Evaluation of kriging interpolation methods as a tool for radio environment mapping

WH Boshoff

Dissertation submitted in fulfilment of the requirements for the degree *Magister in Computer and Electronic Engineering* at the Potchefstroom Campus of the North-West University

Supervisor: Ms MJ Grobler

Co-supervisor: Dr M Ferreira

May 2015

Declaration

I, Willem Hendrik Boshoff hereby declare that the dissertation entitled "Evaluation of kriging interpolation methods as a tool for radio environment mapping" is my own original work and has not already been submitted to any other university or institution for examination.

W.H. Boshoff

Student number: 21625158

Signed on the 28th day of April 2015 at Potchefstroom.

Acknowledgements

Firstly, I would like to thank my King and Heavenly Father for giving me the opportunity, the ability and peace through stressful times, to complete this dissertation.

Thank you to my parents, Nico and Des Boshoff, for leading, supporting and teaching me what is important in life. I love you very much.

Thank you to my beautiful girlfriend, Tania de Nysschen, for your unwavering support and prayers. Thank you for sharing your beautiful heart with me and for being a true example of our Father's unconditional love. I love you very much.

I would like to thank Mrs. Leenta Grobler for her support, motivation and suggestions throughout the two years. I would also like to thank Dr. Melvin Ferreira for his technical guidance and teaching, approachability and honesty. I would not be able to be where I am today without both of your guidance.

Finally, I would like to thank Telkom Centre of Excellence for the financial support and for giving me the opportunity to further my studies.

Abstract

In the journey toward optimal spectrum usage, techniques and concepts such as Cognitive Radio and Dynamic Spectrum Access have enjoyed increasing attention in many research projects. Dynamic Spectrum Access introduces the need for real-time RF spectrum information in the form of Radio Environment Maps. This need motivates an investigation into a hybrid approach of sample measurements and spatial interpolation as opposed to using conventional propagation models.

Conventional propagation models, both path-general and path-specific, require information of transmitters within the area of interest. Irregular Terrain Models such as the Longley-Rice model, further require topographic information in order to consider the effects of obstacles.

The proposed spatial interpolation technique, kriging, requires no information regarding transmitters. Furthermore, Ordinary Kriging requires nothing other than measured samples whereas other kriging variants such as Universal Kriging and Regression Kriging can use additional information such as topographic data to aid in prediction accuracy.

This dissertation investigates the performance of the three aforementioned kriging variants in producing Radio Environment Maps of received power. For practical and financial reasons, the received power measurement samples are generated using the Longley-Rice Irregular Terrain Model and are, therefore, simulated measurements.

The experimental results indicate that kriging shows great promise as a tool to generate Radio Environment Maps. It is found that Ordinary Kriging produces the most accurate predictions of the three kriging methods and that prediction errors of less than 10 dB can be achieved even when using very low sampling densities.

Keywords: *Kriging, Irregular Terrain Model, Longley-Rice, Radio environment mapping, RF propagation modelling, Spatial interpolation, TV broadcasting*

Contents

List of Figures

List of Tables

List of Acronyms

AGL above ground level

AMSL above mean sea level

BLUE Best Linear Unbiased Estimator

BS Base Station

BTS Broadcast Technology Society

CR Cognitive Radio

CV cross-validation

dB decibel

dBd decibel relative to dipole

dBm decibel relative to one milliwatt

DEM Digital Elevation Model

DMS degree, minute, second

DSA Dynamic Spectrum Access

DTT Digital Terrestrial Television

EDA Exploratory Data Analysis

ERP Effective Radiated Power

GHz gigahertz

GSM Global System for Mobile communications

ha hectare

ICASA The Independent Communications Authority of South Africa

IDW Inverse Distance Weighting

ITM Irregular Terrain Model

ITS Institute for Telecommunication Sciences

ITU-R International Telecommunications Union - Radiocommunications

ITWOM Irregular Terrain with Obstructions Model

KED Kriging with External Drift

kHz kilohertz

km kilometre

LOO-CV leave-one-out cross-validation

LTE Long-Term Evolution

ME Mean Error

MAE Mean Absolute Error

MHz megahertz

OK Ordinary Kriging

OSL observed significance level

OLS Ordinary Least Squares

ppm portable pixmap

PSD Power Spectral Density

REM Radio Environment Map

RF Radio Frequency

RGB Red Green Blue

RMSE Root-Mean-Squared Error

RK Regression Kriging

SD standard deviation

SK Simple Kriging

SPLAT! RF Signal Propagation, Loss and Terrain analysis tool

SRS Simple Random Sampling

SRTM Satellite Radar Topography Mission

TPS Thin Plate Splines

TV Television

TVWS TV White Space

UHF Ultra High Frequency

UK Universal Kriging

UMTS Universal Mobile Telecommunications Service

UTM Universal Transverse Mercator

VHF Very High Frequency

WGS84 World Geodetic System 1984

Chapter 1

Introduction

This chapter serves as an introduction to the dissertation. The application domain and proposed solution is briefly introduced in section 1.1. Sections 1.2 and 1.3 provides more detail on the proposed research and the importance of the study, respectively. This is followed by the definition of the research question in section 1.4. The aims and objectives are summarised in section 1.5, and the proposed research methodology is discussed in section 1.6. The chapter is concluded with an overview of this dissertation in section 1.7.

1.1 Introduction

The concept of Cognitive Radio (CR) is defined as a radio system with the ability to assess its surrounding geographic and operational environment. The CR then accordingly adapts to changes in its operating parameters and protocols in a dynamic and autonomous way [1]. This is done to provide reliable communication, independent of its location and which is spectrally efficient [2].

A difficult task in the journey toward CR functionality is providing the ability to access the frequency spectrum dynamically to effectively utilise white space within the Radio Frequency (RF) spectrum. Recently, spatial re-use techniques enjoyed increasing attention, where CRs are allowed to transmit and receive within specified interference constraints [3]. Therefore, research on Power Spectral Density (PSD) maps gained interest as a method of obtaining information on RF traffic in terms of time, space and frequency.

1.1.1 Dynamic Spectrum Access

A proposed solution to improve utilisation of the frequency spectrum is Dynamic Spectrum Access (DSA). It involves wireless devices sharing locally available spectrum based on real-time demands rather than making use of statically allocated frequencies [4]. The shared usage of available spectrum is also known as spectrum sharing [5]. Spectrum sharing can be implemented in a hierarchical method where licensed, or primary, and unlicensed, or secondary, users share spectrum. Another method where users have equal regulatory rights to the shared spectrum, is referred to as horizontal spectrum sharing [6].

Proposed solutions include the use of interference cartography, channel gain maps and PSD maps. These solutions can collectively be referred to as radio environment mapping.

Two popular radio propagation standards used for generating Radio Environment Maps (REMs) are the Longley-Rice Irregular Terrain Model (ITM) and International Telecommunications Union - Radiocommunications (ITU-R) P.1546 propagation models. These two models are discussed in section 2.2.

1.1.2 TV white space

Many countries are already implementing or moving towards the implementation of Digital Terrestrial Television (DTT) [7]. Within the frequency bands allocated to DTT, unoccupied channels exist at certain times in different areas. These unoccupied channels are known as TV White Space (TVWS). Although DTT in South Africa was promised for the 2010 Fifa World Cup, the process has been delayed, and the migration to DTT was postponed to December 2013 [8, 9]. The digital migration is yet to be completed, and no further target dates have been published in the government gazettes.

Currently, TV broadcasting utilises the upper Very High Frequency (VHF) and Ultra High Frequency (UHF) bands [10] which also exhibit very favourable propagation characteristics for data communication networks [11]. Thus, efficient utilisation of TV white space through DSA can be very beneficial for data communications in South Africa.

1.1.3 Kriging interpolation

The kriging interpolation technique is mainly used for interpolating spatial data and has many variations of implementation [12]. Some of the most common variations used for a single target variable, are Simple Kriging (SK), Ordinary Kriging (OK), Universal Kriging (UK) and Regression Kriging (RK). Co-kriging is another variation that is used to predict two target variables simultaneously.

All of these variations are conceptually the same but differs in the parametrical assumptions that are made. The kriging variants applicable to this study are discussed in more detail in chapter 2, section 2.3.

Although kriging originates from mining and geology, it has made its way into many different engineering applications from circuit design to field strength estimation. Kri-

ging has many advantages in comparison to other spatial interpolation techniques which are elaborated on in chapter 3, section 3.3.1.

1.2 Proposed Research

The focus of this research study is to evaluate the accuracy of kriging interpolation methods as a tool for generating REMs by using the Longley-Rice ITM as the baseline. A sample set obtained from the predictions made by the ITM will, therefore, be used as input to a kriging model and for evaluating the accuracy of the kriging predictions.

Comparing the results of these two models should lead to a conclusion regarding the extent of the applicability of kriging in the domain of radio environment mapping. The technique will be implemented on predictions of RF received power of TV channels in the UHF band in South-Africa. The map generated from samples will then be compared to values predicted using radio propagation models, to determine the accuracy of kriging relative to these propagation models.

1.3 Importance of Study

Although DSA is not the definitive characteristic of a CR, it will aid tremendously in the steps toward "anytime, anywhere and spectrally efficient communication" [2]. In order to successfully implement DSA, a device requires real-time information about the current state of the spectrum in its immediate spatial environment.

Propagation models such as the Longley-Rice ITM and the ITU-R P.1546 requires information regarding the transmitting and receiving antennas. This information includes the exact locations of the antennas, the Effective Radiated Power (ERP) and the antenna heights. The proposition of using measured samples and kriging interpolation as a hybrid approach removes the need for knowledge regarding the specifics of the antennae.

Furthermore, kriging holds the advantage of requiring relatively few samples for accurate predictions. Kriging also favours a random sampling approach which, in addition to the small number of samples, could be much more time and cost efficient and practical than taking measurements in a regularly spaced grid.

Finally, the implementation of kriging on samples generated by the Longley-Rice ITM is of importance to draw a conclusion on the promise of the technique for practical implementation. This study attempts to find the most suitable kriging method for radio environment mapping. It also reduces time and money spent on acquiring actual measurements of received power by using simulated sample data as input to the modelling process.

1.4 Research Question

This research aims to answer the following question:

- Does one or more of the kriging interpolation methods provide the accuracy required to generate REMs that can be used to augment or replace the need for conventional propagation prediction methods?

1.5 Research Aims and Objectives

In this study, we will aim to:

- describe and understand the kriging interpolation methods;
- implement kriging on TV broadcast data in order to generate a map of RF received power over a specified area;

- evaluate the accuracy of Ordinary Kriging, Universal Kriging and Regression Kriging when using simulated measurements generated through the Longley-Rice ITM;
- and finally make a recommendation on the better kriging variant for future use of kriging methods for radio environment mapping in applications such as CR.

1.6 Research Methodology

This research project is approached in five consecutive phases. A brief description of each phase follows.

1.6.1 Literature study

In this phase, research is done on related work done in the field of radio environment mapping. The purpose of the literature study is to obtain an in-depth understanding of the applicable study areas, techniques, regulations and standards. It will, thus, comprise of discussions on radio propagation models, the implementation of kriging interpolation methods, prediction accuracy metrics, sampling techniques and coordinate systems. The result of this phase can be found in chapter 2.

1.6.2 Preliminary design

This phase includes a preliminary design for constructing the kriging model implementations following the knowledge gained from the literature study. This phase also comprises various sub-studies in order to reach conclusions regarding different considerations that could have an effect on the results of implementation.

1.6.3 Implementation of kriging model

The samples required to implement kriging is generated using the Longley-Rice ITM in SPLAT! which is an RF Signal Propagation, Loss and Terrain analysis tool. After these samples are generated, the kriging methods are implemented in the R software environment [13]. Finally, the various prediction maps and statistical results are used to evaluate the prediction accuracy visually.

1.6.4 Kriging prediction accuracy evaluation

The accuracy of the kriging prediction results is determined through cross-validation (CV). Considering that the only knowledge on which predictions are based is the measured samples, the CV approach compares the predictions to the sampled values. The results are presented using different metrics discussed in section 2.3.6.

1.6.5 Verification and validation

Finally, the implementations of the kriging methods are verified by confirming that the necessary requirements have been met. The results are verified by cross-validating the predictions with the results produced by the Longley-Rice ITM.

The kriging implementation in the R software environment is validated using the ooDACE toolbox in MATLAB. Correlation between the predicted values using identical input data is determined, and the prediction errors are compared.

1.7 Dissertation Overview

The remainder of this dissertation is structured as follows: Chapter 2 discusses the applicable literature and provides the background required for this project. Chapter 3 describes the conceptual design of the kriging methods for mapping the received power and is then followed by the implementation of the kriging methods in chapter 4. Chapters 6 and 5 shows the results obtained from simulations and also include the validation of the proposed solution. The dissertation is concluded in chapter 7 with a discussion of the efficiency of the proposed solution as well as recommendations on changes that can be made and possible future work.

Chapter 2

Literature Study

This chapter starts with background on radio wave propagation and the Longley-Rice ITM and ITU-R P.1546 propagation models. Section 2.3 discusses the different aspects of kriging interpolation, and section 2.4 reviews possible sampling approaches. Sections 2.5 and 2.6 provide brief discussions on coordinate systems. The chapter closes with a review of related work in section 2.7.

2.1 Radio wave propagation

Radio waves are electromagnetic waves of a certain frequency range. Electromagnetic waves are transverse waves consisting of two components: an electric field component and a magnetic field component. These two components are perpendicular to each other and energy is propagated in a direction perpendicular to both of the field components [14]. The power density of a radio wave in a given time and space can be calculated by determining the product of these two fields. The range of frequencies referred to as radio frequencies stretches from 10 kHz to 300 GHz [15].

Radio waves travel at speed of 3×10^8 metres per second (m/s) in a vacuum (or free space). The propagation speed of radio waves in clear air within the Earth's atmosphere can be approximated to be the same as the propagation speed in a vacuum. When studying radio wave propagation for communication applications, the focus is directed to the power that can be transmitted from one antenna to another.

There are many different types of antennas with different characteristics and, therefore, a generic, theoretically ideal, antenna is used as a reference in antenna calculations. This reference antenna is the isotropic radiator. The isotropic radiator transmits equally in all directions. When the distance (d) and the frequency (f) are known, the loss (in dB) during transmission in free space between two isotropic radiators can be calculated using the following equation [16, 17]:

$$loss = 32.4 + 20\log(d) + 20\log(f) \quad \text{dB} \tag{2.1}$$

This type of loss is referred to as free-space loss [16]. Considering that free-space is a lossless medium, one could say that the term free-space loss is contradictory. It is also known as basic transmission loss. The link loss between any two points is the free-space loss minus any antenna gains plus all other external losses.

$$\text{link loss} = \text{free space loss} - \text{antenna gains} + \text{miscellaneous losses} \tag{2.2}$$

Thus,

$$loss = [32.4 + 20\log(d) + 20\log(f)] - [G_t + G_r] + L_m \quad \text{dB} \tag{2.3}$$

, where G_t and G_r are the transmitter and receiver antenna gains, respectively, and L_m is any miscellaneous losses such as feeder or connector losses given in decibel (dB) [16]. The gains are given in dBi since they are given relative to the reference isotropic radiator, but they can also be given in dBd, relative to the half-wave dipole antenna which is discussed in section 2.1.1.

In radio wave propagation, a very important generalisation is made known as the

inverse square law. This law states that the reduction in power density from the transmitting radio waves is proportional to the square of the distance.

2.1.1 Point-to-area transmission

Point-to-area transmission refers to the manner in which Base Stations (or broadcasting transmitters) provide coverage over a certain area for mobile communications. The two types of antennas most commonly used in point-to-area transmission are the half-wave dipole antenna and the sectored antenna. Examples of the elevation and azimuth patterns of these two antennas are shown in figure 2.1.

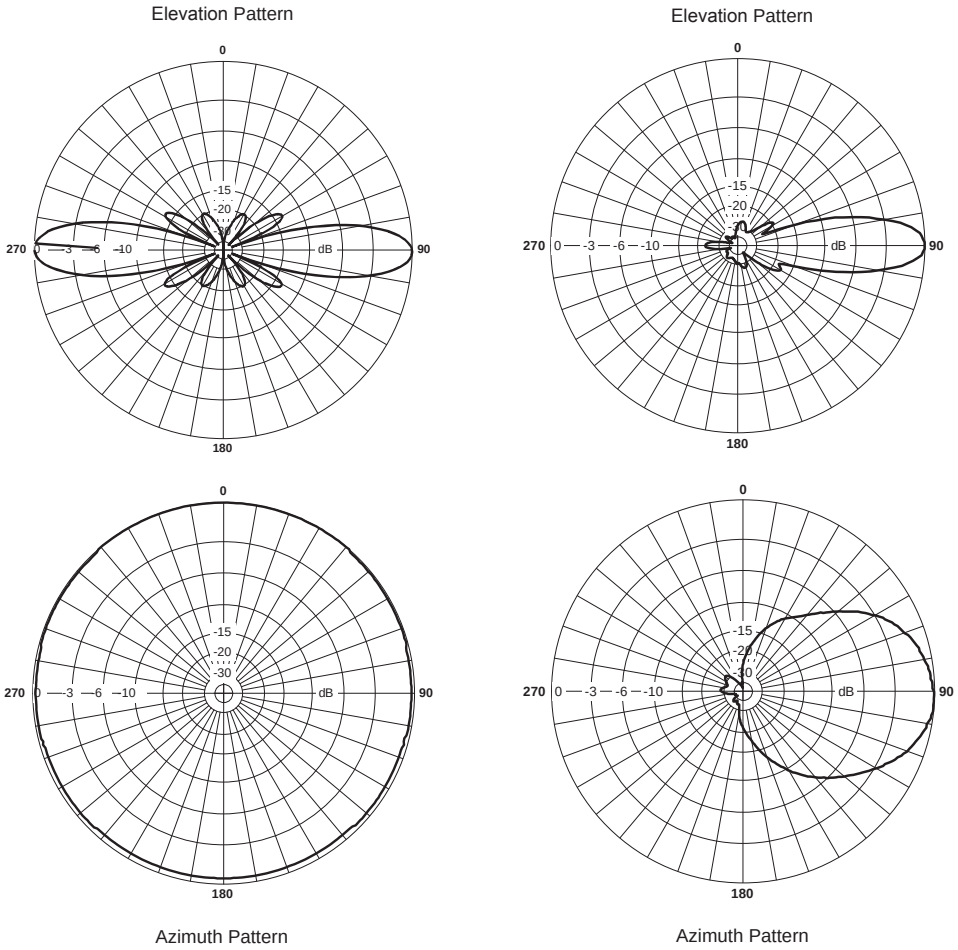

Figure 2.1: Elevation and azimuthal patterns of a half-wave dipole (left) and a sectored antenna (right) [18]

The half-wave dipole antenna radiates in all directions in the horizontal plane. It has a gain of 2.1 dBi and, like the isotropic radiator, is also used as a reference antenna. The standard measuring unit used to refer to this antenna is decibel relative to dipole (dBd). The sectored antenna is more directional and is named according to its 3 dB beamwidth. The 3 dB beamwidth is the range within which the antenna's radiated power has decreased with less than half the maximum radiated power. The sectored antenna normally provides horizontal coverage of less than 180 degrees.

High-power transmitters are used for television broadcasting. These transmitters are usually placed in elevated positions in order to evade obstacles (also known as clutter) such as high buildings that could interfere with the transmission. A single broadcasting transmitter can suffice for a coverage area with a radius of 100 km or more, surrounding the transmitter.

2.1.2 Electric field strength

In point-to-area transmission, the coverage area refers to the area in which a single antenna can transmit or receive signals to or from other transmitters and receivers. The two main applications for point-to-area transmission are digital mobile communications and broadcasting [16]. The latter is mainly used for television and radio whilst the former include Global System for Mobile communications (GSM), Universal Mobile Telecommunications Service (UMTS) and recently Long-Term Evolution (LTE). In television broadcasting predictions, path-general prediction models (such as the ITU-R P.1546) are occasionally used. The reason being that the assumption is made that the receiving antennas are placed on rooftops and directed at the broadcasting station which reduces the effect of surrounding buildings on the received signal.

In broadcasting transmission calculations, electric field strength is preferred to power density. The standard measure for electric field strength is microvolt per metre ($\mu V/m$) since received electric field strengths are usually very small.

2.2 Radio wave propagation models

The more conventional method of generating radio environment maps is through the use of propagation models. Two popular models used for VHF and UHF are the Recommendation ITU-R P.1546 and the Longley-Rice ITM. In this section, both of these models will be discussed.

2.2.1 Longley-Rice irregular terrain model

The Longley-Rice model is a radio propagation model used to predict radio signal attenuation over irregular terrain relative to free-space transmission loss. This method is designed for the frequency range 20 MHz to 40 GHz [17] and path lengths from 1 km to 2000 km [17, 19]. It is based on electromagnetic theory and statistics describing similar radio measurements and terrain features. It is also known as the Institute for Telecommunication Sciences (ITS) ITM. The ranges for which this model is intended are summarised in table 2.1 [17].

Table 2.1: Longley-Rice ITM parameter limits

Parameter	Minimum	Maximum
Frequency	20 MHz	40 000 MHz
Antenna heights	0.5 m	3000 m
Distance	1 km	2000 km
Surface refractivity	250 N-units	400 N-units

The model caters for two telecommunication links: point-to-point and point-to-area and it is path specific. The path parameters taken into account in this model are the effective antenna heights, horizon distances and elevation angles, terrain irregularity and reference attenuation. The reference attenuation includes line of sight, diffraction and forward scatter attenuation.

The model uses the variability of the signal in time and space as well as a distance value in order to predict a median attenuation of the radio signal. The model can be implemented for a broad range of engineering problems such as preliminary estimates

for system design, tactical planning and surveillance in the military and land-mobile systems [20].

Radio propagation is particularly difficult to predict for the VHF and UHF bands since cluttering obstacles and the atmosphere cause scattering. The signal levels, therefore, vary in time and space since the atmospheric conditions change with time and the obstacles in the propagation path depend on the surrounding terrain. The model focuses on received power and is not necessarily concerned with specific channel characterisation, and there are many special circumstances that it does not consider.

The difference between point-to-point and area prediction models is that the area prediction model does not require the detailed propagation path information and may not even require a specified path. The authors of [20] mention five areas in which prediction models play very important roles:

- Equipment design
- General system design
- Specific operational area
- Specific coverage area
- Specific communications link

Considering the above-mentioned areas, one finds that area prediction models can be useful for most problems. The question comes down to the accuracy and precision of the results required. In some cases, specific propagation path information may not be obtainable, and one is forced to use an area prediction model. In other cases, the mere complexity and effort a point-to-point prediction model necessitates could tempt one to rather opt for the area prediction model and sacrifice some accuracy of the results.

Input parameters

For the area prediction model, some parameters are merely estimated values used for similar conditions (e.g. knowledge of the terrain type can be used to fit the conditions to predefined terrain parameter values of a similar terrain). The input parameters for the model are divided into four sets: system parameters, environmental parameters, deployment parameters and statistical parameters [17, 20, 21].

1. *System parameters*:
   These parameters are entirely independent of the environment, and they are directly related to the radio system considered. There are five system parameters:
   - Frequency
   - Distance
   - Transmitting antenna height
   - Receiving antenna height
   - Polarisation
2. *Environmental parameters*:
   The environmental parameters describe the statistics of the specific environment in which the radio system operates or is to operate. These four parameters are:
   - Terrain irregularity parameter (Δh)
   - Electrical ground constant
   - Surface refractivity (N_s)
   - Climate
3. *Deployment parameters*:
   These parameters attempt to describe interactions in the system. This model considers only one deployment parameter: siting criteria. This parameter describes how carefully the positioning of both transmitting and receiving antennas was done.

4. *Statistical parameters*:

   The statistical parameters describe the variety of statistics longed for by the user and is often referred to in the form of quantiles. These parameters go hand in hand with the reliability and confidence of the analysis.

Even though there are about twelve input parameters, many of them can be replaced by nominal values for simplicity. The number of input parameters that are of importance in all scenarios comes down to only five: frequency, distance, antenna heights and terrain irregularity. The reason for the insignificant effect of some of the input parameters is the fact that the atmosphere has very little effect on radio wave propagation for shorter distances. Therefore, nominal values can then be used to assume average conditions.

Calculation of atmospheric and terrain parameters

Longley et al. [17] states the refractive index is the most important atmospheric parameter for "predicting a long-term median reference value of transmission loss". It affects the Earth's effective radius and, therefore, the extent to which a radio ray bends as it passes through the atmosphere. The surface refractivity is calculated using equation 2.4.

$$N_s = N_o \exp(-0.1057 h_s) \quad \text{N-units} \tag{2.4}$$

, where N_s is the surface refractivity, N_o is the surface refractivity reduced to sea level, and h_s is the elevation of the Earth's surface in km.

The irregularity of the terrain is characterised by the parameter Δh. According to Shumate [22], Δh is determined by the amount of deviation from the average height of elevations between the transmitting and receiving antennas. Figure 2.2 shows the terrain profile considered for determining the average height of elevations. The interquartile ranges of the propagation path and elevations are considered. Thus, distance between 10% and 90% of the path from the transmitter to the receiver is used. Within this range,

elevations between 10% and 90% of the highest elevations are used to calculate the average height of elevations through a least-squares method. The deviation from the average elevation is then used as Δh.

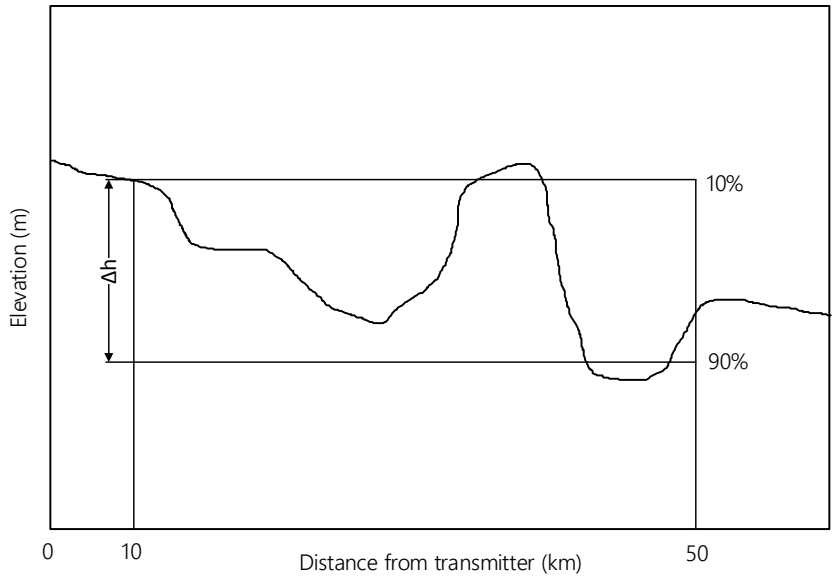

Figure 2.2: Definition of the terrain irregularity factor (Δh) [23]

The implementation of the Longley-Rice ITM in SPLAT!, that will be discussed in section 4.1.3, uses the SRTM Digital Elevation Model (DEM) with a 3-arc-second resolution [24] to determine the path profile. In cases where terrain profiles are unavailable, the estimate values shown in table 2.2 are used for Δh.

Table 2.2: Estimate values for Δh [17]

Terrain type	Δh (m)
Water or very smooth plains	0 - 5
Smooth plains	5 - 20
Slightly rolling plains	20 - 40
Rolling plains	40 - 80
Hills	80 - 150
Mountains	150 - 300
Rugged mountains	300 - 700
Extremely rugged mountains	> 700

Furthermore, the estimate of Δh at a specific distance can be calculated using equation 2.5.

$$\Delta h(d) = \Delta h[1 - 0.8\exp(-0.02d)] \text{ m} \tag{2.5}$$

, where $\Delta h(d)$ and Δh are in metres and the distance (d) at which Δh is desired, is specified in km.

An additional two parameters, known as ground constants, are considered in the calculations for line-of-sight and diffraction attenuation. These are the conductivity (σ) and the relative dielectric constant (ϵ) of the Earth's surface. Once again, some estimate values are proposed for cases where the values of these constants are not known. These estimates are summarised in table 2.3. Hufford et al. [20] propose that the constants for average ground are suitable for most cases.

Table 2.3: Estimate values for the ground constants [17]

Type of surface	σ (℧/m)	ϵ
Poor ground	0.001	4
Average ground	0.005	15
Good ground	0.02	25
Sea water	5	81
Fresh water	0.01	81

The quality of the ground is classified according to the roughness of the terrain. Areas with very rocky soil, steep hills and very mountainous terrain are classified as poor ground. Cities and industrial areas with high buildings also fall into this category. Average ground is found in areas with heavy clay soil, medium hills and forestation. Good ground is defined by low hills, rich soil and, mostly, flat country.

Calculation of additional path parameters [17]

In order to determine the transmission loss, the antenna heights, horizon distances and horizon elevation angles are required. Depending on the scenario, these parameters may be known or estimated. The estimate values for the horizon distances and

the horizon elevation angles are dependent on the terrain irregularity factor (Δh), the heights of the antennas above ground level (AGL) and the method used for selecting antenna sites.

In cases where the transmitting and receiving antenna sites are randomly located, the effective heights of the antennas are assumed to be equal to their heights AGL as shown in equation 2.6.

$$h_{e1,2} = h_{g1,2} \text{ m} \tag{2.6}$$

, where $h_{e1,2}$ denotes the effective antenna heights for the transmitting and receiving antennas, respectively, and $h_{g1,2}$ denotes the antenna heights AGL in m. Using similar notation, equation 2.7 is used to determine $h_{e1,2}$ for antennas located on or near hilltops in radio relay link situations.

$$h_{e1,2} = h_{g1,2} + k \exp(-2h_{g1,2}/\Delta h) \text{ m} \tag{2.7}$$

, where Δh is the terrain irregularity factor, and k is a constant determining the extent to which $h_{e1,2}$ differs from $h_{g1,2}$. k is dependent on how carefully an antenna site is selected, and it will not exceed the value of 50. Thus, in cases where equation 2.7 is used, the effective height of the antenna is larger than its structural height.

The distance to the radio horizon of each antenna is determined by its effective height, smooth-earth horizon distance and Δh. The smooth-earth horizon distance is given by equation 2.8.

$$d_{Ls1,2} = \sqrt{0.002 a h_{e1,2}} \text{ km} \tag{2.8}$$

, where $d_{Ls1,2}$ denotes the smooth-earth horizon distances of the transmitting and receiving antennas in km, $h_{e1,2}$ are in m and a denotes the effective Earth radius in km, given by equation 2.9.

$$a = 6370[1 - 0.04665 \exp(0.005577 N_s)]^{-1} \text{ km} \tag{2.9}$$

, where the real Earth radius is taken to be 6370 km and N_s is the surface refractivity. Whereas, the horizon distances over irregular terrain is given by equation 2.10.

$$d_{L1,2} = d_{Ls1,2} \exp(-0.07\sqrt{\Delta h / h_e}) \text{ km} \tag{2.10}$$

, where

$$h_e = \begin{array}{ll} h_{e1,2} & \text{for} \quad h_{e1,2} \geq 5 \text{ m}, \\ 5 \text{ m} & \text{otherwise.} \end{array} \tag{2.11}$$

Thus, the total distance between the antennas and their horizons is given by equation 2.12.

$$d_L = d_{L1} + d_{L2} \text{ km} \tag{2.12}$$

Finally, the horizon elevations are calculated using the effective antenna heights, the terrain irregularity factor, the smooth-horizon distances and the horizon distances over irregular terrain. The horizon elevations ($\theta_{e1,2}$) is given by equation 2.13.

$$\theta_{e1,2} = \frac{0.005}{d_{Ls1,2}}[1.3(\frac{d_{Ls1,2}}{d_{L1,2}}\Delta h - 4h_{e1,2}] \quad \text{rad} \tag{2.13}$$

The sum of elevation angles and the angular distance for a transhorizon propagation path, which is always positive, are calculated using equations 2.14 and 2.15, respectively.

$$\theta_e = \theta_{e1} + \theta_{e2} \quad \text{rad} \tag{2.14}$$

$$\theta = \theta_e + d/a \quad \text{rad} \tag{2.15}$$

, where d is the propagation path length in km, and a is the Earth's effective radius, also in km. The additional parameters, $h_{e1,2}$, $d_{L1,2}$, $\theta_{e1,2}$ and θ, are required for the computation of transmission loss as discussed in the following section.

Transmission loss calculations

The reference value for transmission loss (L_{cr}) are determined by the sum of free space loss (L_{bf}), as given by equation 2.1, and the reference attenuation relative to free space (A_{cr}). Thus, the reference value for transmission loss is determined using equation 2.16.

$$L_{cr} = L_{bf} + A_{cr} \quad \text{dB} \tag{2.16}$$

A_{cr} is calculated differently depending on the propagation distances. The attenuation relative to free space is calculated using the formulae of two-ray optics for distances

well within line-of-sight. For distances beyond line-of-sight, diffraction is the main cause of attenuation and for greater distances, forward scatter becomes the dominant mechanism affecting propagation.

2.2.2 Prediction accuracy

In research, it was found that the accuracy of propagation models is commonly in the order of 8-10 dB for urban areas and between 10 and 15 dB in rural areas [25–27]. The authors of [20] state that the Longley-Rice ITM's predictions are theoretically within a range of 10 dB of the actual measured values for any given distance within the specifications of the model. Further experiments done by the authors of [28,29] confirm this by finding prediction errors between 5 dB and 10 dB for different situations.

2.2.3 Enhancements on the Longley-Rice ITM

Many enhancements have been made on the implementation of the Longley-Rice ITM by Sidney Shumate [30]. This enhanced implementation is referred to as the Irregular Terrain with Obstructions Model (ITWOM). Shumate primarily used the ITU-R P.1546, discussed in section 2.2.4, along with other ITU-R recommendations, Snell's Law and Beer's law, to derive deterministic approximation equations for the software implementation of the new ITWOM.

Some shortcomings of the previous implementation of the Longley-Rice ITM, pointed out by Shumate in [30], are that it works best for 30-arc-second terrain detail and that the use of finer detailed terrain data, such as 3-arc-second and 1-arc-second, do not provide better results. The ITM also lacks in the consideration of more than two obstructions in a radial path, and the obstructions before the antennas' horizons are not considered. Shumate also brings to light some mathematical errors and outdated approximations found in the core implementation code of the Longley-Rice ITM.

The details of the corrections made by Shumate are discussed in several articles since 2007 which are published in the IEEE Broadcast Technology Society (BTS) Newsletter [22, 31–42].

The ITWOM includes multipath effects of reflected signals caused by obstructions. Among the derivations made from the ITU-R P.1546, are clutter loss function equations for line-of-site ranges and the consideration of the radiative transfer phenomenon in propagation above and below the 'clutter canopy'. Shumate also altered the switch point between diffraction and tropospheric scatter to be true to ranges proposed by Longley and Rice in [17] rather than the implementation in the ITM.

For the remainder of this dissertation, references made to the implementation of the Longley-Rice ITM in SPLAT!, refers to the ITM with the enhancements added by Shumate (i.e., the ITWOM).

2.2.4 International Telecommunications Union - Radiocommunications P.1546

The ITU-R P.1546 model [43] is a point-to-area prediction method and is path-general, which means that it does not consider path specific properties such as terrain irregularity. This method is only valid for the frequency range of 30 MHz to 3 GHz [16, 43] and for distances of 1 km to 1000 km. It is mainly intended for broadcasting with transmitting antennas situated above the local surrounding clutter. The model predicts for a height of 10 m above the ground [16], which is a good approximation of the average height of terrestrial television antennas. The parameters required by this ITU model are effective antenna heights (of both transmitter and receiver), percentages of time and location probability as well as the distance between the transmitter and receiver [43].

The ITU-R P.1546 provides field strength curves as a function of distance, for a few nominal frequencies, time percentages, antenna heights and three different propaga-

tion path types [21]. There are three different sets of curves for three different frequency ranges. The frequency ranges are 30 MHz to 300 MHz, 300 MHz to 1000 MHz and 1000 MHz to 3000 MHz. The three different propagation paths are land, warm sea and cold sea. A mixed-path method is also proposed in the case where propagation prediction is required over land and sea.

The three nominal frequencies of which the curves are given are 100 MHz, 600 MHz and 2000 MHz. The curves of these three frequencies can be interpolated or extrapolated should one require the field strength value of any other frequency within the ITU-R P.1546 model's specified range. As an alternative to the curves, the recommendation proposes using tabulated field strengths provided by the Radiocommunications Bureau when implementing this model using computers.

Transmitting antenna height calculation

The curves and tabulations for field strength versus distance are given for the following transmitting antenna heights: 10 m, 20 m, 37.5 m, 75 m, 150 m, 300 m, 600 m and 1200 m. The calculation of the transmitting antenna height, h_1, differs for land and sea paths. For sea paths, h_1 is the height of the antenna above sea level. For land paths, the effective height, h_{eff}, is determined by using the height of the antenna above the averaged ground clutter from 3 km to 15 km in the direction of transmission or the direction of the receiving antenna.

A method for calculating h_1 is provided for four different cases:

1. Land paths shorter than 15 km where no terrain information is available:
   In this case formulas are given for paths shorter than 3 km and as well as paths longer than 3 km. If the length of the path is represented by d and h_a is the height of the antenna above the ground, the formulas are as follows:

$$h_1 = h_a \quad \text{m} \quad \text{for} \quad d \leq 3\text{km} \tag{2.17}$$

$$h_1 = h_a + \frac{(h_{eff} - h_a)(d-3)}{12} \quad \text{m} \quad \text{for} \quad 3 < d < 15\text{km} \tag{2.18}$$

2. Land paths shorter than 15 km where terrain information is available:
   In this case, only one formula is given since the terrain height is taken into account. An averaged terrain height is calculated for the distances $0.2d$ to d km. The actual height of the antenna is subtracted from the average terrain height in order to find h_b.

$$h_1 = h_b \quad \text{m} \tag{2.19}$$

3. Land paths longer than 15 km:
   In this case, the effective antenna height, h_{eff}, is calculated in a similar manner to the second case. The average terrain height is determined by calculating the average height of the terrain between the distances 3 and 15 km, and the height of the antenna above this average terrain height is taken as h_{eff}.

$$h_1 = h_{eff} \quad \text{m} \tag{2.20}$$

4. Sea paths:
   In the case of sea paths, the actual height of the antenna above sea level can be taken as h_1, but the ITU-R P.1546 becomes unreliable for values $h_1 < 3$ m.

Receiving antenna height calculation

The height of the receiving antenna, h_2, is determined by calculating the height of the antenna above the surrounding ground clutter. Thus, the height is equal to the height of the clutter surrounding the antenna. The recommendation specifies the minimum value for h_2 as 10 m.

Interpolation of propagation curves

It was previously stated that when using the ITU-R P.1546 model in computer implementations, one is encouraged to use tabulated data from the Radiocommunications Bureau. In this case values might be encountered that are not tabulated. If one chooses to use the field strength versus distance curves, the problem could arise that either the antenna height or time percentage or frequencies used, differ from the nominal values used for the graphs. The ITU-R P.1546 provides a solution for both these cases.

When the values obtained during the implementation of this recommendation cannot be read directly from the given graphs or tables, the given values can be interpolated or extrapolated in order to find the correct values for a certain scenario.

The field strength values can be interpolated or extrapolated as function of distance, frequency and percentage time using the closest superior and inferior values found on the graphs or in the tables. When extrapolating the values care should be taken to stay within the limits for which the ITU-R P.1546 is valid. Table 2.4 shows the input parameters and their limits.

Table 2.4: ITU-R P.1546 input parameters and their limits

	Unit	Definition	Limits
f	MHz	Operating frequency	3 to 3000
d	km	Path length	1 to 1000
p	%	Percentage time	1 to 50
h_1	m	Transmitting antenna height	0 to 3000
h_a	m	Transmitting antenna height above ground	$> R$
h_b	m	Transmitting antenna height above terrain height	Only for $d < 15$ km
h_2	m	Receiving antenna height above ground	1 to 3000
R	m	Clutter height	None

Time variability

Time variability refers to the percentage of time that the field strength is at a certain value. The propagation curves show the field strength values that are exceeded for the specified time percentages. The curves only indicate three discrete time percentages, i.e. 1%, 10% and 50%. As mentioned in section 2.2.4, the values can be interpolated for different time percentages but the ITU-R P.1546 is not valid for percentages more than 50% or less than 1%.

Location variability

Location variability, in this case, refers to the variability of field strength within a certain area. For this recommendation, the propagation curves represent an area of 500 m by 500 m and for this area shows field strength values exceeded at 50 % of locations. There are mainly three influences causing variations in field strength over a certain area, namely: multipath variations, local ground cover variations and path variations.

This recommendation mainly considers local ground cover variations and provides a method to estimate the location variability to increase accuracy when terrain clearance angle correction is applied. When implementing method this method, location percentage can be specified to fit the applicable scenario. The values of variability used for the nominal frequencies are given in table 2.5.

Table 2.5: Nominal variability values used for planning

	Standard deviation (dB)		
Broadcasting type	100 MHz	600 MHz	2000 MHz
Analogue	8.3	9.5	-
Digital	5.5	5.5	5.5

2.3 Kriging interpolation

Geostatistics is the area in statistics that focuses on geographical applications such as meteorology, mining exploration and other environmental sciences [5]. Kriging is a very popular spatial interpolation technique used in geostatistics and serves as a method to make inferences on the unknown or unobservable values of a random process [44]. This technique was originally introduced by the South African mining engineer Danie Krige [44, 45] by whom it was used to establish mining maps by using scattered measurements. Today kriging is used in many different fields, such as computer-aided optimal design of aeroplanes and computer chips [46].

The method is based on spatial autocorrelation which originates from the first law of geography (or Toblers first law). This law states that everything is related to everything else, but near things are more related than distant things [47].

The kriging interpolation technique is mainly used for spatial data and has a number of implementation variations. The three most common variations are Simple Kriging (SK), Ordinary Kriging (OK) and Universal Kriging (UK) [48]. Regression Kriging (RK) is a variation of UK and another multivariate variant of kriging, is co-kriging. All of these variations are conceptually the same but differ in the parametrical assumptions that are made.

Kriging is a Best Linear Unbiased Estimator (BLUE) spatial interpolation method since the estimates are weighted linear combinations of the sample data used and it attempts to achieve a mean error of zero by minimising the error variance. The last mentioned feature distinguishes kriging from other spatial interpolation techniques [49].

Another favourable characteristic of kriging is the fact that the points are estimated using the covariances between the data samples and between the estimation point and the data samples. Thus, the estimation does not depend on the locations of the sampled data points but rather the separation between them. The separation between the

locations required by kriging is the Euclidean (or straight-line) distance. Thus, when working with larger areas where the locations are given in terms of geographical coordinates, conversion to a flat surface such as Universal Transverse Mercator (UTM) is required. The UTM coordinate system is discussed in section 2.6.

2.3.1 Data assumptions and input requirements

Although kriging is a very robust spatial interpolation technique, there are a few input requirements and properties that the data is assumed to have. These requirements and assumptions are in most cases not a necessity for one to be able to implement kriging, but they need to be satisfied for kriging to be the optimal predictor [50]. As previously mentioned, the kriging method is based on spatial autocorrelation. Therefore, the input data must be spatially autocorrelated. This means that the variance of samples close to each other is smaller than the variance of samples further apart.

Except for the data being spatially autocorrelated, it needs to be stationary. Second-order stationarity seems to suffice for kriging [44,50,51]. For second-order stationarity, the data must have a constant mean and the variance be independent of location. Cressie [44] states that a spatial dataset is second-order stationary when equations 2.21 and 2.22 is satisfied.

$$Z(\mathbf{s}) = \mu, \quad \forall\, \mathbf{s} \in D \tag{2.21}$$

, where Z is a random function or process. In the application of kriging, Z represents the measured values of the samples as a function of the locations of the samples $\mathbf{s}$ and $\mathbf{s}$ is taken from the area of interest D.

$$cov(Z(\mathbf{s}_1), Z(\mathbf{s}_2)) = C(\mathbf{s}_1 - \mathbf{s}_2), \quad \forall\, \mathbf{s}_1, \mathbf{s}_2 \in D \tag{2.22}$$

, where *cov* indicates the covariance between the sample values at locations $\mathbf{s}_1$ and $\mathbf{s}_2$ and C is the covariogram as a function of the distance between the two locations. The covariogram is discussed in section 2.3.2. Thus, the dataset is second-order stationary if the covariances of the target variable are solely dependent on the distance between

the sample locations rather than the sample locations.

The kriging model requires second-order stationarity since it assumes that a single semivariogram describes the entire area of interest. It implies that the variance is only a function of distance and is not affected by location [52]. The second requirement is that the sampling locations are chosen independently of the values of samples. Finally, for kriging to be the optimal predictor, the fitted semivariogram model should be a true representation of the input data.

In addition to the aforementioned assumptions, each variation of kriging has other additional requirements and assumptions.

2.3.2 The semivariogram

Kriging estimation requires kriging weights that are derived from a fitted model semivariogram. The semivariogram describes the variance between values of sample locations as a function of their separation distance (known as lag). The initial step in finding the model semivariogram that best fits the data is to calculate the experimental semivariogram by finding the average of the semi-variances for all the pairs of sample points for a certain lag. The semivariances for the experimental semivariogram can be calculated using equation 2.23 proposed by the authors of [53].

$$\gamma(\mathbf{h}) = \frac{1}{2}E[(z(\mathbf{s}_i) - z(\mathbf{s}_i + \mathbf{h})^2] \tag{2.23}$$

, where $z(\mathbf{s}_i)$ is the value at a sampled location, s_i, and $z(\mathbf{s}_i + \mathbf{h})$ is a neighbouring sampled value at a lag $\mathbf{h}$ away [50]. When sample locations are chosen randomly instead of by a systematic gridded approach sample pairs are rarely separated by the same lag. In this case a tolerance around a lag h must be defined for which the average semivariance is to be calculated [44]. This could have an effect on how truthful the semivariogram is, but the effect of this on the accuracy of the kriging predictions, is insignificant [54].

Before fitting a model semivariogram to the experimental semivariogram, one has to consider the possibility of anisotropy within the data. Anisotropy means that the variance of the sampled data does not only depend on the separation between sampling locations but the direction as well. The data is said to be isotropic if [51]:

$$\gamma(z(\mathbf{s}_i) - z(\mathbf{s}_j)) = \gamma(|z(\mathbf{s}_i) - z(\mathbf{s}_j)|) \tag{2.24}$$

, where γ is the variance between the sampled values, z, at locations $\mathbf{s}_i$ and $\mathbf{s}_j$. Thus, the condition for isotropy shown in equation 2.24, states that the variance between all samples separated by the same distance should be the same regardless of the direction of their separation.

Since real data is rarely perfectly isotropic, the author of [50] proposes a rule of thumb using the semivariogram confidence bands in two orthogonal directions. This rule of thumb states that one should consider an anisotropic model if the confidence bands in the major and minor directions show an overlap of less than 50%.

Once the experimental variogram is calculated, and a conclusion has been reached on the isotropy of the data, the model semivariogram can be fitted. The model semivariogram can be one or a combination of the standard positive definite variogram models. These models include the linear, spherical, exponential, circular, Gaussian and Matern models [50].

Choosing which of these models to use depends on the location and geometry of the area over which the prediction is done [44]. After the best predictor (model semivariogram) is selected and fitted, it is then used to determine the nugget, sill and range parameters. When the final model semivariogram is fitted to the samples, this model can then be used to solve the kriging weights and predict any of the unknown points within the sampled area.

The semivariogram has three defining properties of interest for modelling spatial data which are shown in figure 2.3.

1. Nugget:

   The nugget is the initial value of the semivariogram, $\gamma(0)$, and therefore shows the variability of the samples at $h = 0$. It is an indication of sampling and analytical errors, possibly caused by equipment tolerances, etc.

2. Range:

   The range of the semivariogram is the lag at which it reaches 95% of the sill. This means that it is the separation distance beyond which the semivariance is spatially independent. Since the kriging weights sum to one, the weights at lag distances greater than the range are usually negligible.

3. Sill:

   The sill shows the variability of spatially independent samples (i.e., the semivariance of samples beyond the range).

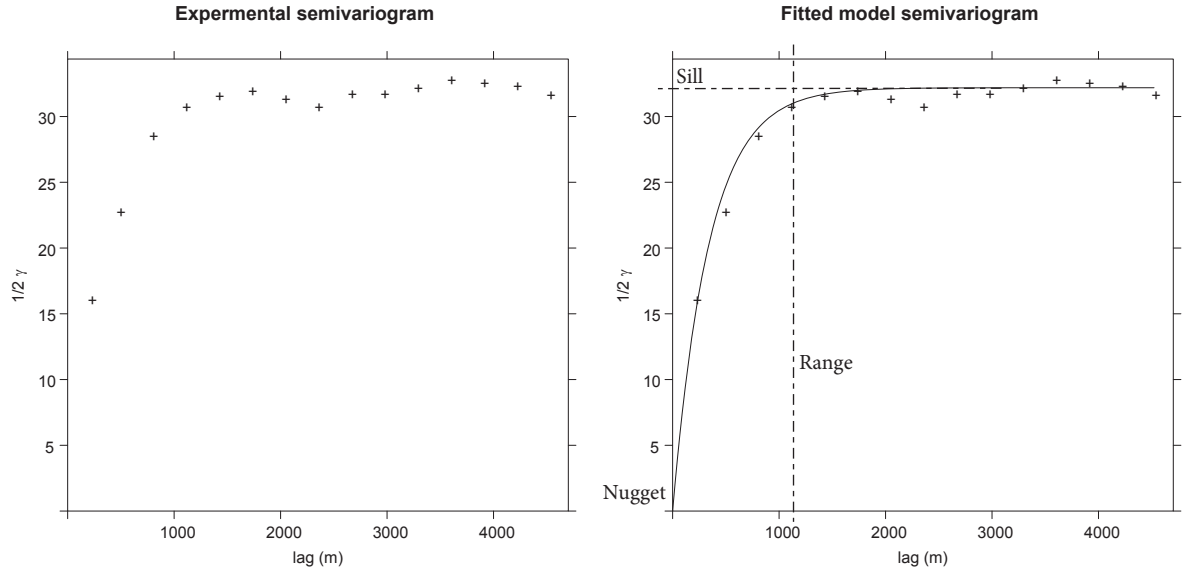

Figure 2.3: Experimental and model semivariogram

It is common practice to use the semi-variances to model the variogram after which the covariances are used for further calculations [50, 55]. When determining the kriging weights, the same results are found when using either semi-variances or covariances.

The relationship between these two is given by equation 2.25.

$$C(\mathbf{h}) = C_0 + C_1 - \gamma(\mathbf{h}) \tag{2.25}$$

, where C is the covariance as a function of lag, $\mathbf{h}$, C_0 is the nugget, C_1 is the sill of the semivariogram and γ is the semivariogram as a function of $\mathbf{h}$.

2.3.3 Ordinary kriging

What defines OK as a spatial prediction method is the following two assumptions [53, 56]:

1. Model assumption:

$$\begin{aligned} &Z(\mathbf{s}) = \mu + \delta(\mathbf{s}), \quad \mathbf{s} \in \mathbf{D}, \\ &\mu \in \Re, \text{ and } \mu \text{ is unknown} \end{aligned} \tag{2.26}$$

   , where $Z(\mathbf{s})$ is a Gaussian process which is a function of the location, $\mathbf{s}$, from the area of interest, $\mathbf{D}$, μ is a constant unknown regression function (i.e. $\mu = \alpha_0$ with α_0 being a constant unknown value) and δ is a Gaussian process constructed from the residuals. The constant regression function means that the technique assumes an unknown constant trend in the data [57].

2. Predictor assumption:

$$Z(\mathbf{s}_0) = \sum_{i=1}^{n} \lambda_i Z(\mathbf{s}_i), \quad \sum_{i=1}^{n} \lambda_i = 1 \tag{2.27}$$

   , where λ_i in this case represents the kriging weights [44, 58] which are assigned to each sample value, $Z(\mathbf{s}_i)$, and are used as a linear combination to predict the unknown value $Z(\mathbf{s}_0)$. The condition of the kriging weights summing to unity in equation 2.27 ensures unbiasedness.

2.3.4 Universal and regression kriging

UK assumes a more general and less idealistic scenario than OK, where μ from equation 2.26 is no longer constant but an unknown linear combination of identified functions [44,57]. These functions are dependent on location, and the most commonly used functions are those with values of explanatory variables. These explanatory variables are referred to as covariates [50]. While the predictor assumption remains the same as for OK, the modified model assumption for UK is given by equation 2.28.

$$Z(\mathbf{s}) = \sum f(\mathbf{s})\boldsymbol{\beta} + \delta(\mathbf{s}), \quad \mathbf{s} \in \mathbf{D} \tag{2.28}$$

, where $f(\mathbf{s})$ represents the known functions of explanatory variables listed in the vector $\boldsymbol{\beta}$, as a function of location, $\mathbf{s}$, and δ is a zero-mean normally distributed process containing the residuals produced by fitting the regression function to the target variable.

This variation of kriging is known by a few different names such as Universal Kriging (UK), Kriging with External Drift (KED), RK as well as SK with varying local means [50]. Hengl states in [50] that the only difference between UK and RK lies in the computational steps of the implementation. For RK, the predictions for fitting the trend model and the consequent residuals are made separately after which they are added together to find the final predicted value.

In cases where kriging needs to be used for spatial extrapolation, UK is proposed to be the best candidate since it uses a trend function [49].

2.3.5 Kriging model validation

The output of kriging and most other statistical prediction models are commonly maps of the predicted values and prediction variances. The latter can be used to deter-

mine the accuracy of the prediction map by calculating the overall prediction variance (which is the mean of the prediction variances). The overall prediction variance is evaluated against the global variance. The closer it is to the global variance, the more inaccurate the predictions are, and if it tends to zero the predictions tend to optimal accuracy. But the kriging variance cannot be used as the sole measure of prediction uncertainty [59].

Common practice for validating kriging models is a method known as CV [16, 58, 60, 61]. Though there are many different statistical metrics which can also provide information on the accuracy of the model, CV is one especially suitable for scenarios in which kriging is used. The reason for this is that the sample data is usually limited and requires time and expensive equipment to be collected. By using CV, the entire set of sample data used to generate the kriging model can also be used to validate the kriging model.

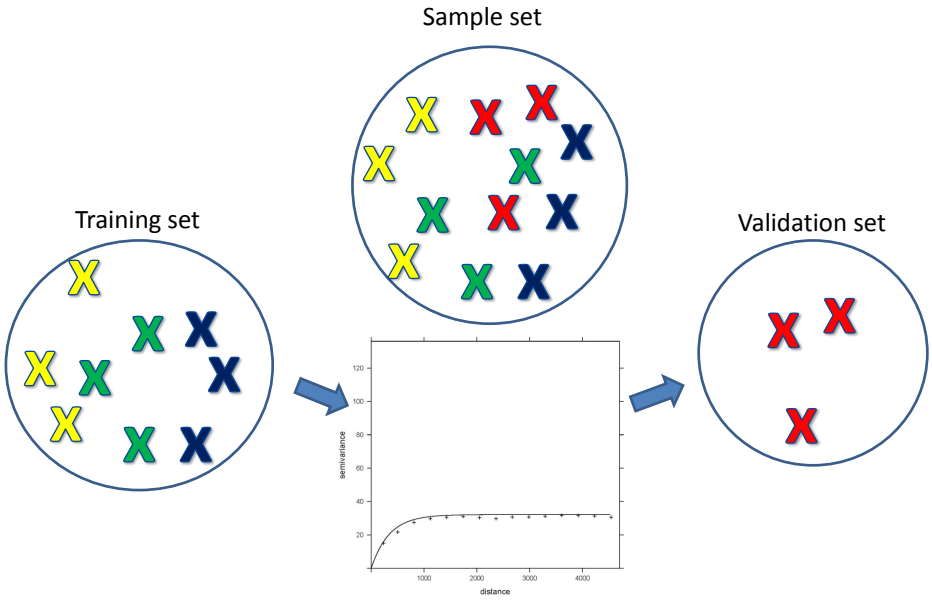

Figure 2.4: *k*-fold CV illustration

A popular form of CV used for kriging is *k*-fold CV. This form of CV is implemented by dividing the sample data set into *k* disjoint subsets, with the value of *k* typically being in the order of 3 to 10 [62]. The CV process is iterative and is repeated *k* times.

Figure 2.4 illustrates one iteration of k-fold CV where $k = 4$. A different subset is omitted as the validation set for each of the k iterations while the remaining $k - 1$ subsets are used to fit the kriging model. The kriging model is then used to predict the points of the validation set and an error function such as the ME or MAE is used to calculate the prediction error. The final CV prediction error is then found by obtaining the mean value for the errors found in all k iterations.

A special case of k-fold CV where $k = 1$, is known as leave-one-out cross-validation (LOO-CV). LOO-CV is both the most accurate and computationally the most expensive form of CV.

Although CV is an effective way of evaluating the fit of the semivariogram to the data, it does have some limitations. It is entirely dependent on the accuracy and the comprehensiveness of the input data [55]. This means that CV does not give any indication of what is missing in the input data.

2.3.6 Model evaluation metrics

Summarising the results obtained through CV, can be done using various metrics. This section discusses a few metrics useful for evaluating the accuracy and efficiency of the kriging models.

The Mean Error (ME) can be used to give an indication of the bias of predictions, i.e. it determines if the model is more likely to under-predict or over-predict. The ME is calculated using equation 2.29.

$$ME = \frac{1}{n}\sum_{i=1}^{n}(Z_{CV,i} - Z(\mathbf{s}_i)) \tag{2.29}$$

, where n is the number of samples, $Z_{CV,i}$ is the predicted value and $Z(\mathbf{s}_i)$ is the corresponding sample value. Using similar notation, the Mean Absolute Error (MAE) and

Root-Mean-Squared Error (RMSE) are determined through equations 2.30 and 2.31.

$$MAE = \frac{1}{n}\sum_{i=1}^{n}|Z_{CV,i} - Z(\mathbf{s}_i)| \tag{2.30}$$

The MAE calculation through equation 2.30 ignores under-prediction as well as over-prediction. It only considers the mean of all errors regardless of the direction of the errors.

$$RMSE = \sqrt{\frac{1}{n}\sum_{i=1}^{n}(Z_{CV,i} - Z(\mathbf{s}_i))^2} \tag{2.31}$$

Since the larger errors are given more weight by squaring the errors in the RMSE approach, the RMSE values also give an indication of the variance in the errors. For this reason, it is to be expected that the RMSE values will always be greater or equal to the MAE values.

The RMSE relative to the standard deviation (SD) of the input data is also considered using equation 2.32.

$$RMSE_{SD} = \frac{RMSE}{\sqrt{\frac{1}{n-1}\sum_{i=1}^{n}(Z(\mathbf{s}_i) - \overline{Z})^2}} \tag{2.32}$$

, where n is the number of samples and $\overline{Z}$ is the mean of all the samples. This is proposed to be a better representation of the actual performance of the model [63]. A similar method referred to as the model efficiency (EF) is proposed by the authors of [64]. The EF is determined using equation 2.33.

$$EF = 1 - \frac{\sum_{i=1}^{n}(Z_{CV,i} - Z(\mathbf{s}_i))^2}{\sum_{i=1}^{n}(\overline{Z} + Z(\mathbf{s}_i))^2} \tag{2.33}$$

The value of EF is desired to be as close to one as possible. In cases where EF is very close to zero, the authors of [65] found that the mean of the observations gives more reliable estimations than the model.

Pearson's correlation coefficient is used to determine if there is a linear relation between the predictions made and the true or baseline values. The formula used to de-

termine the correlation coefficient, r, is shown in equation 2.34 [66].

$$r = \frac{\sum_{i=1}^{n}(Z_{P,i} - \overline{Z_P})(Z_{T,i} - \overline{Z_T})}{\sqrt{\sum_{i=1}^{n}(Z_{P,i} - \overline{Z_P})^2}\sqrt{\sum_{i=1}^{n} Z_{T,i} - \overline{Z_T})^2}} \tag{2.34}$$

, where n again denotes the number of samples, $Z_{P,i}$ is a predicted value using CV and $Z_{T,i}$ is the corresponding true sampled value or baseline predicted values. $\overline{Z_P}$ and $\overline{Z_T}$ denote the mean of the values of the predictions and the baseline values, respectively.

2.4 Statistical sampling techniques

Quantitative statistical sampling techniques are divided into two groups: probability sampling and non-probability sampling. Figure 2.5 illustrates some important terminological definitions when dealing with sampling.

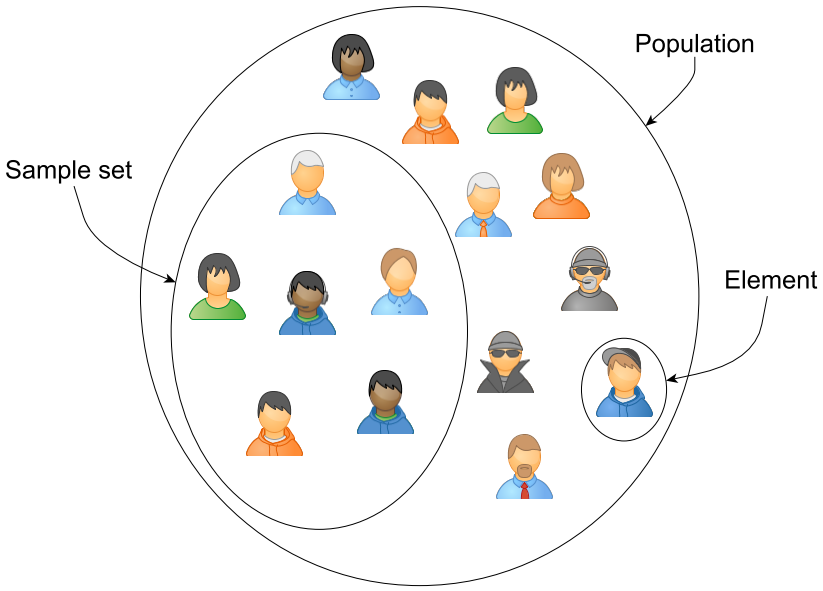

Figure 2.5: Important sampling terminology

When sampling data, the samples (or observations) are taken out of the population which is all possible items that possess the property of importance to the analysis.

Each item within the population is known as an element, and the group of elements used for the analysis is called the sample set.

2.4.1 Probability sampling

Probability sampling is sampling approaches in which each element in the population has the same probability to be chosen for the sample set. A brief description of the four most popular probability sampling approaches follows [67].

1. Simple random sampling:
   Simple Random Sampling (SRS) is implemented exactly as the name suggests. Depending on the nature of the analysis, each element can be assigned a number, and the sample set could be selected using a random number generator. Either way, the sample set selection is totally random.

2. Systematic sampling:
   A systematic approach is used to select samples. This is done by selecting a starting point or initial sample and then continuing by selecting every n-th element after that for the sample set.

3. Stratified sampling:
   In stratified sampling, the population is divided into different groups according to a single property each group shares. These groups or subsets are called strata [66]. This is followed by any other sampling approach to select elements out of each group for the sample set.

4. Cluster sampling:
   Cluster sampling is similar to stratified sampling in that the population is also divided into groups sharing a property, but these groups are known as clusters [66]. The difference for cluster sampling is that one or more of the groups are chosen as the sample set using another approach such as SRS.

2.4.2 Non-probability sampling

Contrary to probability sampling, some elements are more likely to be selected for the sample set when using non-probability sampling approaches. These approaches are common when people are the subject of the statistical analysis. A few non-probability sampling approaches are briefly described below [68].

1. Convenience sampling:
   In this approach to sampling, the samples are selected mainly due to their convenient accessibility to the researcher. Although the sampling is biased, it does have some advantages for certain types of research experiments.

2. Purposive sampling:
   Also referred to as judgemental or selective sampling, this method consists of many different variations. The samples are selected by focusing on particular characteristics of the population that would have the best chance, according to the researcher, of answering the research question.

3. Quota sampling:
   In quota sampling, the population is divided into subgroups according to certain characteristics. The proportions of the subgroups in the population are taken into consideration when sampling to ensure that each subgroup is proportionally represented in the sample set.

4. Snowball sampling:
   This sampling technique is only possible when human subjects are being sampled since the sampled subjects are asked to refer the researcher to other possible subjects.

2.4.3 Preferred sampling approach for kriging

Considering the kriging assumptions discussed in 2.3.1, the calculation of the semivariogram using equation 2.23 and the different sampling techniques discussed in section 2.4, the preferred method is concluded to be Simple Random Sampling. This preference is motivated by the findings of the authors of [54] that the effects of different sampling patterns on the performance of kriging, are quite insignificant. The authors of [69] also found marginally smaller prediction errors, using random sampling. Thus, the SRS approach is chosen mainly for its advantages for practical implementation.

SRS also provides value and location independent sampling with a greater variety of separation distances between sampling locations which should make for a very accurate experimental semivariogram. The SRS method is unbiased with the only exception of ensuring that the samples are representative of the entire area of interest since the kriging methods are designed for interpolation rather than extrapolation.

2.5 Geographic coordinate system

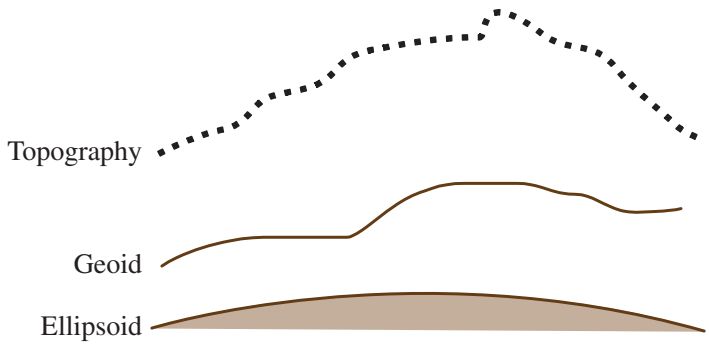

Figure 2.6: The Earth's main geodetic surfaces [57]

The shape of the Earth has demanded continuous research since the days when man started exploring different continents and drawing maps. The actual shape of the surface is quite irregular, as shown by the topography in figure 2.6. However, for most cal-

culations, can be approximated to a reference ellipsoid [57]. The third surface shown in figure 2.6 is the geoid which is the best approximation of the level of the Earth's oceans [70].

The location of a point on the Earth's surface is described in terms of latitude and longitude which are collectively referred to as the point's geographic coordinates. The latitude is referenced to equator. Figure 2.7 illustrates how the geographic coordinates are calculated.

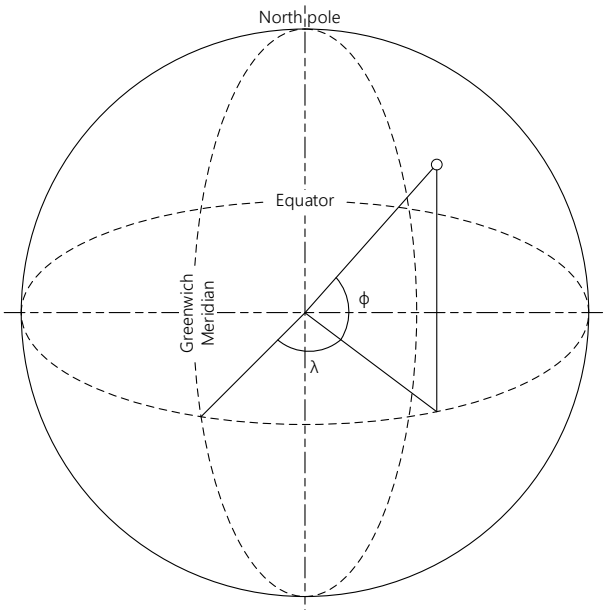

Figure 2.7: Geographic coordinates [70]

Thus, the latitude, ϕ, is determined by finding the angle between the equatorial plane and the line that passes through a point and which is perpendicular to the reference ellipsoid. The longitude, λ, is given by the angle between the meridian passing through the point and the reference meridian [70].

2.6 Universal Transverse Mercator coordinate system

The UTM system is a coordinate projection system that is used to produce a fairly accurate depiction of the Earth's ellipsoidal surface as a flat, two-dimensional surface. The Earth is divided into 60 longitudinal zones starting from 180 degrees West. The zones are 6 degrees wide and are known as UTM zones.

The longitudinal UTM zones are further vertically divided into 8 degree zones stretching from 84 degrees North to 80 degrees South, with the exception of the most northerly zone (zone X) which is 12 degrees in latitude. These zones are denoted by the letters C to X, only leaving out I and O to prevent possible confusion with the numbers 1 and 0. South Africa is covered in its entirety by ten UTM tiles, eight of which are the H and J tiles of UTM zones 34 to 36. The northern part of the Limpopo province lies in 35K and 36K.

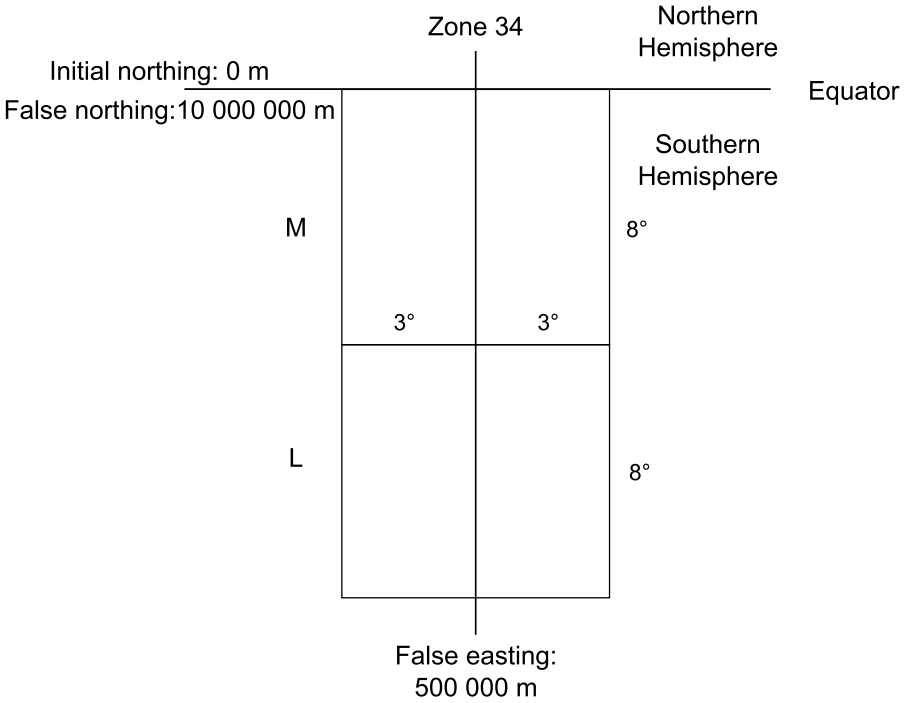

Figure 2.8: UTM zone illustration

The UTM system defines coordinates in the unit of metres. Figure 2.8 illustrates a few core aspects of UTM zones. The system uses the terms northing and easting as opposed to latitude and longitude.

The northing of a position increases when moving in the northern direction. Likewise, does the easting increase when moving in the eastern direction. Figure 2.8 shows that each UTM zone's meridian is designated by a false easting of 500 000 metres. The equator is designated by both an initial northing of zero metres for the northern hemisphere and 10 000 000 metres for the southern hemisphere.

The fact that the UTM system defines coordinates in terms of metres makes it quite an appealing and popular choice for applications using spatial interpolation techniques such as kriging.

2.7 Related Work

Kriging has enjoyed increasing attention in the field of radio environment mapping in recent years [5, 69, 71–76]. It has especially been investigated in applications for mapping TV white space [5, 77–79]. The authors of [5, 69, 71, 72, 77–79] all investigate the use of OK for generating REMs and find that it produces promising results.

Alaya-Feki et al. [5, 75] proposed OK as a tool for interference cartography with the aim of secondary spectrum usage. The authors found the power of OK to lie in the low sample density required to provide a viable solution for accurate interference mapping.

The authors of [69] conducted an investigation into the use of three spatial interpolation techniques for generating REMs for indoor and outdoor scenarios. The results showed that, although OK necessitates the highest computational intensity, it produced the lowest relative MAEs in both cases. It was also found that OK performs better for outdoor prediction of received power than in indoor environments.

Phillips et al. investigated the effectiveness of OK in coverage mapping of a 2.5 GHz WiMax network in [71, 76]. The authors used a gridded sampling approached with a one hundred metre spacing, and predicted WiMax coverage and performance on the University of Colorado campus.

Phillips found that the performance of kriging is superior to other measurement-based methods. This statement followed results showing a reduction of up to 10 dB in the prediction errors produced by kriging. It was concluded that the small amount of samples required by kriging and its robustness and scalability reveals the true value of kriging in radio environment mapping.

Achtzehn et al. found that OK produces consistently accurate predictions with a MAE of approximately 5 dB for very small and large areas [77,79]. From the experiment conducted in [77], it was also concluded that OK produces accurate coverage prediction for TV networks with multiple transmitters.

Ojaniemi et al. proposed an optimal field measurement technique when using kriging for radio environment mapping [80]. The same authors also investigated the use of kriging to update a geolocation database used for white space devices in [78].

This study expands the research into the application of some other variations of the kriging family in radio environment mapping. The use of OK is motivated by the little information required to implement it, in most cases. The availability of additional, possibly explanatory, data required for UK and RK provides the opportunity to investigate the efficiency of these two methods in radio environment mapping.

2.8 Conclusion

This chapter gave a brief overview of the fundamentals of radio wave propagation and investigated the implementations of two conventional propagation models namely, the Longley-Rice ITM and the ITU-R P.1546. A discussion on the proposed solutions, OK, UK and RK, was conducted in terms of the data required and the steps that need to be followed for implementation of the technique. This chapter also considered different sampling techniques, coordinate systems of interest and related work.

Chapter 3

Design

In this chapter, the different aspects of designing the experiment in which kriging is evaluated as a tool for radio environment mapping, are discussed. Section 3.2.1 proposes a procedure for randomly selecting TV broadcasting sites. This is followed by a discussion of the experimental flow of the implementation in section 3.2. The chapter ends off with a discussion of different experimental parameters taken into account and conclusions regarding their effect on the kriging prediction results.

3.1 Flow diagram syntax

There are many different methods for referencing and discussing flow diagrams. This section serves to define the flow diagram syntax used in throughout the dissertation.

The flow diagrams to be discussed in this chapter are referenced within the text by using similar syntax. Each functional block is labelled with a unique number. Since there are functional blocks of which the flow within the blocks are expanded in subsequent sections, each level of flow is denoted by a new level of sub-numbers.

The highest level of flow is denoted by {x.0}, where x is the unique integer assigned to each block. The second level is denoted by {x.y}, where x is the block that is expanded and y is a unique integer assigned to each block in this level. The flow diagrams discussed in the following sections follow this syntax and is expanded only to the third level which is denoted by {x.y.z}.

3.2 Logical flow of experiment

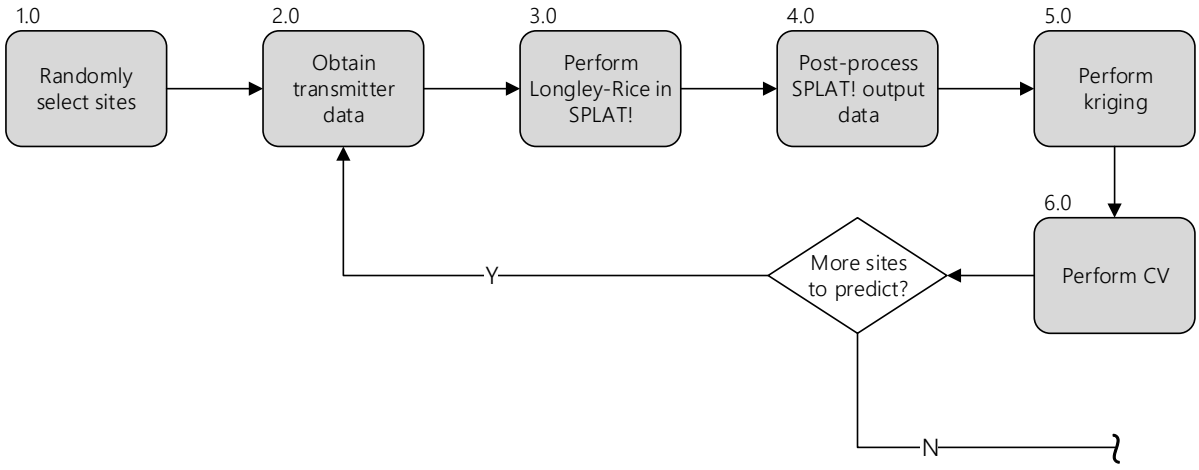

Figure 3.1: Logical flow: Experiment

The execution of the proposed experiment requires completion of the six phases shown in figure 3.1. Each phase is represented by a functional block. Firstly, a number of sites are randomly selected {1.0}. The data required to perform the Longley-Rice ITM for each randomly selected site is then obtained {2.0}. This process is discussed in section 3.2.2. Thereafter the Longley-Rice ITM can be implemented {3.0}.

SPLAT! produces the prediction results in a data file formatted as discussed in section 4.1.3. This data file requires some post-processing {4.0} before it can be used to perform kriging {5.0}. After the SPLAT! data file is processed, kriging can be performed, and the kriging model can be validated through CV {6.0}.

3.2.1 Random site selection

The first phase in conducting this experiment requires the selection of a number of sites in a random fashion. The site refers to a TV broadcasting station of which the coverage measurements will generated and used for kriging. The procedure for the random selection is shown in figure 3.2.

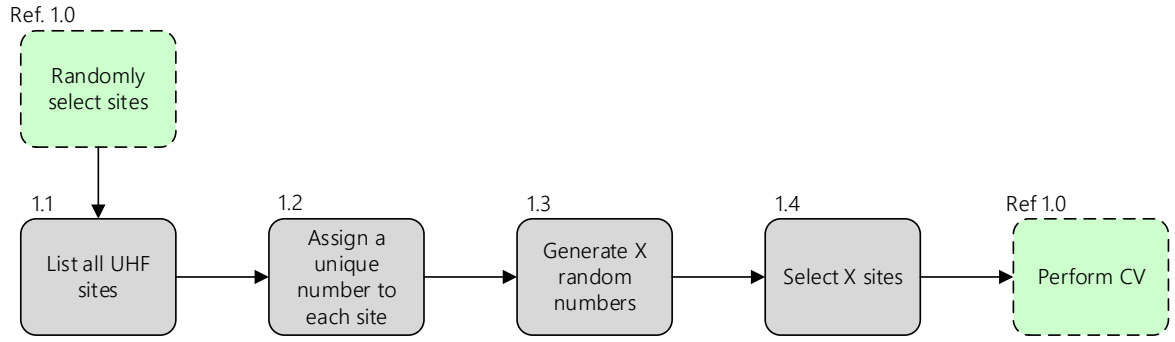

Figure 3.2: Logical flow expansion: Experiment, Block 1.0

Since the performance of kriging for the UHF TV band is being investigated, the random selection is initiated by listing all sites of which the first channel is a UHF channel {1.1}. Each site is then assigned a unique integer between one and the total number of sites listed{1.2}.

If X random sites are required, X random numbers are generated in {1.3} from a pool containing the range of the numbers assigned to the sites in {1.2}. This random number generation is done in R using the *sample* function provided by the *sampling* package [81].

Finally, the X sites associated with the random numbers generated are selected as the random sites {1.4}. This method of selecting sites is used in all cases where a random selection of sites is required and each site is investigated separately neglecting the possible effects of other surrounding sites.

3.2.2 Obtain transmitter data

As stated in section 4.1.3, SPLAT! requires two input files containing information regarding the transmitting station. Thus, obtaining the required transmitter data consists of two phases, as shown in figure 3.3. The transmitter's name, latitude, longitude and its antenna height AGL are extracted from the TV broadcasting transmitter database to create the site location (QTH) file {2.1}.

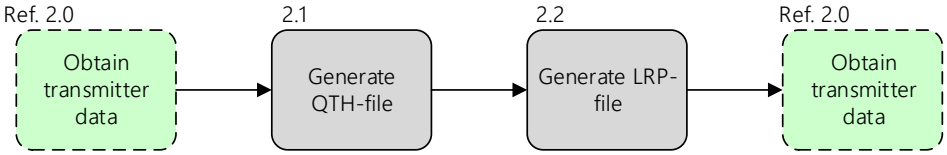

Figure 3.3: Logical flow expansion: Experiment, Block 2.0

An LRP file with default ITM parameters is provided by SPLAT!. The channel frequency, polarisation and ERP in the default LRP file are modified for each particular transmitter and channel {2.2}. These parameters are also obtained from the TV broadcasting transmitter database discussed in section 4.2.

3.2.3 Kriging implementation

The flow of implementing kriging is illustrated in figure 3.4. Building the kriging model {5.0} requires sample data that can only follow when SPLAT! has produced the results of the Longley-Rice ITM. The kriging phase starts by loading the ITM results {5.1}. In section 2.3, it was stated that kriging requires the Euclidean distances between sample locations. Therefore, the geographic coordinates of the locations predicted by SPLAT! need to be transformed to UTM coordinates {5.2}. The random selection of samples {5.3} can then follow.

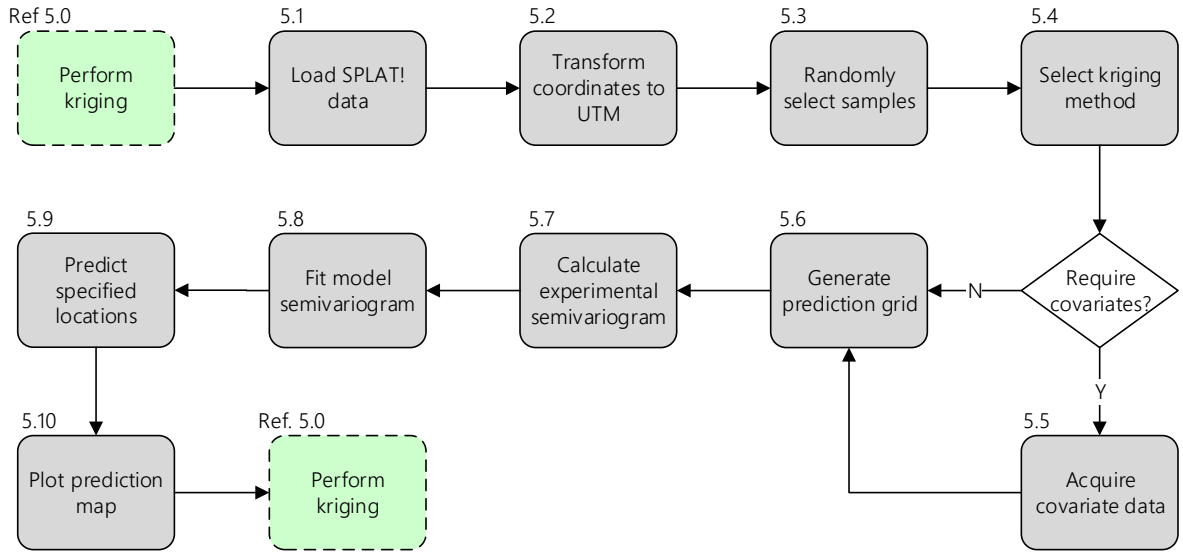

Figure 3.4: Logical flow expansion: Experiment, Block 5.0

For the selection of samples, the sample set size need to be specified which should naturally be less than the number of points predicted by SPLAT!. The selection of the kriging method {5.4} to be used can then continue. This requires a choice between the options of OK, UK and RK.

Should UK or RK be selected, covariate data is required to fit a regression function to the trend in the sample data. The acquisition of covariate data {5.5} comprises of not only obtaining covariate data for the sample locations, but for the locations to be predicted as well. Thus, covariate data for the entire area of interest is required as will be discussed in section 3.2.4. The acquisition of covariate data is not required if OK is the selected kriging method to be implemented.

Before the kriging method can be implemented with the purpose of mapping the area of interest, the locations that are to be predicted need to be specified in a gridded format {5.6}. Although the sampling is done randomly, a prediction grid covering the area of interest is required for an accurate contour plot of the predicted received power. In the case of OK, the prediction grid should consist only of the gridded locations. For

the implementation of UK and RK, the required covariate data should be added to the gridded prediction locations.

After the prediction grid is generated, the experimental semivariogram can be calculated {5.7} as discussed in section 2.3.2 and model semivariogram can be fitted {5.8}. The fitted model semivariogram can then be used to determine the kriging weights for each location and predict the values of the target variable {5.9} at all the locations specified in the prediction grid.

Finally, the predicted values can be used to plot a prediction map {5.10} of the results and the model can be validated using CV {6.0}.

3.2.4 Covariate selection

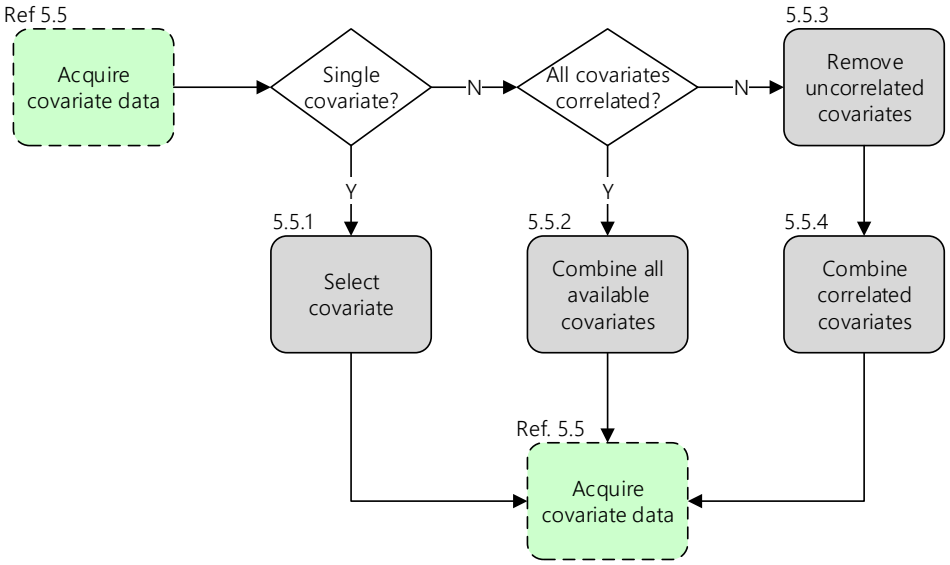

Figure 3.5: Logical flow expansion: Perform kriging, Block 5.5

As briefly mentioned in section 2.3.4, UK and RK both use covariates as additional predictors in the attempt to improve the accuracy of the predictions. Covariates are also referred to as explanatory variables [50].

The covariates selected for a certain situation mainly depends on the availability of information for the area of interest and the correlation between the covariate and the variable for which the kriging predictions are required. The variable predicted using the kriging method is also known as the target variable, which in this case is the received power.

Figure 3.5 describes the flow of covariate selection. If a single covariate is required for the implementation of UK or RK, the applicable covariate data is obtained for the sample and prediction locations {5.5.1}. In the case where all the available covariates show correlation with the target variable, a combination of all the covariates is used {5.5.2}. Finally, if only some of the available covariate data show a correlation with the target variable, the uncorrelated covariates are not considered {5.5.3}, and a combination of the correlated covariates are used {5.5.4}.

3.2.5 Cross-validation design

The implementation of the kriging model needs to be evaluated as mentioned in section 2.3.5. Figure 3.6 illustrates the logical flow for the implementation of k-fold CV {6.0}.

For k-fold CV, the sample set is loaded {6.1} and needs to be divided into k equally sized subsets {6.2}. Each iteration extracts one of the subsets as a validation set {6.3} until all samples have been used for validation. The remaining $k-1$ subsets are also extracted and used as a training set {6.4}. The training set can then be used to calculate the experimental semivariogram and fit a model semivariogram {6.5} similar to the phases {5.7} and {5.8} in section 3.2.3.

The target variable at locations of the single subset kept apart for validation, are then predicted {6.6} using the semivariogram fitted to the training set. The predicted values are then compared to the actual sampled values of the validation set using error

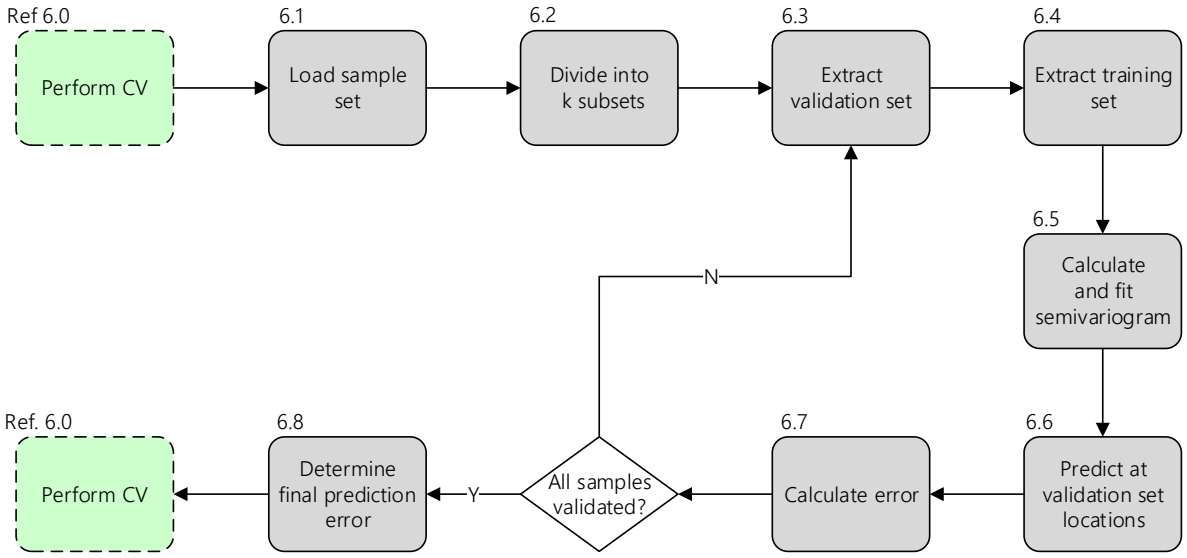

Figure 3.6: Logical flow expansion: Experiment, Block 6.0

functions {6.7}. Finally, after all samples have been used for validation, the calculated prediction errors are summarised to quantify the accuracy of the kriging model {6.8}.

3.3 Considerations

This section considers variables in the study to be conducted. Firstly, different spatial interpolation techniques are investigated in order to justify the use of kriging in this particular case. Secondly, experiments are conducted in order to determine the effect of the prediction error made by the Longley-Rice ITM, the sampling density and the prediction radius, on the results produced by kriging.

3.3.1 Spatial interpolation techniques

Considering the large number of spatial interpolation techniques available today, the use of kriging in this particular case requires some form of justification. The authors of [12] performed an extensive review on spatial interpolation techniques for applica-

tions mainly in the field of environmental science.

Spatial interpolation techniques are divided into three categories. These categories are non-geostatistical, geostatistical and combined methods. As the name suggests, the combined methods use a combination of techniques that fall into the first two categories. The geostatistical techniques are further subdivided into univariate and multivariate techniques based on the amount of information required for their implementation.

Some of the most popular non-geostatistical spatial interpolation techniques include Inverse Distance Weighting (IDW), linear regression models and splines while most of the geostatistical techniques are variants of kriging [12]. Should it be necessary, selection of the appropriate interpolation can be done using various proposed decision trees [12,50,82].

Non-geostatistical techniques

The popularity of IDW and Thin Plate Splines (TPS) demands consideration. A brief description of these techniques follows.

IDW, similar to kriging, uses a weighted linear combination of sampled values to interpolate to a unsampled value. These weights are are calculated by the inverse function of the distance between the interpolated value and the sampled values shown in equation 3.1.

$$\lambda_{\mathbf{s}_i} = \frac{1/d_{\mathbf{s}_i}^p}{\sum_{i=1}^{n} 1/d_{\mathbf{s}_i}^p} \tag{3.1}$$

, where $\lambda_{\mathbf{s}_i}$ is the weight given to the sampled value at the location $\mathbf{s}_i$, $d_{\mathbf{s}_i}$ is the distance between the location of the interpolated value and the location $\mathbf{s}_i$, p is a power parameter and n is the number of sampled values. The accuracy of IDW is mainly affected by the power parameter [49].

Using the decision tree developed by the authors of [12], IDW is a good option when the input data shows no spatial data structure, no secondary or explanatory variables are available, no abrupt estimation is allowed and distance is the determining factor of the value of the interpolated variable. Abrupt estimation refers to a discrete interpolated surface rather than a smooth surface.

While IDW is a univariate interpolation technique, TPS provides the option of multivariate use. Multivariate techniques can use auxiliary data to aid in the interpolation accuracy. TPS is a deterministic spatial interpolation technique which also provides a smooth interpolated surface [83]. This technique is not as computationally intensive as other spatial interpolation techniques and is quick to implement.

TPS is preferred when no error estimation is required, and a smooth local prediction surface is required with the possibility of using explanatory data.

Advantages and disadvantages of kriging

Through the investigation of kriging as an interpolation technique, it is found that kriging, like any other spatial interpolation technique, has its set of advantages and disadvantages. It is, therefore, necessary to determine the influence of these characteristics on the particular application of the method.

The first advantage that kriging has over IDW and TPS is that it is a stochastic interpolation technique. Thus, in addition to the predictions made, it provides an assessment of the uncertainty of the predictions through the kriging variance. It is an exact interpolator since the predicted values at sampled locations are equal to the sampled values [12].

The performance of kriging is almost unaffected by the sampling pattern while TPS is found to perform quite poorly when using irregularly spaced sample data [54, 84].

Finally, kriging provides the best linear unbiased prediction. It is, therefore, known as the optimal predictor provided all the input data requirements are met and is robust enough to perform well even when these requirements are not met [50].

Some drawbacks of kriging are that the definition of the best fitting semivariogram and the computational intensity of the predictions could sometimes be time-consuming. Furthermore, the assumption of spatial stationarity is violated more often than not but as previously mentioned this violation does not prohibit the use of kriging. Finally, in some application domains the minimum requirement of about 100 to 200 samples [50,85] is a disadvantage but in the field of radio environment mapping this is not out of the ordinary and not necessarily a disadvantage as such.

3.3.2 Longley-Rice ITM prediction variance

The theoretical and practical prediction errors made by the Longley-Rice ITM, discussed in section 2.2.2, motivates an investigation into the affect that these errors have on the performance of a kriging model when using the ITM prediction as measured samples.

Considering a prediction error of 10 dB [20], it is assumed that each value predicted by the ITM is the expectation or mean value of a normal distribution characterised by a standard deviation, σ, of 10 dB. Thus, the actual value at that specific location, if physically measured, will most probably be very close to the mean but could lie anywhere within the range of the normal distribution.

Therefore, in order to investigate the effect of this possibility, the prediction error is introduced to the input of the kriging model. Rather than using the SPLAT! output of the Longley-Rice ITM as is, each sampled value is used as the mean of the normal distribution with $\sigma = 10$ dB. A random value from that particular normal distribution is selected using the *normrnd* function in MATLAB, which is then used as the simulated

measurement value. The results of the comparison between the SPLAT! input data and the simulated measurement data is shown in figure 3.7.

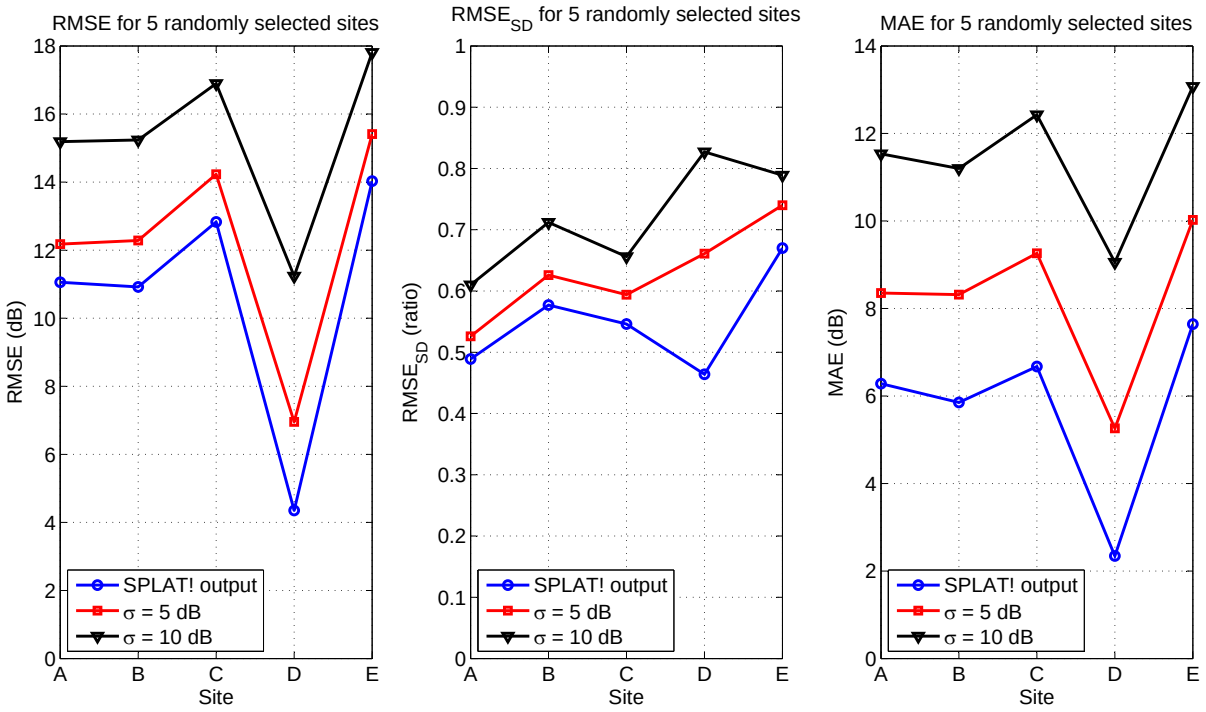

Figure 3.7: Comparison of using direct SPLAT! output and simulated measurements

The experiment is done for five randomly selected sites, using the random selection process discussed in section 3.2.1. Refer to table B.1 in appendix B for all information regarding the randomly selected sites. Figure 3.7 shows a clear correlation between the predictions made using the three different sets of input values, namely the unadjusted SPLAT! output data, values randomly selected from a normal distribution with $\sigma = 5$ dB and values randomly selected from a normal distribution with $\sigma = 10$ dB.

It is evident that, though the predictions are well correlated, the results obtained from using the unadjusted SPLAT! data consistently perform better. This can be explained by the difference in the standard deviations of the three input data sets. Table 3.1 shows the standard deviations of the input data sets. As expected, the input data set with the lowest variance in its values produce the best results.

Table 3.1: Sample set standard deviations for 5 randomly selected sites

	Sample set standard deviation (dB)		
Site	SPLAT!	$\sigma = 5$ dB	$\sigma = 10$ dB
A	22.606	23.155	24.906
B	18.936	19.619	21.396
C	23.483	23.937	25.766
D	9.373	10.515	13.589
E	20.047	20.837	22.564

These results show that the OK model prediction accuracy shows a slight decrease when the measured values show greater variance. It should also be mentioned that the high prediction errors produced by the OK model is mostly due to the low sampling density used for this test, i.e. approximately one sample for every eight hectares. The low sampling density was used due to limited time since greater sample sets exponentially increase the execution time of the kriging process. The low-density sample sets were also sufficient to draw a conclusion regarding this specific consideration.

It should also be considered that the theoretically simulated measurements could exaggerate the variance in measurements should the case be, for example, that the Longley-Rice ITM consistently over-predict for a site and some of the values are randomly selected from the upper half of the normal distribution. This could lead to the simulated measurement value being more than 10 dB higher than the actual value at that location. This scenario is illustrated by equation 3.2.

$$\begin{aligned} P_{actual} &= x \text{ dBm}, \\ P_{ITM} &= x \text{ dBm} + 7 \text{ dB}, \\ P_{sim} &= P_{ITM} \text{ dBm} + 8 \text{ dB} \end{aligned} \tag{3.2}$$

, where P_{actual} is the real or true received power at a certain location, P_{ITM} is the received power predicted by the ITM for the same location and P_{sim} is the simulated received power measurement. Thus, the simulated measurement for this scenario, P_{sim}, is 15 dB higher than the actual received power, P_{actual}. The possibility, therefore, exists that the simulated measurements could produce unrealistic values.

That being said, simulating measurements with $\sigma = 5$ dB still produce MAEs of less than 10 dB. It can thus be concluded that the prediction error of the Longley-Rice ITM could have a slight effect on the accuracy of the kriging model though the effect is not too significant.

3.3.3 Effect of prediction radius and sample density

In order to effectively investigate the potential that resides within the kriging methods to produce accurate REMs, it is necessary to determine the extent to which the size of the prediction area and the sampling density, affects the results. Once again, five randomly selected sites were chosen for this investigation using the process discussed in section 3.2.1. Refer to table B.2 in appendix B for all information regarding the randomly selected sites.

In investigating each of these sites, the Longley-Rice ITM was implemented for a prediction radius of 1 km, 2 km, 3 km, 4 km, 5 km, 10 km and 15 km. From each prediction radius of each site, values were sampled at densities of one sample per eight ha, one sample per four ha, one sample per two ha and one sample per ha. The maximum sampling density of one sample per ha is limited by the density of predicted points produced by SPLAT!. Table 3.2 numerically describes the sampling densities in terms of the actual number of samples rounded to the nearest ten. The area in ha is calculated using equation 3.3.

$$A = \pi \times r^2 \times 100 \tag{3.3}$$

, where A is the area in ha and r is the prediction radius in km. It should be mentioned that the use of the "per hectare" convention for describing the sampling densities does not refer to a gridded sampling approach. It is a mere indication of the total number of samples taken for a given prediction area. The sampling approach used for this investigation is SRS as discussed in section 2.4.3.

Table 3.2: Sampling densities per prediction radius

Prediction radius (km)	Area (ha)	Number of samples			
		1 per 8 ha	1 per 4 ha	1 per 2 ha	1 per 1 ha
1	314.16	40	80	160	320
2	1256.64	160	320	630	1260
3	2827.43	350	710	1410	2820
4	5026.55	630	1260	2510	5020
5	7853.98	980	1960	3930	7850
10	31415.93	4290	8590	17180	31410
15	70685.83	9440	18960	37450	70680

Following the random sample selection, with the sample densities shown in table 3.2, for each of the five randomly selected sites, the OK model and CV procedures discussed in sections 3.2.3 and 3.2.5 were implemented. Figure 3.8 shows the consequent results.

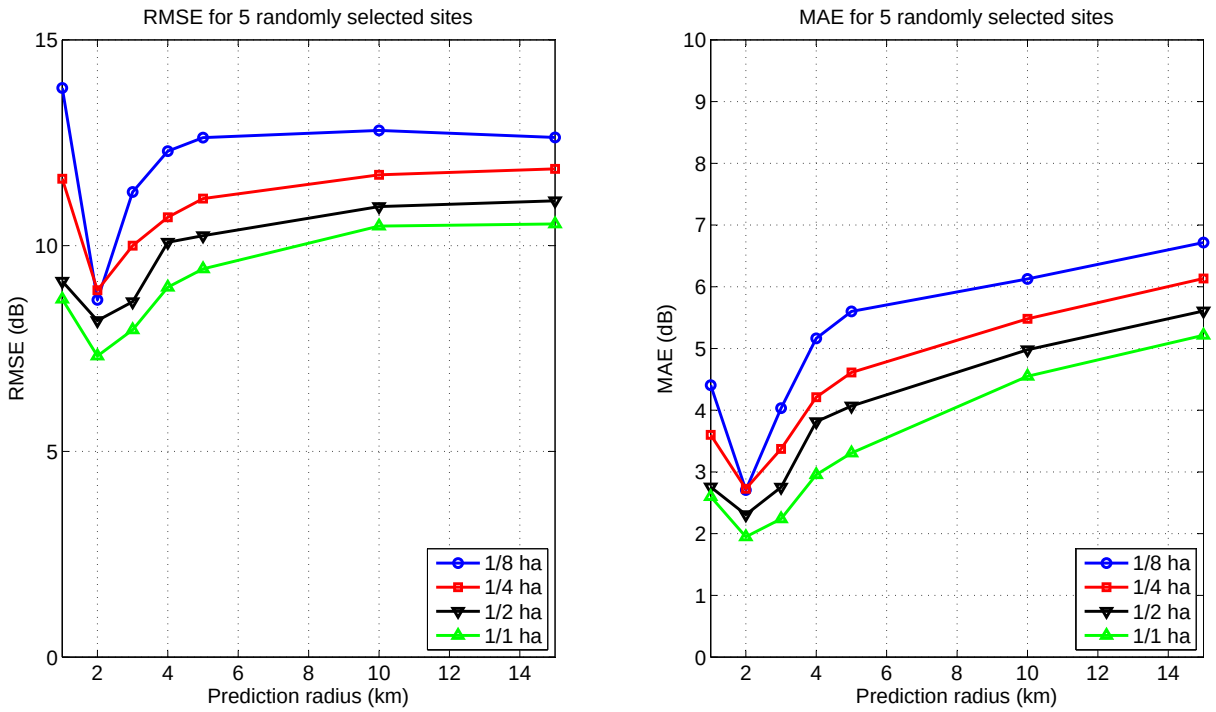

Figure 3.8: Effect of prediction radius and sample density on OK accuracy

The prediction errors shown in figure 3.8 firstly indicates that the OK model consistently performs better as the sample density increases. Although the prediction accuracy clearly increases with higher sampling densities, the increase seems to be approximately 1 dB while the number of samples required, doubles.

It is also evident from figure 3.8 that the prediction accuracy does not degrade significantly as the prediction radius increases. The results show that the prediction errors vary by approximately 3 dB, which is quite insignificant considering that the prediction area almost doubles with each increment of prediction radius.

It can, therefore, be concluded that both the prediction radius and the sample density have minimal effect on the prediction accuracy of the kriging model. Granting the fact that there is a clear increase in accuracy as the sample density increases. This also proves the statement made in section 2.4.3 that the most important requirement of the sample data is for it to be representative of the entire area of interest.

Thus, for any prediction radius the deciding factors are the available time and data. The experimental parameters are, therefore, dependent on the time available for generating the kriging predictions, the time available to physically measure sample data or obtain available data and the amount of sample data that is available.

3.3.4 Effect of using a single covariate

Considering the available covariate data, it is important to determine which of the covariates has the largest positive effect on the prediction accuracy. This section discusses different methods of obtaining covariate data, the available data in this particular case as well as the results obtained from using each of the available covariates separately in the implementation of UK.

Acquiring covariate data

Covariate data for an experiment can be obtained in three ways, depending on the specific covariate. The first option, if possible, is to measure the value of the covariate while measuring samples of the target variable. This method could require expensive equipment and could also be very time-consuming since covariate data are required for the sampled locations as well as all locations that are to be predicted.

Secondly, and most preferably, if the covariate data is available in an accessible database, it can be extracted from the database. This can potentially be very time-efficient, while problems could arise should data for the exact sampled locations not be contained within the database.

Finally, some covariate data may be calculated. This will be possible in a case where, for example, the distances of the locations from a specified reference point are used as a covariate. Since the locations of the sampled measurements as well as the location that are to be predicted are known, the distances from the reference point can be calculated.

Available covariates

The most restrictive aspect in selecting a covariate is obviously the availability of data. By using SPLAT! to generate the sample data, some possible covariate data are also produced. As described in section 4.1.3, the SPLAT! output file provides the azimuth referenced to true North, and the elevation to the first obstruction along with the received power for each predicted location.

Since the locations of the samples as well as the locations where predictions are to be made are known, the locations can also be used as a covariate. This leads to another possibility. The knowledge of the sampling and predictions locations and, in this case, the location of the TV broadcasting transmitter, makes it possible to deter-

mine the distance of each location from the transmitter. This could prove to be a useful covariate for this situation considering the inverse square law mentioned in section 2.1.

Thus, the available covariates are as follows:

- Azimuth referenced to true North
- Elevation to first obstruction
- Sample and prediction point location
- Distance from transmitter

Results

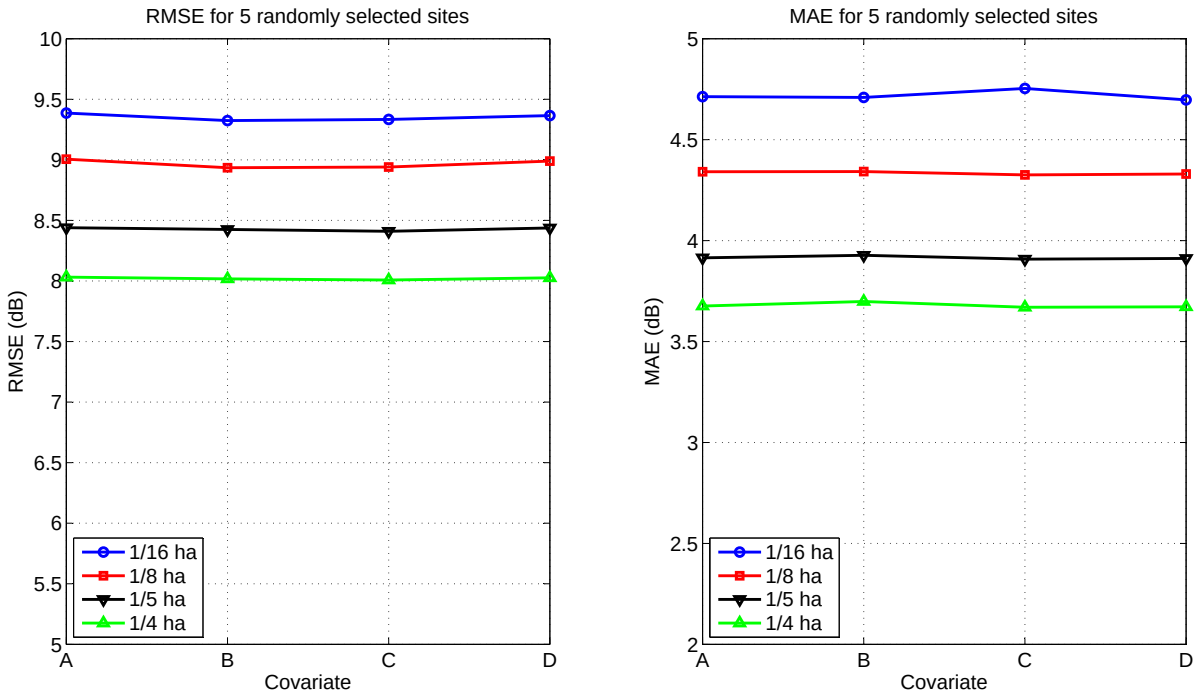

Figure 3.9: Comparison of prediction error using different covariates

The value of each covariate for the use of predicting received power is evaluated by implementing UK using each covariate separately. The same sample set is used in all four cases of covariates, and the results are evaluated and compared using CV.

Figure 3.9 shows the results after comparing the four different covariates for five randomly selected sites using four different sampling densities for a prediction radius of 5 km. Refer to table B.3 in appendix B for all information regarding the randomly selected sites.

It is evident from figure 3.9 that all the covariates produce similar prediction errors and that the accuracy of the predictions is more affected by the sampling density.

It can, therefore, be concluded that no single covariate produces better results than the others. A combination of these covariates might show a better correlation with the trend of the target variable and produce better results.

Using a combination of covariates

Both UK and RK provide the ability to use a combination of covariates rather than a single covariate. The best combination of covariates is determined by fitting linear models to all covariate data and by using a stepwise algorithm provided by the *stats* package in R [86, 87]. This stepwise algorithm finally produces a formula describing the best combination of covariates along with the residuals of the fitted linear model. Since the covariates are combined in a stepwise fashion, uncorrelated covariates are excluded from the formula and the result will, therefore, be the most suitable covariate if there is no combination that will improve the predictions.

3.4 Conclusion

This chapter served as the conceptual design phase in the process of investigating the use of kriging methods for generating REMs. Different aspects with the potential to affect experimental results were considered. It was found that kriging provides some advantages over other spatial interpolation techniques and that the experimental parameter having the largest effect on prediction results is the sampling density. A proposed experimental flow was presented and discussed and in the implementation of UK and RK it was proposed that using a combination of the available covariates might be the best approach.

Chapter 4

Kriging model implementation

In this chapter, the implementation of the kriging methods is discussed. Section 4.1 provides a brief background on the simulation tools used for the implementation while section 4.2 describes the TV transmitter database used. Section 4.3 discusses all the requirements for implementing the Longley-Rice ITM in SPLAT!. Finally, the exploration of the kriging input data is discussed in section 4.4, and the implementation of the kriging methods in R concludes the chapter in section 4.5.

4.1 Simulation tools

The simulation tools that were chosen for this research project is MATLAB, R and SPLAT!. Each of these simulation tools shows characteristics required for this research to be successful. Since kriging is an interpolation technique used mainly in geographical applications and not very common in radio environment applications, the tools designed for radio wave propagation models do not necessarily provide capabilities for implementing techniques such as kriging.

It was found that the best platform for implementing the kriging technique in this case, is R. The other two tools (MATLAB and SPLAT!) were chosen for validation and verification of the results obtained from the kriging implementation in R because of their popularity and specialised capabilities. A detailed discussion of these tools follows.

4.1.1 MATLAB

MATLAB was chosen because of its popularity, power and versatility. For this research application, a kriging toolbox called ooDACE [88,89] will be used. This toolbox implements the "Gaussian Process based Kriging surrogate models" [90]. ooDACE [88,89] is capable of implementing ordinary kriging, co-kriging, blind kriging and stochastic kriging. When implementing ordinary kriging, three different plots are obtained as output. These are two contour plots showing the estimated values and the variance and a landscape plot which shows the final interpolated values of the interpolated area.

4.1.2 R

R is a programming environment designed and created for statistical computing and graphics. It provides many different software facilities; from data handling and storage to graphical data display and analysis as well as simple and user-friendly programming syntax [13]. R is a very popular programming environment in geostatistics and its use is proposed by many authors [50,52,55].

Since the purpose of this study is to investigate kriging interpolation, the R packages of interest are *geoR* [91] and *gstat* [92]. These packages provide the implementation of kriging interpolation as well as the handling of geographical data such as coordinates and different coordinate systems. The *rgdal* package [93] is also required for the conversion of the geographical coordinates to UTM coordinates.

4.1.3 SPLAT!

SPLAT! is an acronym for an RF Signal Propagation, Loss and Terrain analysis tool. This tool implements the Longley-Rice ITM with enhancements, and one of its main applications is in analogue and digital television and radio broadcasting [94]. RF Signal Propagation, Loss and Terrain analysis tool (SPLAT!) is a very popular tool among researchers in the radio propagation field [94]. Interoperability with Google Earth also provides scaled and good quality graphical presentation of results.

In order for SPLAT! to implement the Longley-Rice ITM, two input files are required in addition to the digital elevation data describing the topography of the Earth's surface. These files are a site location file containing the broadcasting transmitter's name, its location in geographical coordinates and its height AGL, and an ITM parameter file. The parameter file defines all the input parameters required by the Longley-Rice ITM as discussed in section 2.2.1.

SPLAT! has different options for point-to-point predictions as well as point-to-area predictions. The output is given in the form of two text files; a portable pixmap (ppm) image and a data file.

The output file of importance is the alphanumerical data file. This file contains the boundaries of the analysed area as well as the coordinates, azimuths, elevations to first obstruction and the received power in decibel relative to one milliwatt (dBm) at that specific point [95]. Another file of interest to us is the *.dcf* (SPLAT! colour definition) file. This colour definition file assigns a Red Green Blue (RGB) colour value to each 10 dBm increment of received power and it is used to plot the ppm image which marks the transmitter location and shows the received power in dBm for the specified radius.

In this study, version 1.4.1 of SPLAT! is used.

4.2 TV broadcasting transmitter database

The data used for this research is provided by The Independent Communications Authority of South Africa (ICASA). In the past, the regulation and operation of telecommunication and broadcasting services were done separately. ICASA is the independent regulatory body established to regulate both the telecommunications, broadcasting and postal sectors, in 2000 [96]. The data contains information of all analogue and digital broadcasting stations in South Africa as given by the ICASA final terrestrial broadcasting plan of 2013 [97].

The database contains 745 transmitter stations in total and of each station information about its identification, position, transmitting and physical properties is given. Within the data, all the information required for the implementation of the propagation models is provided. The only information not given is the terrain detail required for the implementation of the Longley-Rice ITM.

4.3 Longley-Rice ITM implementation

As mentioned in section 4.1, SPLAT! is used to implement the Longley-Rice ITM in order to generate the samples for the kriging models. This section discusses the files required by SPLAT!, the command generation required for executing the point-to-area received power analysis in SPLAT! as well as the output files generated after execution and their importance in this particular case.

4.3.1 QTH and LRP file generation

Both the site location (QTH) and ITM parameter (LRP) files are generated in MATLAB. The TV broadcasting transmitter database discussed in section 4.2 is used to obtain the information required to generate a QTH file and an LRP file for each site. Detailed

examples of these files can be found in appendix A.

The QTH file is generated by extracting the site's decimal geographic coordinates as well as the antenna height AGL for the selected channel. Since the database contains multiple entries with identical site names, it was decided to designate each site entry numerically. Thus, the sites were named numerically with a number between 1 and 745.

The QTH file is, therefore, composed of the site's numerical name, its latitude and longitude, both in decimal format and the antenna height AGL.

The LRP file for each site is generated using the SPLAT! default LRP file. The parameter values required for this file are specific to the channel used and the terrain surrounding the site.

The channel information required for the LRP file is the channel frequency in MHz, the polarisation of the antenna and the ERP in watts. Since the ERP is specified in dB referenced to 1 W, a unit conversion of the ERP value to watt is done using equation 4.1.

$$y\ \mathrm{W} = 10^{x\ \mathrm{dBW}/10} \tag{4.1}$$

, where y is the ERP in watts and x is the ERP in dBW. The conversion shown in equation 4.1 is implemented by using the *db2pow* function provided by MATLAB. The remaining parameter values specified in the LRP file are obtained from the SPLAT! default LRP file.

When the Longley-Rice ITM is implemented, SPLAT! searches for an LRP file with an identical name to that of the QTH file with the only difference of the *.lrp* extension. Therefore, in generating the QTH and LRP files, they are given the same numerical site name generated for the QTH file. If an LRP file with the same name is not found, SPLAT! uses the default LRP file.

4.3.2 SPLAT! command generation

Since SPLAT! is a command-line driven program, a MATLAB script is created to generate a text file containing the SPLAT! commands to predict the received power for each site using the Longley-Rice ITM.

The following is an example of a command to execute the point-to-area propagation prediction for site 422:

```
splat -t 422.qth -L 10.0 -metric -R 4.0 -dbm -ano 422
```

The *-t* switch specifies that the site location file, *422.qth*, is to be used on this occasion. It is followed by the receiving antenna height through the *-L* switch along with the *-metric* switch indicating that the receiving antenna height and prediction radius, *-R*, is specified in metres and kilometres, respectively. Finally, the *-dbm* switch is required for a received power analysis while the *-ano* switch specifies the name of the output alphanumeric file discussed in section 4.3.3.

4.3.3 SPLAT! output files

In point-to-area prediction mode, SPLAT! always produces three output files. These files are a prediction map in ppm format, a colour definition file and a site report. The colour definition file defines the colour regions for the prediction map. The site report contains the sites location in geographic coordinates and its height above mean sea level (AMSL). Furthermore, it contains the antenna's heights AMSL and average terrain as well as height of the average terrain calculated toward the azimuth bearings of 0, 45, 90, 135, 180, 225, 270 and 315 degrees [95].

When prompted, SPLAT! produces an additional alphanumeric data file containing the every point predicted within the prediction radius. In addition to the geographic coordinates and the predicted received power of each point, this file provides the azimuth

of each point relative to the site and true North. This file also provides the elevation to first obstruction for each point.

4.4 Exploratory Data Analysis

When using any data type for experimental purposes, especially in geostatistics, it is important to understand and summarise characteristics of the data being used by performing statistical tests on the data. This process is referred to as Exploratory Data Analysis (EDA), and it may reveal structure and problems possibly existing in the data [98]. Many procedures of the EDA phase of an experiment, are done in the form of hypothesis tests.

A hypothesis is an assumption or claim being made regarding any number of characteristics of a population. These characteristics of interest can range from a measured parameter to the form of the distribution of the population [66]. Hypothesis tests are methods to compare two hypotheses (null hypothesis and alternative hypothesis) about a dataset using sample data. The outcome of a hypothesis test can either be that the null hypothesis is rejected or that it is not rejected. The following terminology are of importance when considering hypothesis tests:

- Null hypothesis, H_0: This is the assumption which is initially considered to be the truth. H_0 will only be rejected if the sample data strongly contradict the assumption. Otherwise, H_0 will be accepted as the truth.
- Alternative hypothesis, H_A: This contradicts H_0 and is assumed to be true if the null hypothesis is proven false.
- Type I error: This is the case in which the outcome of a test rejects H_0 when it is actually true.
- Type II error: This is when the result of the test erroneously does not reject H_0 when it is not true.

- Significance level: This is denoted by α and is the probability of making a type I error. This means that if $\alpha = 0.05$ is selected, a type I error will occur 5% of the time if the test is repeatedly executed.

The hypothesis test returns a p-value (also known as the observed significance level (OSL)) which is used to determine the outcome of the test [66]. The two aforementioned outcomes of the test is determined as follows:

- If $p > \alpha$: Sample data do not reject H_0.
- If $p < \alpha$: Sample data reject H_0.

4.4.1 Test for spatial autocorrelation

As briefly mentioned in section 2.3.1, spatial autocorrelation is a characteristic of spatial data which refers to how the data is spatially related. If the values of locations that are close to each other have more similar values than locations further apart, the data is said to be spatially autocorrelated.

The data is tested for spatial autocorrelation, using Mantel's test [99] in R. The test is implemented by generating two distance matrices. One matrix contains the distances between all sample locations and the other contains the distances (or differences) of the values for all pairs of sample locations. The relation between the two matrices is then used to arrive at a conclusion on the spatial autocorrelation of the data. The null and alternative hypotheses for Mantel's test [99] are:

- H_0: The two matrices are unrelated.
- H_A: The two matrices are spatially autocorrelated.

Thus, in order for the test to be successful rejection of H_0 is desired. Table 4.1 summarises the results of Mantel's test conducted on ten randomly selected sites. A sam-

ple set with a density of one sample per eight hectares is drawn from each of the ten sites, and these sample sets are tested for spatial autocorrelation through Mantel's test. Refer to table B.4 in appendix B for all information regarding the randomly selected sites.

Table 4.1: Results of Mantel's test for spatial autocorrelation at a 5% significance level

Site	1	2	3	4	5	6	7	8	9	10
Accepted hypothesis	H_A	H_0	H_A	H_A	H_A	H_A	H_A	H_A	H_A	H_A

The results of the test, shown in table 4.1, show that only one of the sample sets failed to reject the null hypothesis. The sample sets of the remaining nine sites successfully rejected H_0 and, thus, are spatially autocorrelated. It can, therefore, be assumed that the received power values to be investigated are spatially autocorrelated.

4.4.2 Test for spatial stationarity

Although second-order stationarity is a requirement for the data used, kriging can still be applied to non-stationary data. The model assumes that the data is stationary by assuming that a single fitted semivariogram describes the entire area of interest as discussed in section 2.3.1. The spatial stationarity of the input data is, therefore, assumed rather than physically tested.

4.5 Kriging implementation

The kriging models are implemented through various phases discussed in section 3.2.3. The actual implementation of each of these phases is discussed in this section. Sections 4.5.3 and 4.5.5 only apply to the implementation of UK and RK.

4.5.1 SPLAT! output data post processing

The alphanumeric data files produced by SPLAT! require some processing before they can be imported into R or MATLAB, as a matrix. This is due to the structure of these files. The first two lines of the file describe the bounding box of the prediction area, i.e. the minimum and maximum latitude and longitude values. These two lines appear as follows:

```
119, 117 ;max_west, min_west
35, 34   ;max_north, min_north
```

This is overcome by skipping the first two lines when importing the files into R. Secondly, SPLAT! indicates that the path between the transmitter and the predicted location is obstructed by adding an asterisk, *, at the end of the line as shown in the example below.

```
-32.7238565, 339.0887544, 5.496, -2.067, -72.400
-32.7528335, 339.0920919, 5.391, -6.830, -106.628 *
-32.7453798, 339.0912557, 5.391, -5.279, -65.434
```

This causes an inconsistent number of columns when importing the file to a matrix. Since the SPLAT! predictions are used as simulated measurements and when physically measuring these values one does not necessarily know the location of the transmitter, these asterisks are simply removed. After the removal of the asterisks, the alphanumeric files are ready to be imported into R for the sampling to be done.

4.5.2 Sampling

After the SPLAT! output data file is processed, and it is imported to a matrix in R, the received power values are sampled. Since each predicted point occupies a row, the row indexes are used to sample the values.

In order to determine the range within which the random number generator should operate, the number of rows in the SPLAT! data matrix is determined. The number of values to be sampled is determined by the selected sample density. This is done using equation 4.2.

$$\text{Number of samples} = \text{Prediction area (ha)} \times \text{Sample density} \tag{4.2}$$

, where the sample density is given as $1/x$ ha. The number of samples and the total number of rows in the SPLAT! output matrix are then used to randomly select the samples using the *sample* function provided by R.

The *sample* function produces a vector containing the row numbers of the values to be sampled. The sampled values and their corresponding locations are stored in a new matrix to be used as the input matrix to the kriging model.

4.5.3 Obtain covariates

The acquisition of covariates is only required for the implementation of UK and RK. All the covariate data available in this case is discussed in section 3.3.4.

The azimuthal bearing of the each sample location relative to the transmitter and the point's elevation to first obstruction are provided in the SPLAT! output matrix. These two covariates are obtained while sampling is done to find the covariate value corresponding to each sample value. Since the locations of the samples are required for kriging, there is no additional process required to obtain the coordinates as covariate data.

Finally, the knowledge of the transmitter locations allows the distance of each point from the transmitter to be used as a covariate. The use of the UTM coordinate system provides the ability to determine the Euclidean distance of each sample location from

the transmitter through Pythagoras's theorem:

$$d = \sqrt{(lat_t - lat_p)^2 + (lon_t - lon_p)^2} \tag{4.3}$$

, where d is the separation distance in metres, lat_t and lat_p are the UTM northings of the transmitter and the sample location, respectively, and lon_t and lon_p is the UTM eastings of the transmitter and sample location, respectively.

4.5.4 Prediction grid

In order to plot a prediction map of the entire area of interest, a prediction grid needs to be generated. This prediction grid is generated with a resolution of approximately 60 metres and is only contained within the prediction radius since the scope of this investigation does not include extrapolation.

The implementation of UK and RK requires the covariate data for each prediction point as well, as mentioned in section 3.3.4. Again, the use of location as a covariate does not require any additional calculation since the locations of the prediction grid are already known. In the case where the distance from the transmitter is used as a covariate, equation 4.3 is used to determine the covariate values for the prediction grid.

The covariate data provided by the SPLAT! output, on the other hand, requires some calculation. Since the SPLAT! prediction locations do not lie in a regularly spaced grid, the covariate values are interpolated to the prediction grid locations using bicubic interpolation.

4.5.5 Fit linear model

For the implementation of RK, a linear regression model must be fitted between the covariate data and the target variable. The residuals produced by fitting the linear model are then used to create the semivariogram, discussed in section 4.5.6.

The linear model is fitting using the *lm* function provided by the *stats* package in R [86, 87]. An example of how the linear model is fitted is shown below.

```
lm.dBm <- lm(dBm ~ azi+dists+elev,samples)
```

In this example, the linear model is fitted between the received power, *dBm*, and a combination of the covariates - azimuth, *azi*, distance from the transmitter, *dists*, and elevation to first obstruction, *elev*. The *samples* parameter is a matrix containing all the aforementioned sample data.

4.5.6 Fit semivariogram

The semivariogram is calculated and fitted differently for each of the variations of kriging.

In the implementation of OK, only the sampled received power values are used. UK requires the semivariogram to be calculated given the received power samples as a function of the covariates used, and RK constructs the semivariogram solely from the residuals produced by fitting the linear model discussed in section 4.5.5.

The remaining details of generating the semivariograms are discussed as part of the verification in section 5.2.

4.5.7 Predictions

Finally, the kriging predictions can commence. The R function used to perform kriging requires the input samples and their locations, the fitted model semivariogram, the locations at which the predictions are to be made and the kriging method to be used, as input parameters.

The remaining details of performing the kriging interpolation is discussed as part of the verification in section 5.2.

4.6 Conclusion

This chapter discussed the details of implementing the experimental flow proposed in chapter 3. A discussion of the simulation tools to be used was followed by a description of the process of obtaining the sample data using SPLAT! and the Longley-Rice ITM. An exploratory data analysis was performed in order to determine whether the data meets kriging requirements prior to a discussion of the implementation of the kriging methods in R.

Chapter 5

Verification and validation

In this chapter, the verification of the implementations of OK, UK and RK are discussed as well as the procedures for validating the OK implementation in the R programming environment.

5.1 Introduction

In any research project, it is crucial to ensure that the correct procedures and implementations are followed. This phase of the research project is known as validation and verification.

In our case, the verification is done by confirming that all the required phases of the implementation of OK was followed correctly, and that expected results were obtained. The validation is done to ensure that our kriging implementation in the R software environment is correct and produces acceptable results.

5.2 Verification

In this section, we aim to verify the implementation of the OK, UK and RK models, as well as the 10-fold CV algorithm.

5.2.1 OK implementation

In order to verify that the OK model was correctly implemented, the process of implementation is discussed step-by-step. The overview of the procedure performed for validation in section 5.3 gives some background on the steps taken to implement OK.

The remainder of this section discusses the detail of each step shown in figure 5.1. The implementation of these steps are verified against the proposed requirements of various authors [44, 49, 50, 100].

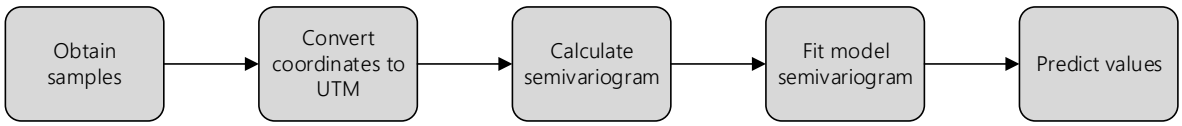

Figure 5.1: Functional flow: OK implementation

Obtain samples

After importing the SPLAT! output data into the R software environment, the *sample* function [101, 102] is used to draw the specified number of samples from the data. For each session, the seed value of the random number generator is reset in order to keep the sampling random and the results comparable.

The SRS method is used in order to stay within the requirement that sampling should be done independently of the values and locations of samples (see section 2.4.3). The randomised sampling approach also ensures that the samples are representative of the entire area of interest [50, 100].

Convert coordinates to UTM

The conversion of the geographical coordinates to UTM coordinates is done after the samples are obtained. The reason for this is that there is no use in converting the entire data set produced by SPLAT! when all the locations are not being used.The centre of the area of interest is determined using equation 5.1.

$$[lon_{centre}, lat_{centre}] = [\frac{lon_{max} - lon_{min}}{2}, \frac{lat_{max} - lat_{min}}{2}] \tag{5.1}$$

, where lon_{centre} and lat_{centre} are the geographical coordinates for the centre of the area of interest and lon_{max}, lon_{min}, lat_{max} and lat_{min} are the geographical coordinates defining the bounding box for the area of interest. The centre of the area is then used to find the UTM zone in which it lies. The UTM zone is found using the MATLAB function *utmzone*. After the UTM zone is determined, the geographical coordinates can be transformed.

The *rgdal* package in R provides a command *project* which uses the UTM zone and a reference ellipsoid to transform the geographical coordinates to UTM. The World Geodetic System 1984 (WGS84) reference ellipsoid is used since this is also the reference ellipsoid used by SPLAT! to specify the coordinates of locations. The transformed coordinates are verified by transforming the coordinates in both R and MATLAB and comparing the results of the transformation.

MATLAB uses the *mfwdtran* function which also requires the UTM zone and reference ellipsoid as input parameters. The difference between the results of R and MATLAB is that R indicates coordinates in the southern hemisphere with a negative northing

value. The conversions to UTM resulted in identical eastings and the relationship of the northing coordinates is indicated in equation 5.2.

$$UTM\ N_{MATLAB} = 10000000 + UTM\ N_R \tag{5.2}$$

, where $UTM\ N_{MATLAB}$ is the UTM northing calculated using the MATLAB functions and $UTM\ N_R$ is the UTM northing calculated in R. The relationship between the northings is correct since the equator is defined by the false northing of 10 000 000 metres as discussed in section 2.6.

Test for spatial autocorrelation

The test for spatial autocorrelation is performed on every sample data set before using it as input to OK as suggested in section 2.3.1. The data is tested by performing Mantel's test [99] in the R software environment as described in section 4.4.1.

Calculate experimental semivariogram

The experimental semivariogram is calculated using the *variogram* command in R. This command uses the input data to determine the semivariance of the sample set as a function of distance using equation 2.23 discussed in section 2.3.2. An additional input parameter specifies the cut-off distance (maximum distance) for which the semivariogram should be determined.

Fit model semivariogram

R uses the *fit.variogram* command to fit a model semivariogram to the experimental semivariogram. The input parameters required by this command are the calculated experimental semivariogram, the type of model semivariogram that should be fit and the initial model semivariogram parameters. Hengl [50] proposes a rule of thumb for the last-mentioned initial values as follows:

- Nugget - Zero
- Sill - The variance of the input sample data
- Range - 10% of the spatial extent of the data or twice the mean distance to the nearest neighbour.

Predict values

The locations at which values are to be predicted as well as the fitted model semivariogram are supplied as input parameters for the *krige* command provided by the *gstat* package. The model semivariogram is used to determine the kriging weights for each of the locations before the prediction is done.

5.2.2 UK implementation

Since the implementation of UK is mostly similar to OK, and the implementation of OK has been verified in section 5.2.1, this section will only verify the parts particular to UK.

The first aspect of UK that differs from OK, as mentioned in section 2.3.4, is that it utilises covariate data. Therefore, a covariate is selected from the additional available data. The procedure followed to determine the most effective covariate is discussed in section 3.3.4. The covariate selection is followed by the generation of a prediction grid since the covariate data is required for both the sample locations and the prediction locations.

The available covariate data is not in a regularly spaced grid and, therefore, have to be interpolated into a grid. This is done using bivariate interpolation functions provided by the *akima* package [103] in R. Since the covariates serve solely as explanatory data, the small errors made by interpolating the data into a grid have a negligible effect on the kriging results.

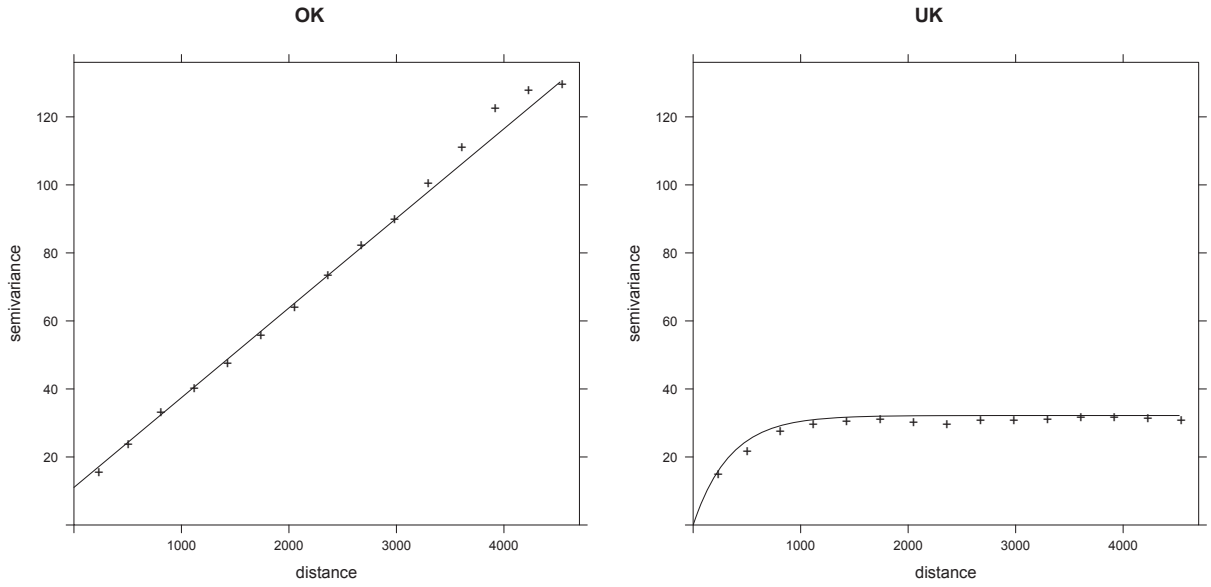

Figure 5.2: Comparison between the OK semivariogram and the UK semivariogram constructed for a single site

The semivariogram for the UK implementation is calculated and fitted by specifying the target variable as a function of the covariate. Furthermore, an Ordinary Least Squares (OLS) regression line is fitted between the target variable and covariate, and the consequent residuals are used to construct and fit the semivariogram. Figure 5.2 shows the difference between the OK semivariogram which is calculated and fitted using only the sample values of the target variable, and the UK semivariogram constructed from the residuals of the OLS regression function.

Finally, UK is executed by specifying the target variable, which is the received power, as a function of the selected covariate and given the semivariogram constructed from the residuals to determine the kriging weights.

Thus, the main difference between OK and UK is verified through figure 5.2 in that the semivariogram is constructed from the residuals of the regression function obtained by using the covariate data.

5.2.3 RK implementation

This section attempts to verify the implementation of RK. As in the case of UK in section 5.2.2, only the aspects of RK implementation differing from that of OK and UK are discussed and verified.

As stated by Hengl in [50], the only difference between RK and UK is the computational steps. In the implementation of RK, a regression line is fitted between the target variable and the covariate, separately. The residuals produced by the regression line are then used as a singular input to the command which calculates and fits the semivariogram. Thus, the result is also a semivariogram constructed from the residuals of the regression function as with UK. The comparison between the semivariograms constructed for OK, UK and RK is shown in figure 5.3.

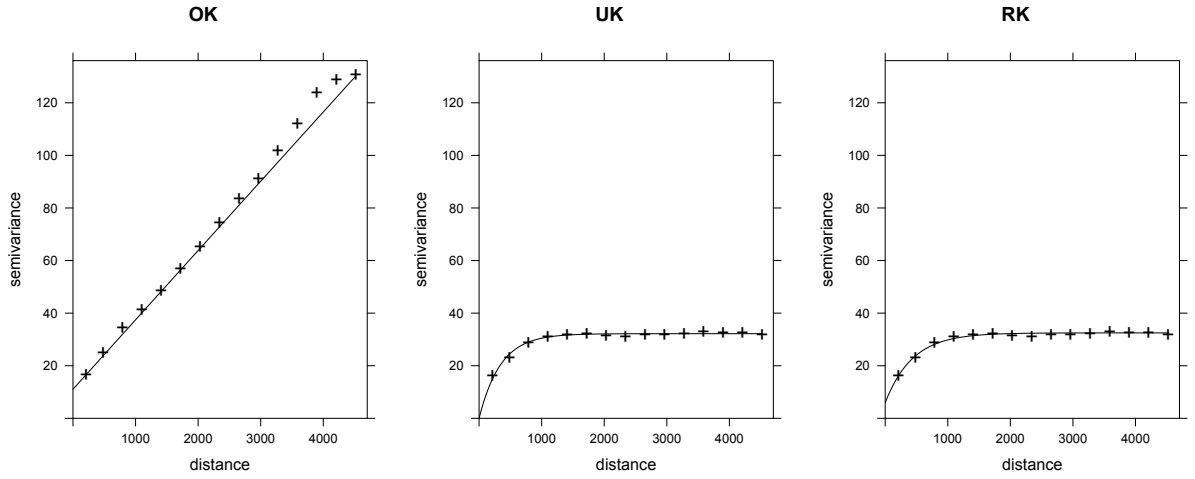

Figure 5.3: Comparison between the OK, UK and RK semivariograms constructed for a single site

Figure 5.3 thus verifies the implementation of RK since it also constructs a semivariogram from the residuals produced by fitting a regression function with the covariate data and delivers a similar semivariogram to that of UK.

5.2.4 10-fold CV

Although both the ooDACE toolbox and R provides CV functions, it was decided to write an algorithm for 10-fold CV. This was done to be able to examine different error functions. The CV algorithm is verified using the *krige.cv* function provided by the *gstat* package [92] in R. Thus, the CV algorithm is verified by comparing its results to those produced by *krige.cv*.

The created algorithm is proposed to be a more accurate indication of the performance of the kriging model, since the *krige.cv* function does not re-fit the semivariogram to the training dataset [55]. Therefore, considering that the semivariogram is only fitted to the original sample set, the results of *krige.cv* is expected to show lower error values than the created CV algorithm. Section 3.2.5 describes the CV process and re-fitting of the semivariogram.

In order to determine the RMSE and MAE correctly, the absolute error as well as the squared error are calculated for all predicted values in each iteration. After the ten iterations, the square-root of the mean of all squared errors is calculated to find the RMSE, and the mean of all absolute errors is calculated to find the MAE.

Figure 5.4 shows the comparison of the results obtained by implementing both *krige.cv* and the created CV algorithm for OK on five randomly selected sites. Refer to table B.7 in appendix B for all information regarding the randomly selected sites.

Table 5.1 summarises the comparison of the two CV implementations through the correlation coefficients r and r^2.

Table 5.1: Correlation between R built-in CV and created CV algorithm

	r	r^2
RMSE	0.9951	0.9903
MAE	0.9959	0.9917

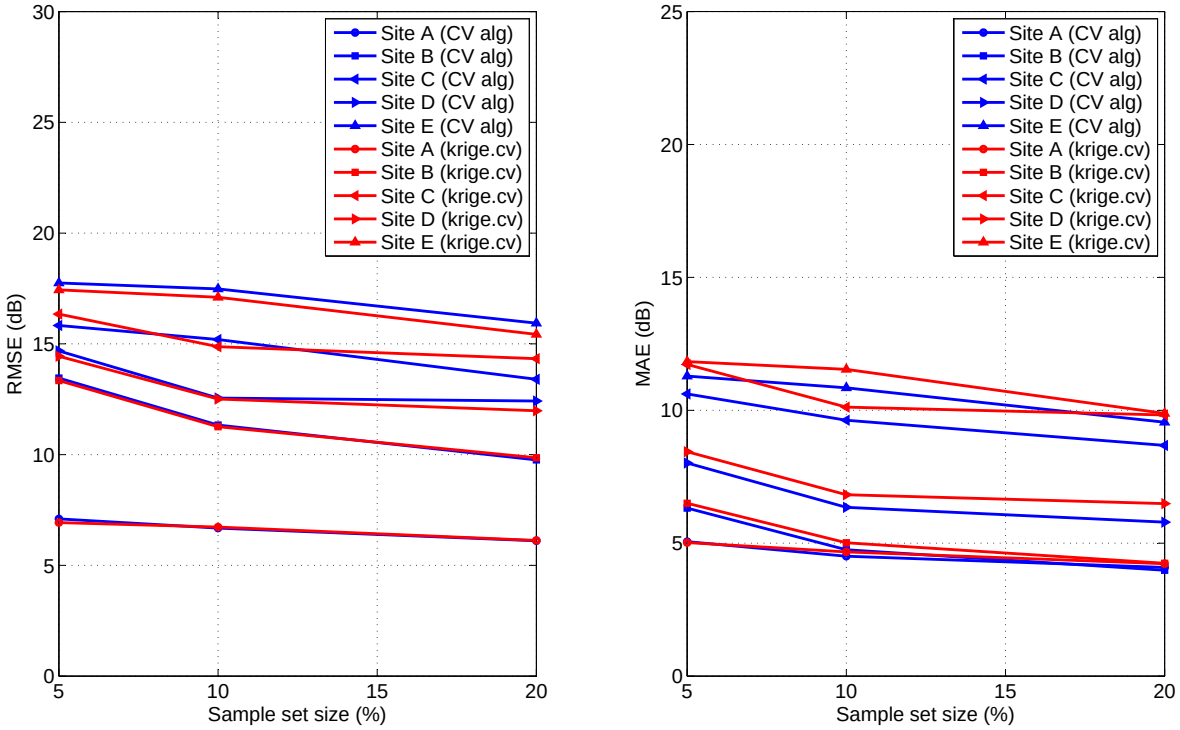

Figure 5.4: Error comparison of CV results for five randomly selected sites

These results verify the created implementation of CV since the results of both error functions show near perfect correlation. The near negligible difference between results obtained by re-fitting the model for each training set and those obtained by neglecting to re-fit the model, could be explained by the large sample sets and the relatively small number of samples used for the validation set.

5.3 Validation methodology

The implementation of OK in the R software environment is validated by statistically comparing the results to that of the ooDACE toolbox used in MATLAB. For the validation, five TV transmitter sites in South Africa are randomly selected using the process discussed in section 3.2.1. Refer to table B.8 in appendix B for all information regarding the randomly selected sites. The validation process is described in figure 5.5.

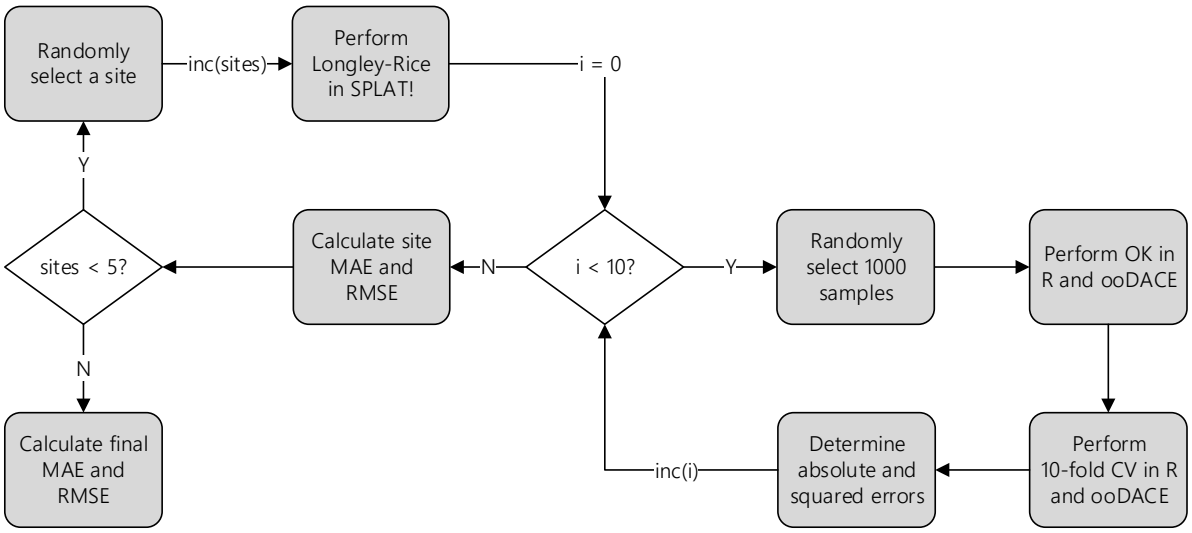

Figure 5.5: Flow diagram for the validation process

The coverage of each transmitter is predicted for a radius of 5 km using the Longley-Rice ITM implemented in SPLAT!. The ITM results are then used as a sample pool from which 1000 samples are selected randomly. These samples are then used as the input data for the OK model implemented both in R and ooDACE after which 10-fold CV is performed in each software environment respectively. The CV results are used to determine the absolute error, as well as the squared error.

This process is repeated ten times for each of the five randomly selected sites. Finally, after all results are obtained the MAE and RMSE are determined.

5.3.1 Validation metrics

The validation of the kriging implementation in R is also done using metrics discussed in section 2.3.6. In addition to calculating the RMSE and MAE, Pearson's correlation coefficient is determined between the R predictions and the baseline ooDACE predictions.

Pearson's correlation coefficient is used to determine if there is a good linear relation between the predictions made using R and those using ooDACE. Equation 2.34 is used with modified variables particular to the validation of the model implementation in R and is shown in equation 5.3.

$$r = \frac{\sum_{i=1}^{n} (Z_{R_{CV},i} - \overline{Z_{R_{CV}}})(Z_{ooDACE_{CV},i} - \overline{Z_{ooDACE_{CV}}})}{\sqrt{\sum_{i=1}^{n} (Z_{R_{CV},i} - \overline{Z_{R_{CV}}})^2} \sqrt{\sum_{i=1}^{n} Z_{ooDACE_{CV},i} - \overline{Z_{ooDACE_{CV}}})^2}} \tag{5.3}$$

, where n again denotes the number of samples, $Z_{R_{CV},i}$ is a predicted value using CV in R and $Z_{ooDACE_{CV},i}$ is the corresponding value predicted through CV in ooDACE. $\overline{Z_{R_{CV}}}$ and $\overline{Z_{ooDACE_{CV}}}$ denote the mean of the values predicted in R and ooDACE, respectively.

5.3.2 Validation results

The results from table 5.2 are visually summarised in figure 5.6 which clearly shows the similarities in the trends of both the MAE and RMSE for R and ooDACE.

Table 5.2: Cross-validation errors for each site

	RMSE (dB)		MAE (dB)	
Site	ooDACE	R	ooDACE	R
A	13.2021	12.2449	8.1518	7.1501
B	13.8230	12.9000	6.9507	6.3463
C	12.7654	11.6592	6.8369	6.2845
D	7.1845	6.1570	4.2793	3.7602
E	23.5107	22.0100	15.9966	14.5104

Table 5.3 summarises the error results for all the validation sites. The Pearson correlation coefficient of $r = 0.9844$ and an $r^2 = 0.9691$ shows a very strong linear relationship between the predictions made by R and ooDACE. A perfect linear relationship is indicated by $r = 1$. Thus, it can be concluded that there is a nearly perfect linear relationship between the predictions made by R and those by ooDACE.

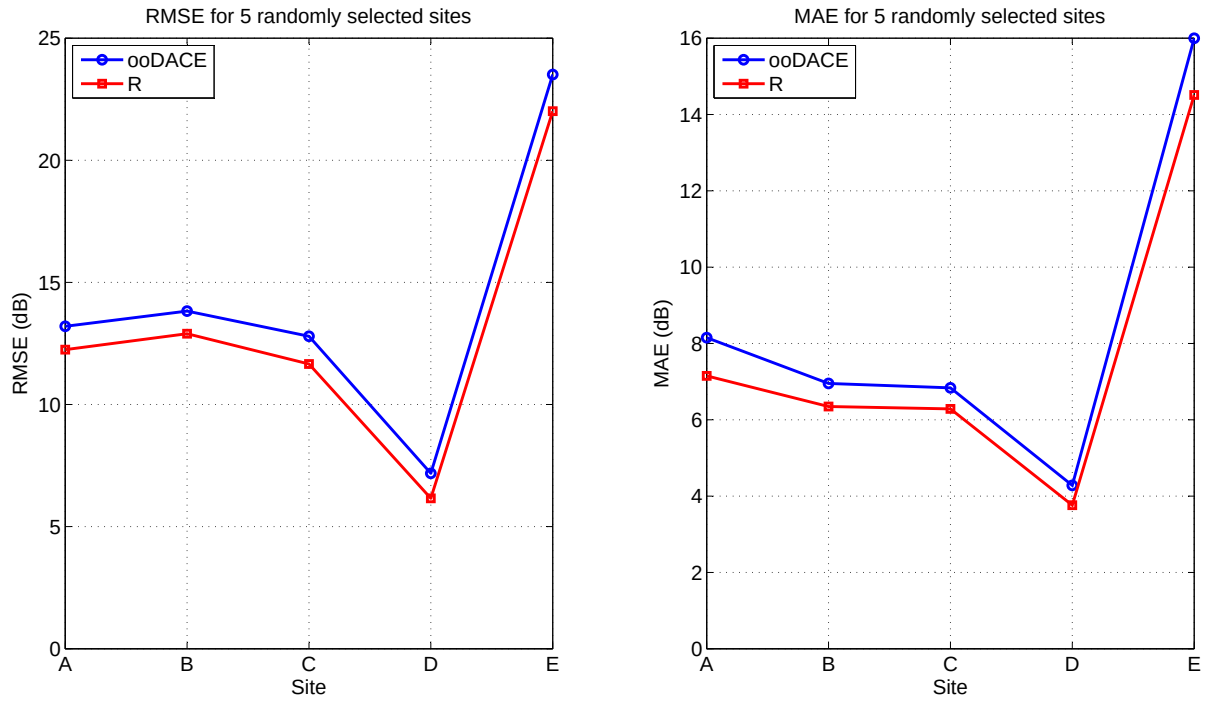

Figure 5.6: RMSE and MAE for five randomly selected sites

Table 5.3: Cross-validation errors for all sites

	RMSE (dB)	MAE (dB)
R	13.9616	7.6103
ooDACE	15.0560	8.4431

For the validation of the OK results produced using R, the ooDACE results are used as a baseline. Therefore, the differences between the two sets of results are examined and expressed as a percentage relative to the baseline. This is done using equations 5.4 and 5.5.

$$\%\ \text{RMSE difference} = \frac{RMSE_{ooDACE} - RMSE_R}{RMSE_{ooDACE}} \times 100 = 7.269\% \tag{5.4}$$

$$\%\ \text{MAE difference} = \frac{MAE_{ooDACE} - MAE_R}{MAE_{ooDACE}} \times 100 = 9.863\% \tag{5.5}$$

, where $RMSE_{ooDACE}$, $RMSE_R$, MAE_{ooDACE} and MAE_R respectively denote the RMSEs and MAEs calculated from the CV results of the R and ooDACE implementations.

These results show that the errors made during predictions using R are within 10% of those made by the baseline, ooDACE. A very strong linear relationship exists between the predictions made with the two different software environments as shown in table 5.3, and that is also clearly evident in the graphs shown in figure 5.6. It can, therefore, be concluded that the implementation of the OK model in R is valid.

5.4 Conclusion

In this chapter, the implementations of the three kriging methods were verified through a step-by-step confirmation that the requirements are met as proposed by various authors in literature. The created CV algorithm is also verified by comparing the results to that of an R CV function provided by the *gstat* package. The implementation of kriging in R is validated by the results obtained using the ooDACE MATLAB toolbox and finding that the results differ by less than 10%.

Chapter 6

Results

In this chapter, OK, UK and RK are performed on one hundred randomly selected sites, and the results are discussed. Section 6.2 presents the experimental parameters while section 6.3 discusses the distribution of the prediction errors for each site and each kriging method as well as the mean prediction error for all sites.

6.1 Introduction

In this study, one hundred sites were randomly selected from which the Longley-Rice ITM predictions were obtained to serve as input data for the different kriging models following the experimental flow described in section 3.2.3. The experimental parameters, as well as the covariate data used, are selected according to the conclusions made in section 3.3. Refer to tables B.5 and B.6 in appendix B for all information regarding the randomly selected sites.

6.2 Experimental parameters

The experimental parameters particular to this case is shown in table 6.1. These parameters were selected as a result of the conclusions made in chapters 3, 4 and 5.

Table 6.1: List of experimental parameters

Parameter	Value
Software environment	R
Number of sites	100
Prediction radius	5 km
Sample density	1/8 ha
Evaluation metrics	RMSE
	MAE
	ME

The implementation of the kriging methods in R is justified by the verification and validation results from chapter 5. A total of one hundred sites are selected for the experiment to come to a conclusion regarding the efficiency of these kriging methods independent of the location and terrain type.

The prediction radius and sample density are chosen following the conclusions made in section 3.3.3. Since it was found that both these parameters have a minimal effect on the prediction results, the 5 km radius and low sampling density were chosen to decrease the execution time for the one hundred sites.

The RMSE, MAE and ME functions are chosen to describe different aspects of the prediction accuracy. The RMSE is chosen to provide an indication of the variance in the prediction errors. The MAE gives an average of the pure error the kriging method makes, regardless of the direction of the error, and the MEs show each method's tendency to over-predict or under-predict.

6.3 Kriging prediction results

The results produced by the different kriging results are, initially, evaluated by considering the distribution of the errors. Figure 6.1 shows the box plots of the prediction error using different error functions. The numerical results are shown for the minimum, first quartile, median, third quartile, and maximum cases over the one hundred sites, in table 6.2.

Table 6.2: Box plot results summary

	RMSE (dB)			MAE (dB)			ME (dB)		
	OK	UK	RK	OK	UK	RK	OK	UK	RK
Minimum	0.150	0.186	0.182	0.021	0.028	0.026	-0.213	-0.202	-0.111
Q1	6.929	6.897	6.844	2.543	2.570	2.629	-0.075	-0.062	-0.033
Median	11.871	11.792	11.687	5.979	6.074	6.190	-0.012	-0.003	0.002
Q3	14.639	14.392	14.083	8.520	8.557	8.997	0.038	0.051	0.032
Maximum	20.468	20.349	20.338	12.739	12.847	13.247	0.192	0.212	0.119

The difference between the distributions of the prediction errors for the different kriging methods, is very small. It can, however, be seen that the range of RMSE values resulted from using RK is the smallest of the three methods. This means that the variance found in the RK prediction errors are consistently smaller. It is also evident from the ME box plots in figure 6.1 that the spread of the RK errors are less than that of OK and UK.

That being said; the MAEs show that if the prediction error of each point is treated equally, OK consistently outperforms UK and RK. This is confirmed by considering the means of the errors over all the sites. The results are summarised in table 6.3.

Table 6.3: Mean prediction error summary

Error function	OK	UK	RK
RMSE (dB)	11.872	11.716	11.571
MAE (dB)	5.850	5.916	6.124
ME (dB)	-0.017	-0.007	-0.002

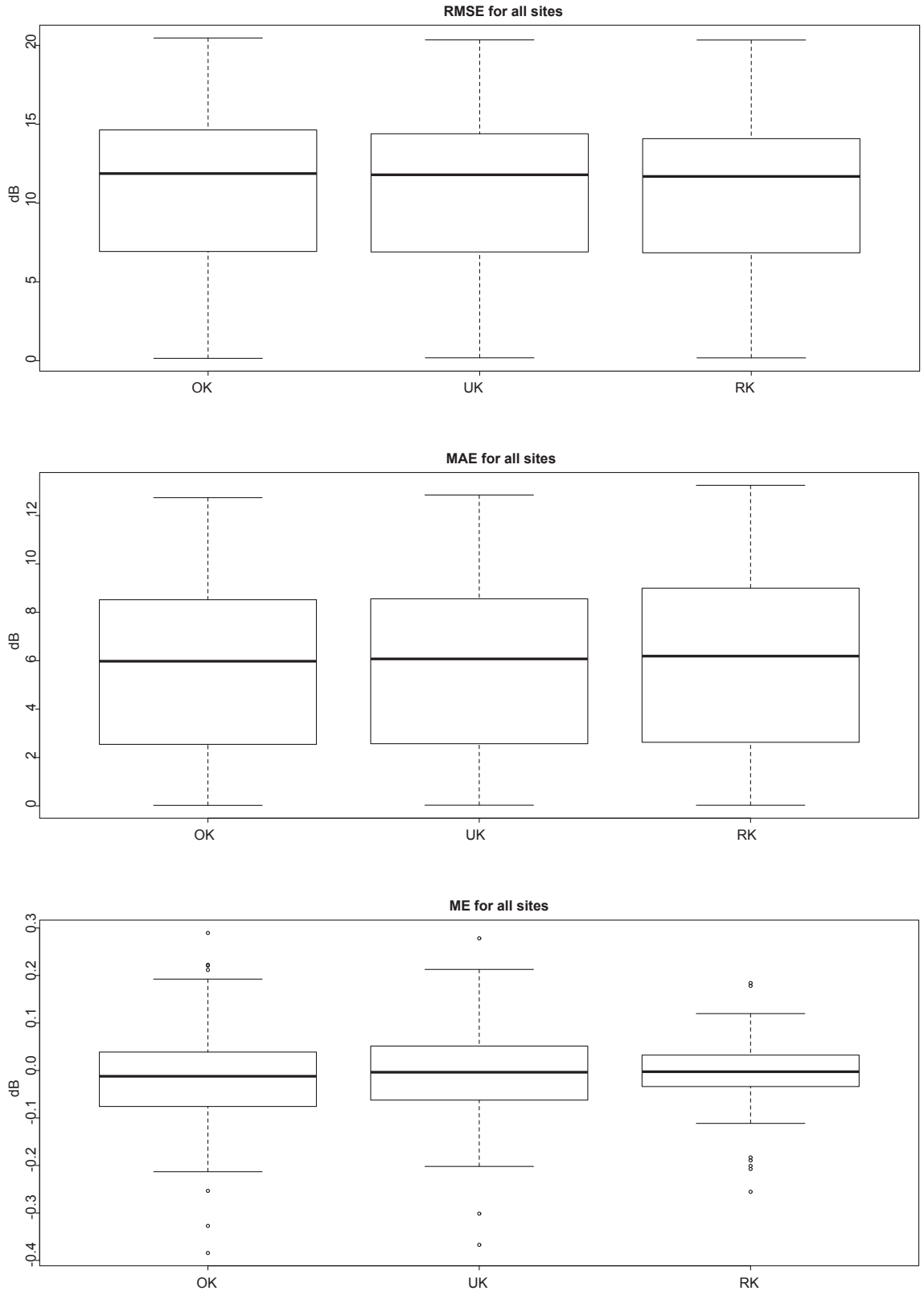

Figure 6.1: Box plots of the RMSEs, MAEs and MEs for OK, UK and RK

6.3.1 Received power prediction maps

Since the aim of this study is to determine the efficiency of the kriging methods for generating REMs, three sites are chosen to present the predicted received power maps. These three sites are selected according to the prediction errors made by the kriging methods in order to demonstrate the maps produced by the best predictions, worst predictions and predictions closest to the means of table 6.3. The MAEs for these three sites are shown in table 6.4.

Table 6.4: Prediction errors for example prediction maps

	Site	MAE (dB)		
		OK	UK	RK
Best	319 (Fig. 6.2)	0.188	0.206	0.206
Worst	586 (Fig. 6.3)	11.826	12.305	13.053
Average	433 (Fig. 6.4)	5.939	6.005	6.168

The received power prediction maps generated through the use of the different kriging methods are compared to the map produced using the Longley-Rice ITM in figures 6.2, 6.3 and 6.4, for the best, worst and average sites respectively.

It is evident from figure 6.2, depicting site 319, that the extremely accurate predictions made by the kriging methods are mostly due to the very little obstruction found within the predicted area. Thus, the received power gradually decreases as the distance from the transmitter increases.

Since the distance from the transmitter was used as a covariate, as discussed in section 4.5.3, it could be expected that the UK and RK predictions should be more accurate than that of OK. The reason that this is not the case, is most probably that the effect that the distance has on the received power is sufficiently portrayed by the raw received power samples.

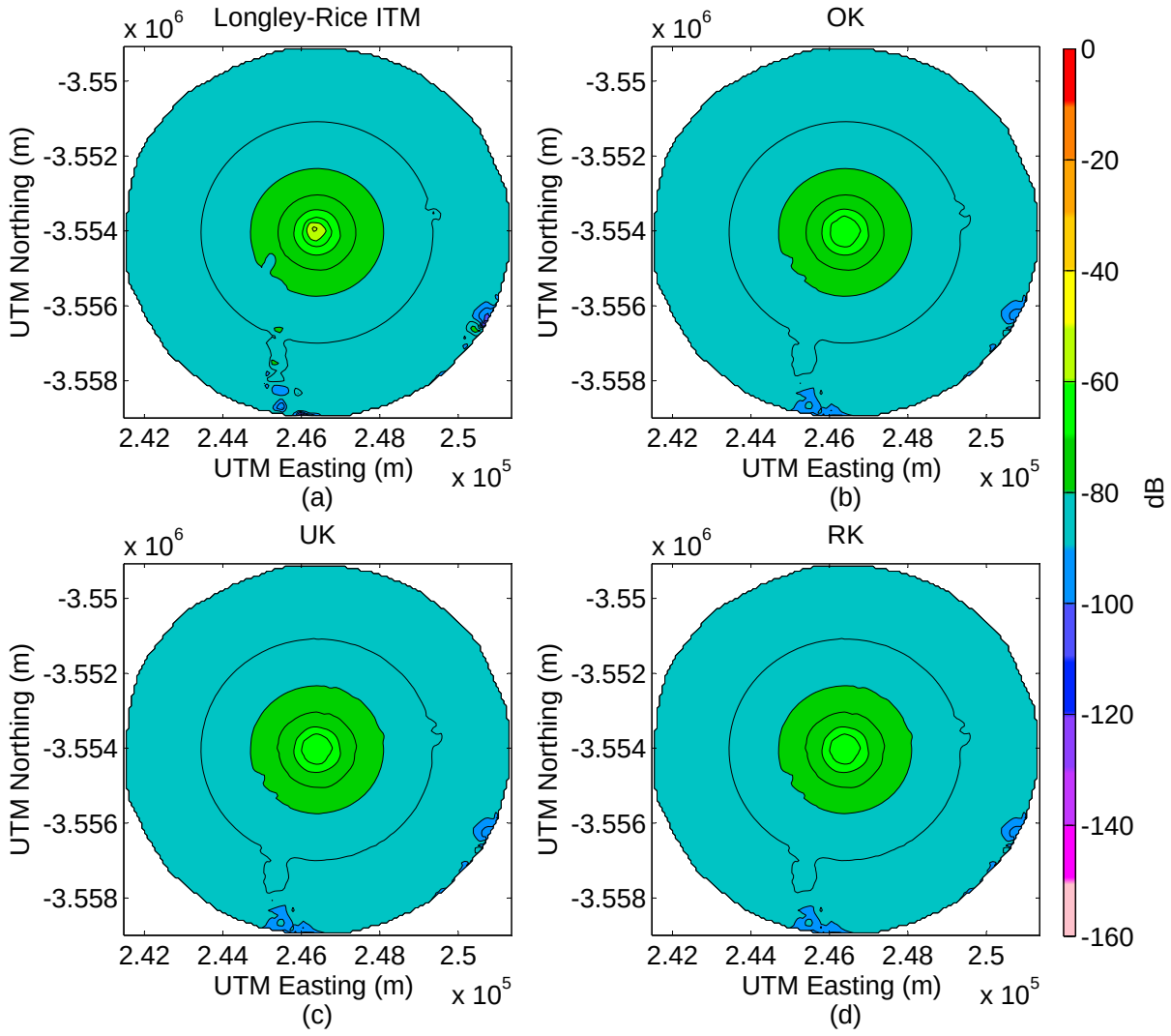

Figure 6.2: (a) Prediction map produced by SPLAT! using the Longley-Rice ITM and prediction maps produced using (b) OK, (c) UK and (d) RK for a site with very small prediction errors (site 319)

Figure 6.3 shows the prediction maps for site 586, where the kriging methods produced very large prediction errors.

Contrary to the case of figure 6.2, the obstructions in the prediction area has a much greater effect on the prediction accuracy. Many abrupt changes of between 20 dB and 40 dB take place over the entire area of the map produced by the ITM. Although figure 6.3 represents a worst case scenario, the kriging prediction maps show a significant resemblance to the ITM map.

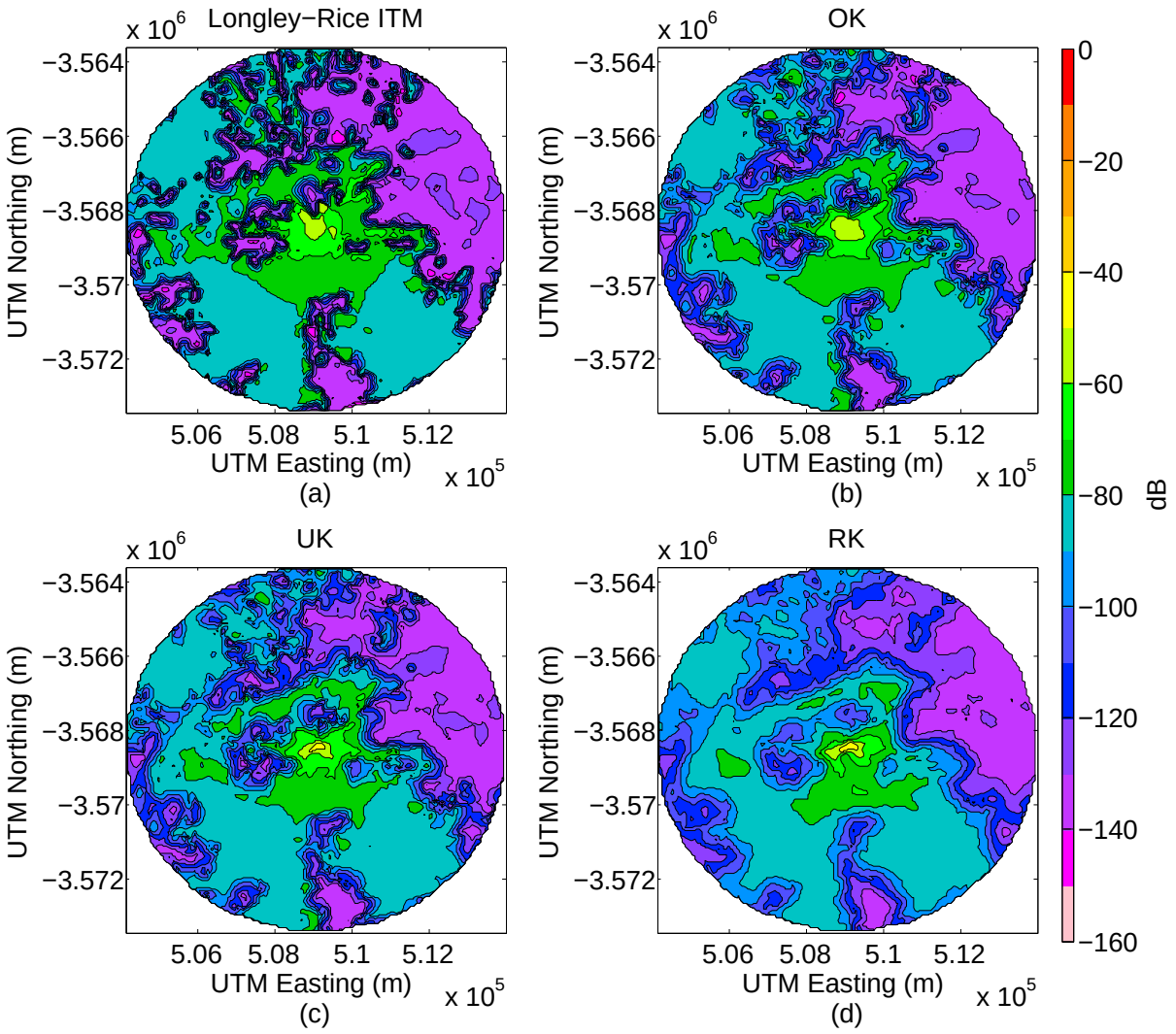

Figure 6.3: (a) Prediction map produced by SPLAT! using the Longley-Rice ITM and prediction maps produced using (b) OK, (c) UK and (d) RK for a site with very large prediction errors (site 586)

Finally, figure 6.4 presents site 433, the average case found in this study of one hundred randomly selected sites.

Considering figures 6.2, 6.3 and 6.4, it is evident that the kriging prediction errors are dependent on the amount of obstruction affecting the received power within the area of interest. Further investigation into the comparison between the actual values given by the Longley-Rice ITM and the kriging predictions, is performed through error maps in section 6.3.2.

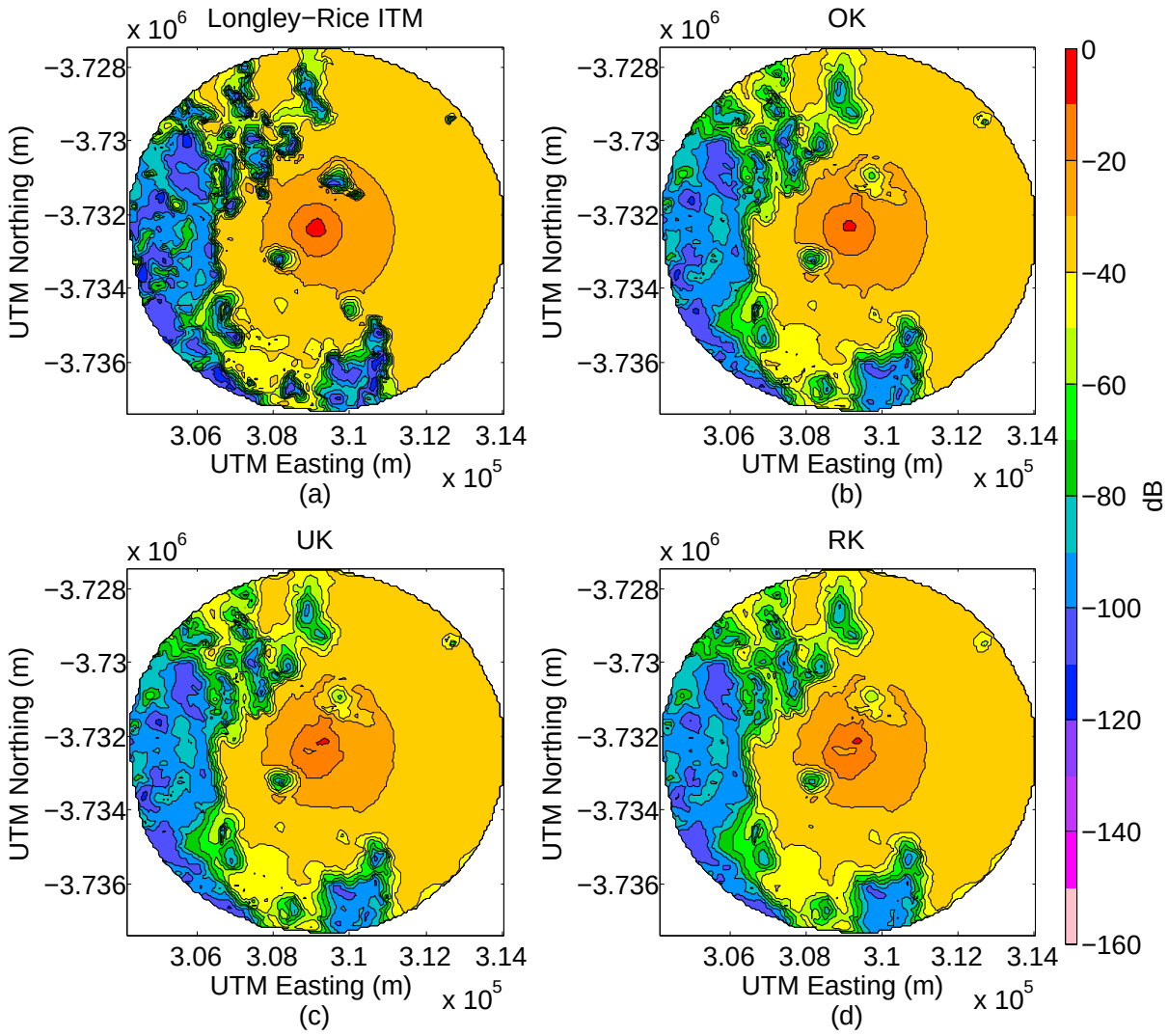

Figure 6.4: (a) Prediction map produced by SPLAT! using the Longley-Rice ITM and prediction maps produced using (b) OK, (c) UK and (d) RK for a site with average prediction errors (site 433)

6.3.2 Prediction error maps

Prediction error maps are generated in order to display the areas in which the largest errors are made. The figures in this section show the mean absolute prediction errors made by the three different kriging methods. Along with these error maps, is a prediction map produced by the ITM. This is done to show the effect of abrupt changes in received power on the prediction accuracy.

Figures 6.5.a, 6.6.a and 6.7.a show the prediction maps produced by the Longley-Rice ITM using the same scale as in section 6.3.1. The error maps produced by OK, UK and RK in figures 6.5.b, 6.5.c, 6.5.d, 6.6.b, 6.6.c, 6.6.d, 6.7.b, 6.7.c and 6.7.d, are scaled according to the colour bars shown in the figures.

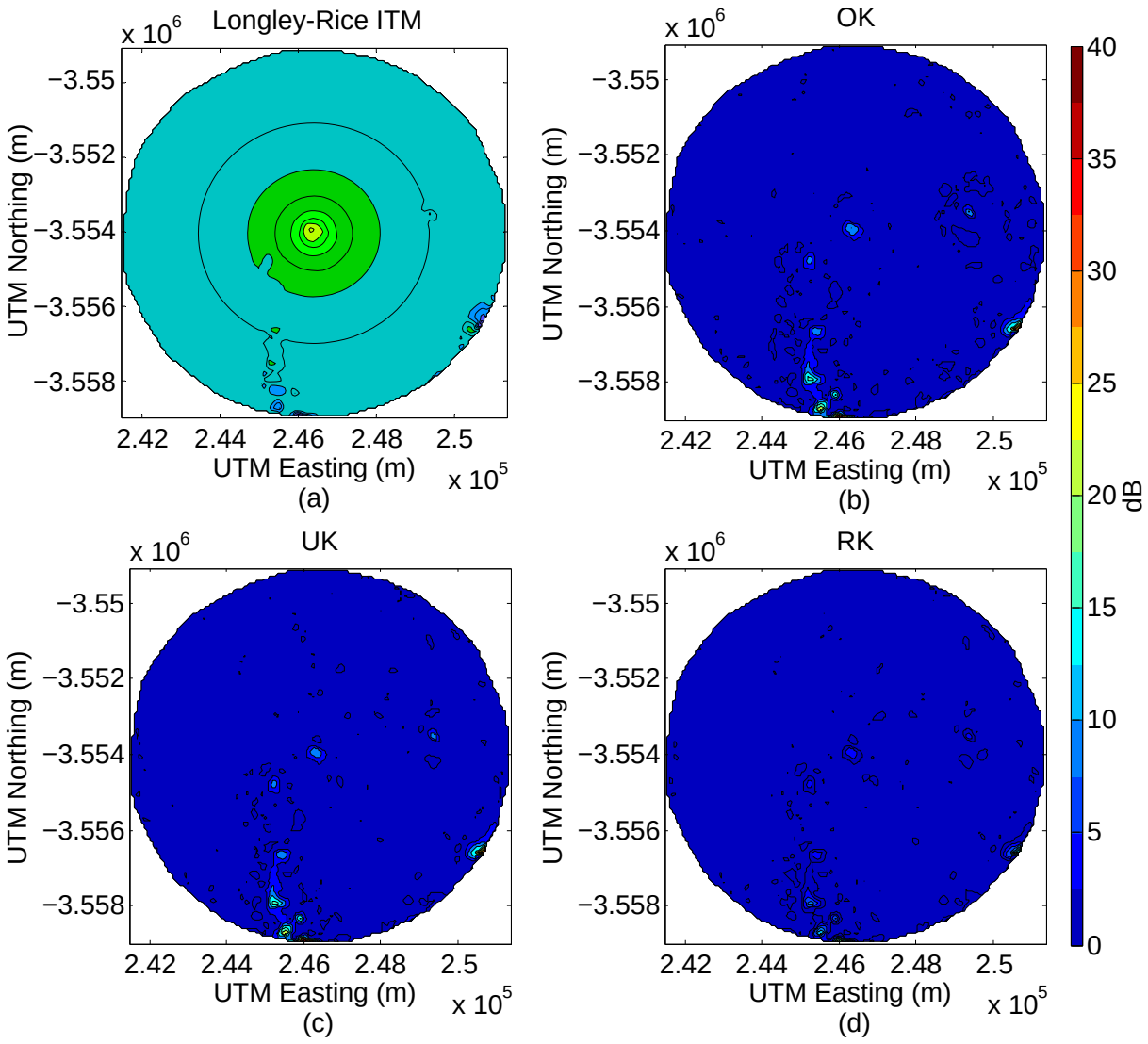

Figure 6.5: (a) Prediction map produced by SPLAT! using the Longley-Rice ITM and error maps produced using (b) OK, (c) UK and (d) RK for a site with very small prediction errors (site 319)

Figures 6.5 and 6.6 again represent the sites with the most accurate (site 319) and least accurate (site 586) predictions. While the prediction errors of the three different kriging methods are nearly identical in figure 6.5, it is clear that UK and RK produce larger errors than OK in the case where there is more obstruction.

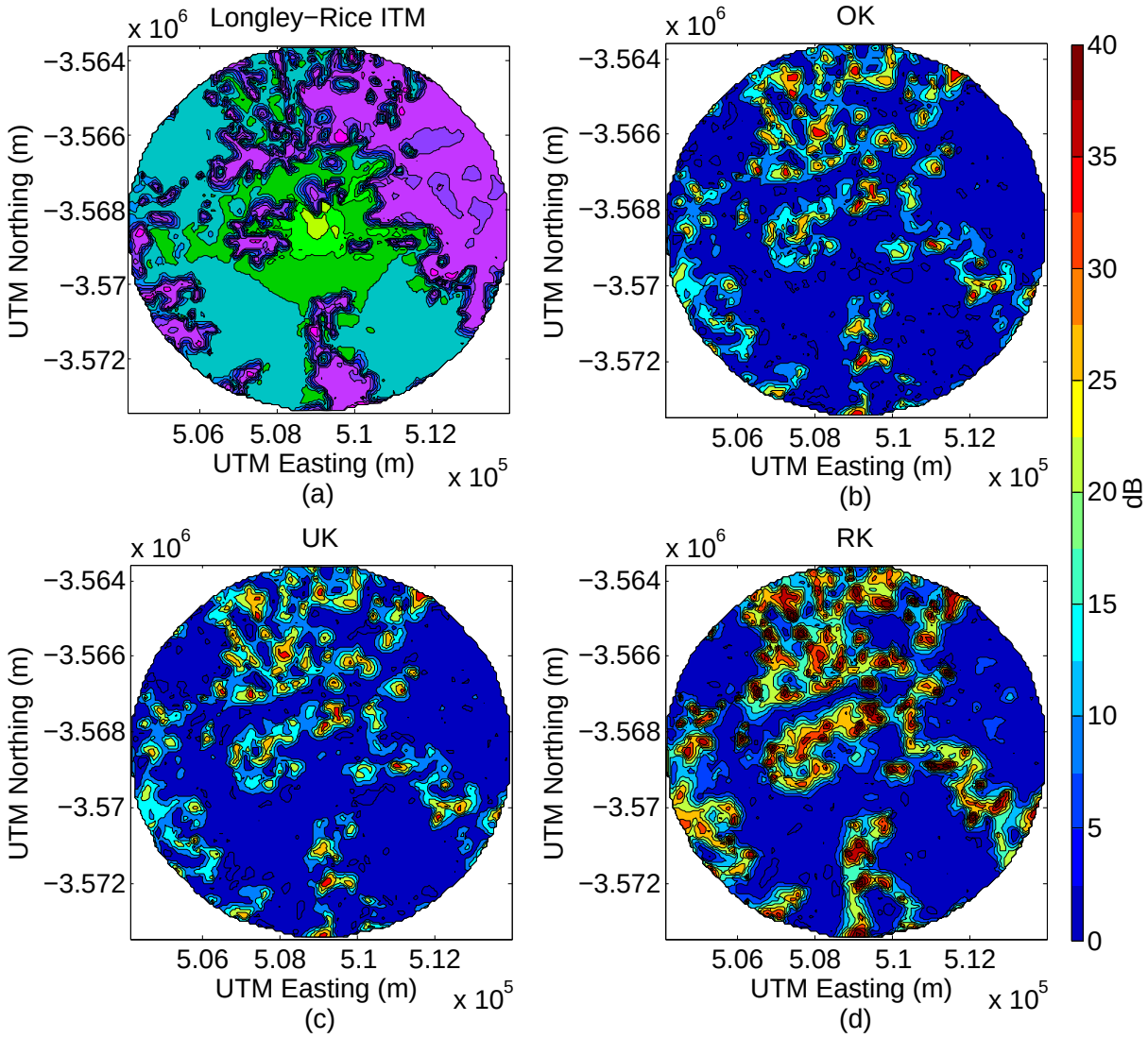

Figure 6.6: (a) Prediction map produced by SPLAT! using the Longley-Rice ITM and error maps produced using (b) OK, (c) UK and (d) RK for a site with very large prediction errors (site 586)

As in the cases of figures 6.5 and 6.6, the site representing average prediction errors (site 433), in figure 6.7, also indicates the majority of large errors at locations where abrupt changes in received power is found.

It is, therefore, evident from the discussed prediction error maps and the mean prediction errors calculated in table 6.3, that the absolute errors made by OK are consistently less than that of UK and RK.

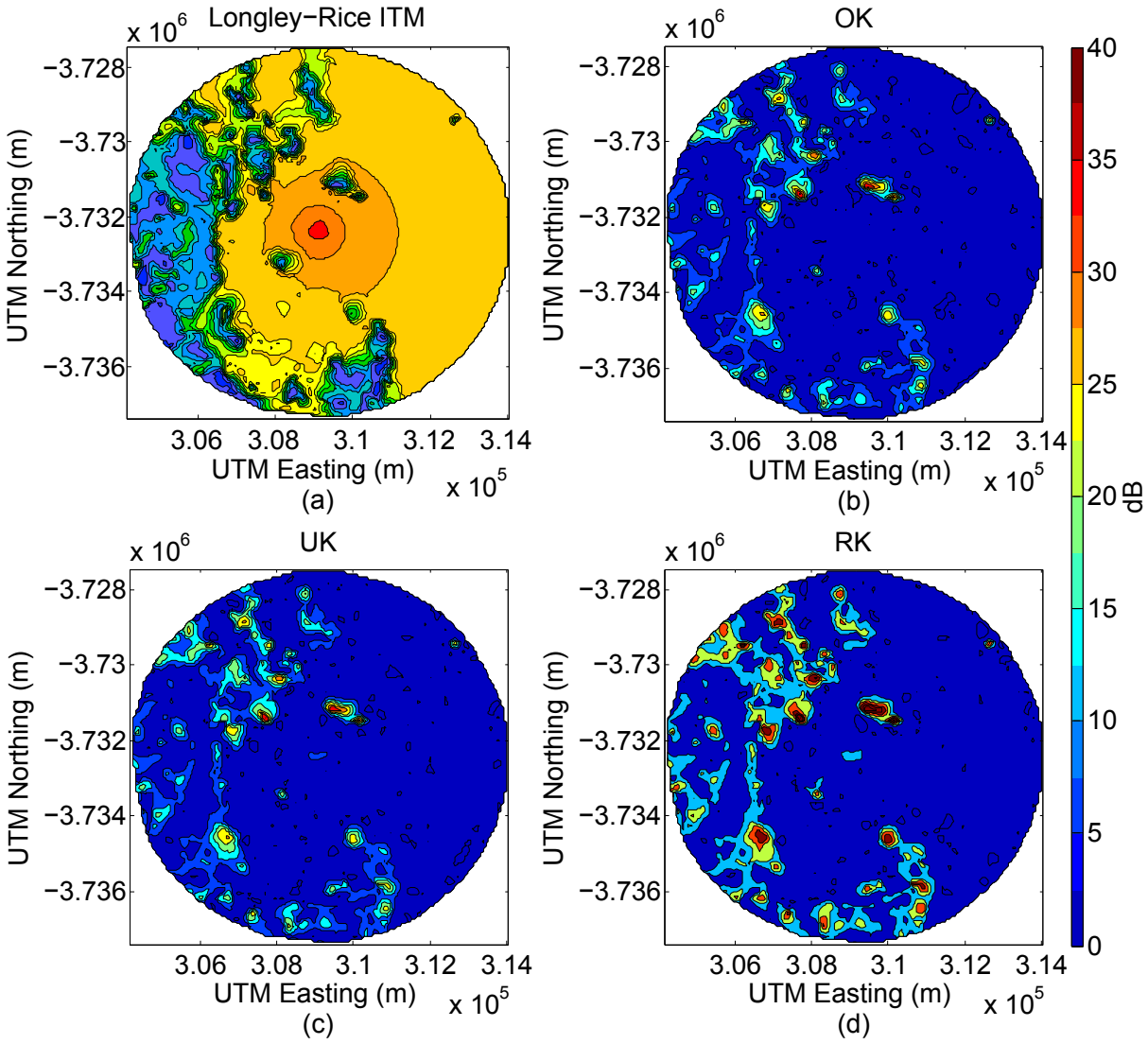

Figure 6.7: (a) Prediction map produced by SPLAT! using the Longley-Rice ITM and error maps produced using (b) OK, (c) UK and (d) RK for a site with average prediction errors (site 433)

6.4 Conclusion

This chapter discussed the results obtained from implementing OK, UK and RK on one hundred randomly selected sites. It was found that while UK and RK consistently produced smaller variances in errors as observed from the RMSEs and MEs, OK performed the best considering the MAEs. The error maps discussed in section 6.3.2 also brought to light that the largest errors made by all the kriging methods were due to abrupt changes in the received power caused by topographical obstructions. The performance of the kriging predictions for sites with large prediction errors can be improved by increasing the sampling density as shown in section 3.3.3. In that case, the available time and financial resources, as well as the accuracy required for the specific scenario, should be considered to determine the feasibility of increasing the number of samples.

Chapter 7

Conclusion

In this chapter, an overview of the entire dissertation is given. This is followed by a discussion of the obtained results. The chapter and dissertation are brought to closure with recommendations for future work.

7.1 Dissertation overview

This dissertation, "Evaluation of kriging interpolation methods as a tool for radio environment mapping", introduced the possibility of using various spatial interpolation techniques of the kriging family to augment or replace the need for conventional propagation models.

The research process was initiated by defining the problem at hand. Definite objectives were proposed and the methodological approach was discussed as an introduction to the dissertation. This was followed by a detailed literature study on radio wave propagation as well as the Longley-Rice ITM and ITU-R P.1546 propagation models in order to obtain a better understanding of the application domain. The concept and mathe-

matical implementation of the kriging methods were investigated, and the sampling approaches and applicable coordinate systems were also considered.

The conceptual design took into account different aspects that could affect the results of the proposed experiment. This included the consideration of other spatial interpolation techniques and the advantages that kriging presents. The effects of sampling density, prediction radius and the use of different covariates for UK and RK were evaluated, and the proposed experimental flow and flow of implementation were also discussed in this chapter.

The conceptual design was followed by a discussion of the actual implementation of the proposed experiment in chapter 4. This included an overview of the simulation tools used to implement the different models and a discussion of the initial phases and requirements for generating the samples needed to implement kriging, through the Longley-Rice ITM. This section further discussed the exploratory data analysis as a prelude to kriging, as well as each phase of the kriging implementation.

Chapter 5 served to verify and validate the implementation of the kriging methods to generate REMs. The kriging implementations were verified by confirming that the requirements proposed by various authors were met, and the CV algorithm was verified through a comparison of the results to those of a built-in R CV function. The implementation of kriging in R was validated by comparing the results to the validated MATLAB kriging toolbox, ooDACE.

The selected variations of kriging were implemented on one hundred randomly selected TV broadcasting sites. The results chapter presented the kriging predictions in various formats. Firstly, the prediction errors, determined through 10-fold CV, were presented as box plots showing the statistical distribution of different error functions for each kriging method.

This was followed by a comparison between the prediction maps generated through kriging and the prediction map obtained from the Longley-Rice ITM. Finally, error maps were generated in order to display the absolute errors over the predicted area for each kriging method.

7.2 Findings

The initial findings were made as part of the preliminary design and sub-studies performed, as discussed in chapter 3. Through investigating the effect of prediction radius on the kriging results, it was found that the accuracy of predictions remained consistent regardless of the size of the prediction area. It was also found that the sampling density has the most notable effect on the prediction accuracy. Although this is the case, the prediction error decreased merely by approximately 1 dB when the sampling density is doubled.

An investigation into the use of only one of the available covariates resulted in the conclusion that none of these covariates, used in solitude, have a greater effect on the accuracy than the sampling density. Therefore, a combination of the available covariates was used in the final experiment.

The results obtained from implementing the three kriging methods on one hundred randomly selected sites in the UHF band, proved that OK delivered the best MAE of the three. This brings into question the feasibility of using the additional covariate data for predicting with UK and RK. It can, therefore, be concluded that the time spent on the acquisition of covariate data as well as the time spent because of the increase in computational complexity of UK and RK, is not justified by the results in this case.

Finally, the MAE of 6 dB produced by OK, using a sampling density of one sample for every eight hectares, is very promising in comparison to the prediction accuracy of the Longley-Rice ITM. As discussed in section 3.3.2, the authors of the Longley-

Rice ITM state the model produce an average prediction error of 10 dB. Thus, the results from this study allude that kriging has the potential to outperform a propagation model such as the ITM. That being said; the comparison between prediction accuracies of these two methods can only be completely verified by using real measured sample data.

This study can conclude that there is no doubt that kriging can be used to generate REMs and that OK provides adequate accuracy without the additional data and computational complexity required by UK and RK.

7.3 Recommendations for future work

Since this study only made use of simulated measurements by using the Longley-Rice ITM predictions as input to the kriging models, the question remains if the kriging prediction accuracy is better than that of the ITM. This could be investigated by using actual measurements for a certain area and by comparing both the kriging and ITM predictions to the measured data.

Furthermore, a case is to be made regarding the use of covariate data which shows a better correlation with the received power samples. This could improve the accuracy of UK and RK to such an extent that the trouble of obtaining the covariate data can be justified.

Future work may also include an investigation considering anisotropy which could produce better results considering that the obstacles in propagation paths of different directions surrounding the transmitter, vary.

Finally, an option to expand this study is to investigate the efficiency and accuracy of kriging for multiple sites and find the limits of kriging for radio environment mapping in terms of prediction radius and multiple broadcasting sources.

7.4 Closure

The experimental results from this study answer the initial research question. Kriging does provide the necessary accuracy to generate REMs. More particularly, OK provides the most accurate predictions of received power for transmission in the UHF band, using the least information. Since kriging is measurement-based, it cannot fully replace conventional propagation models in applications such as network planning where there is no existing network.

The most astounding finding is, probably, the low sample density required by kriging. The combination of the small number of samples and the suitability of random sampling could also have great advantageous financial and practical implications.

Looking forward to the analogue switch-off and the arrival of DTT in South-Africa, kriging presents an answer to the efficient use of TV white space through DSA. Considering the ever increasing demand for mobile data communications, kriging could prove to be very useful in the implementation of CR using REMs.

Bibliography

[1] IEEE Standards Association, "IEEE Standard Definitions and Concepts for Dynamic Spectrum Access: Terminology Relating to Emerging Wireless Networks, System Functionality, and Spectrum Management," *IEEE Std 1900.1a-2012*, no. January, 2013.

[2] S. Haykin, "Cognitive Radio : Brain-Empowered Wireless Communications," *IEEE Journal on Selected Areas in Communication*, vol. 23, no. 2, pp. 201–220, 2005.

[3] S. Kim, "Cooperative spectrum sensing for cognitive radios using kriged kalman filtering," *IEEE Journal of Selected Topics in Signal Processing*, vol. 5, no. 1, pp. 24–36, 2011.

[4] L. Cao and H. Zheng, "Balancing Reliability and Utilization in Dynamic," *IEEE/ACM Transactions on Networking*, vol. 20, no. 3, pp. 651–661, 2012.

[5] A. B. H. Alaya-Feki, S. B. Jemaa, B. Sayrac, P. Houze, and E. Moulines, "Informed spectrum usage in cognitive radio networks: Interference cartography," in *2008 IEEE 19th International Symposium on Personal, Indoor and Mobile Radio Communications*. Cannes: IEEE, Sep. 2008, pp. 1–5.

[6] M. Ferreira, "Spectral opportunity analysis of the terrestrial television frequency bands in South Africa," Ph.D. dissertation, North-West University, Potchefstroom, 2013.

[7] The Digital Video Broadcasting Project. DVB Worldwide. [Nov. 12, 2014]. [Online]. Available: https://www.dvb.org/worldwide

[8] "Explanatory Memorandum on the Repeal of the Digital Migration Regulations and the Publication of the Draft Digital Terrestrial Television Regulations for Public Comment," in *Government Gazette*, Republic of South Africa, 2011, vol. 34642, notice 680.

[9] "Position Paper on Digital Migration Regulations," in *Government Gazette*, Republic of South Africa, 2013, vol. 36170, notice 119.

[10] M. Ferreira and A. Helberg, "Spectral Opportunity Modelling in the Terrestrial Broadcast Frequency Spectrum," in *Southern Africa Telecommunication Networks and Applications Conference (SATNAC)*, George, Western Cape, RSA, 2012.

[11] M. Lazarus, "The Great Spectrum Famine," *IEEE Spectrum*, vol. 47, no. 10, pp. 26–31, 2010.

[12] J. Li and A. D. Heap, "A review of spatial interpolation methods for environmental scientists," Record 2008/23, p. 137, 2008, [Jul. 21, 2014]. [Online]. Available: http://ga.gov.au/webtemp/image_cache/GA12526.pdf

[13] R Core Team and R Foundation For Statistical Computing, "R: A Language and Environment for Statistical Computing," Vienna, Austria, p. 2673, 2014, [Aug. 11, 2014]. [Online]. Available: http://www.r-project.org

[14] D. J. Griffiths, "Electromagnetic Waves," in *Introduction to Electrodynamics*, 3rd ed., A. Reeves and K. Dellas, Eds. Pearson Education, 2008, ch. 9, pp. 364–415.

[15] D. Roberson and W. Webb, "Radio frequency spectrum and regulation," in *Cognitive Radio Communications and Networks*, A. M. Wyglinski, M. Nekovee, and Y. T. Hou, Eds. Academic Press, 2010, ch. 2, pp. 15–39.

[16] C. Haslett, *Essentials of radio wave propagation*. John Wiley & Sons, Inc., 2007, [Jun. 6, 2013]. [Online]. Available: http://onlinelibrary.wiley.com/doi/10.1002/cbdv.200490137/abstract

[17] A. G. Longley and P. L. Rice, "Prediction of tropospheric radio transmission loss over irregular terrain - A computer method," Institute for Telecommunication Sciences, Boulder, Colorado, Tech. Rep., 1968.

[18] H. Boudreau, E. Boudreau, R. Duville, I. Wireless, and P. Consortium, "TIL-TEK Antenna Seminar," [Nov. 4, 2014]. [Online]. Available: http://www.streakwave.com/til-tek/antenna_course.pdf

[19] O. Thoke, "The Longley-Rice Propagation Model and TV White Space for Ultra WiFi," 2011, [Sep. 16, 2013]. [Online]. Available: http://www.brighthubengineering.com/consumer-appliances-electronics/102752-the-longley-rice-propagation-model-and-tv-white-space-for-ultra-wifi/

[20] G. Hufford, A. Longley, and W. Kissick, "A guide to the use of the ITS irregular terrain model in the area prediction mode," Institute for Telecommunication Sciences, Tech. Rep. April, 1982, [Aug. 13, 2013]. [Online]. Available: http://www.its.bldrdoc.gov/pub/ntia-rpt/82-100/82-100.pdf

[21] D. Wicek and D. Wypiór, "New SEAMCAT Propagation Models : Irregular Terrain Model," *Journal of Telecommunications and Information Technology*, vol. 2011, no. 3, pp. 131–140, 2011.

[22] S. E. Shumate, "Longley-Rice's terrain irregularity parameter, Delta-H," *IEEE Broadcasting Technology Society Newsletter*, vol. 16, no. 4, pp. 23–25, 2008.

[23] "Engineering Charts," in *Federal Communications Commission (FCC)*, USA, 2012, vol. 4, regulation 73.333, p. 118.

[24] E. Rodriguez, C. Morris, J. Belz, E. Chapin, J. Martin, W. Daffer, and S. Hensley, "An assessment of the SRTM topographic products," Jet Propulsion Laboratory, Tech. Rep. JPL D-31639, 2005.

[25] C. Phillips, D. Sicker, and D. Grunwald, "Bounding the Practical Error of Path Loss Models," *International Journal of Antennas and Propagation*, vol. 2012, pp. 1–21, 2012.

[26] N. Faruk, A. A. Ayeni, and Y. A. Adediran, "On the study of empirical path loss models," *Progress In Electromagnetics Research B*, vol. 49, no. February, pp. 155–176, 2013.

[27] C. Phillips, S. Raynel, J. Curtis, S. Bartels, and D. Sicker, "The efficacy of path loss models for fixed rural wireless links," in *Passive and Active Measurement: 12th International Conference*, N. Spring and G. F. Riley, Eds. Springer-Verlag, 2011, pp. 42–51.

[28] P. Lazaridis, A. Bizopoulos, S. Kasampalis, J. Cosmas, and Z. Zaharis, "Evaluation of prediction accuracy for the Longley-Rice model in the FM and TV bands," in *Proceedings of the XI International Conference ETAI 2013*, no. September, Ohrid, Republic of Macedonia, 2013.

[29] S. Kasampalis, P. I. Lazaridis, Z. D. Zaharis, A. Bizopoulos, J. Cosmas, and S. M. Ieee, "Comparison of Longley-Rice , ITM and ITWOM propagation models for DTV and FM Broadcasting," in *GWS-2013 conference*, Atlantic City, NJ, USA, 2013.

[30] S. E. Shumate, "Longley-Rice and ITU-P.1546 Combined: A New International Terrain-Specific Propagation Model," in *72nd IEEE Vehicular Technology Conference Fall*. Ottawa, ON: IEEE, 2010, pp. 1–5.

[31] ——, "NTIA releases updated Version 7.0 of the Longley-Rice Irregular Terrain Model," *IEEE Broadcasting Technology Society Newsletter*, vol. 15, no. 3, pp. 20–22, 2007.

[32] ——, "More on Longley-Rice: Error Codes Decoded, Out-of-Date Instructions, and An Updated Free Wrap-Around," *IEEE Broadcasting Technology Society Newsletter*, vol. 15, no. 4, pp. 18–21, 2007.

[33] ——, "On Replacing a 30-Year-old Temporary Patch in Longley-Rice," *IEEE Broadcasting Technology Society Newsletter*, vol. 16, no. 1, pp. 16–18, 2008.

[34] ——, "Longley-Rice and the Irregular Terrain Model," *IEEE Broadcasting Technology Society Newsletter*, vol. 16, no. 2, pp. 22–23, 2008.

[35] ——, "The Irregular Terrain Model (ITM) Averaging System," *IEEE Broadcasting Technology Society Newsletter*, vol. 16, no. 3, pp. 19–21, 2008.

[36] ——, "Longley-Rices Faulty Subroutines, Part 1: Z1SQ1," *IEEE Broadcasting Technology Society Newsletter*, vol. 17, no. 1, pp. 16–17, 2009.

[37] ——, "Longley-Rices Faulty Subroutines, Part 2: dlthx:," *IEEE Broadcasting Technology Society Newsletter*, vol. 17, no. 3, pp. 26–27, 2009.

[38] ——, "Longley-Rices Faulty Subroutines, Part 3: Log vs. Ln Confusion," *IEEE Broadcasting Technology Society Newsletter*, vol. 17, no. 4, p. 26, 2009.

[39] ——, "Longley-Rices Faulty Subroutines: Background on the c++ alos," *IEEE Broadcasting Technology Society Newsletter*, vol. 18, no. 1, pp. 28–31, 2010.

[40] ——, "Longley Rices Most Complex Line of Code," *IEEE Broadcasting Technology Society Newsletter*, vol. 18, no. 2, pp. 29–33, 2010.

[41] ——, "Testing the Fix for Longley-Rices Most Complex Line of Code," *IEEE Broadcasting Technology Society Newsletter*, vol. 18, no. 3, pp. 22–25, 2010.

[42] ——, "An Error in Diffraction Calculation in the ITM?" *IEEE Broadcasting Technology Society Newsletter*, vol. 19, no. 1, pp. 20–21, 2011.

[43] ITU-R, "Method for point-to-area predictions for terrestrial services in the frequency range 30 MHz to 3 000 MHz P Series Radiowave propagation," *Technical Report*, vol. 4, 2009.

[44] N. A. Cressie, "Spatial Prediction and Kriging," in *Statistics for Spatial Data*, revised ed. Wiley Interscience, 1993, ch. 3, pp. 105–210.

[45] D. G. Krige, "A Statistical Approach To Some Basic Mine Valuation Problems on the Witwatersrand," *Journal of Chemical Metallurgical and Mining Society of South Africa*, pp. 201–215, 1952.

[46] W. C. M. van Beers and J. P. C. Kleijnen, "Kriging interpolation in simulation - A survey," in *Proceedings of the 2004 Winter Simulation Conference*, Washington, D.C., 2004, pp. 113–121.

[47] W. R. Tobler, "A computer movie simulating urban growth in the Detroit region," *Economic Geography*, vol. 46, pp. 234–240, 1970.

[48] E. Asa, M. Saafi, J. Membah, and A. Billa, "Comparison of linear and nonlinear kriging methods for characterization and interpolation of soil data," *Journal of Computing in Civil Engineering*, vol. 26, no. 1, pp. 11–19, 2011.

[49] E. H. Isaaks and R. M. Srivastava, *An Introduction to Applied Geostatistics*, A. G. Journel, Ed. New York, United States of America: Oxford University Press, 1989.

[50] T. Hengl, *A Practical Guide to Geostatistical Mapping*, 2nd ed., 2009, [Jul. 15, 2013]. [Online]. Available: http://spatial-analyst.net/book/

[51] R. Christensen, "Linear Models for Spatial Data: Kriging," in *Linear Models for Multivariate, Time Series, and Spatial Data*. Springer-Verlag, 1991, pp. 262–299.

[52] D. O'Sullivan and D. Unwin, *Geographic information analysis*, 2nd ed. John Wiley & Sons, Inc., 2010.

[53] G. Matheron, *The Theory of Regionalized Variables and Its Applications*, 5th ed., Fontainebleau, France, 1971.

[54] E. Englund, D. Weber, and N. Leviant, "The effects of sampling design parameters on block selection," *Mathematical Geology*, vol. 24, no. 3, pp. 329–343, 1992.

[55] R. Bivand, E. Pebesma, and V. Gómez-Rubio, *Applied spatial data analysis with R*, R. Gentleman, K. Hornik, and G. Parmigiani, Eds. Springer, 2008.

[56] A. Journel and C. Huijbregts, *Mining Geostatistics*. Academic Press, London, 1978.

[57] "Geostatistics," in *Handbook of Geographic Information*, W. Kresse and D. M. Danko, Eds. Springer, 2012, pp. 43–59.

[58] D. Arroyo, X. Emery, and M. Peláez, "Sequential Simulation with Iterative Methods," in *Quantitative Geology and Geostatistics*, 17th ed., P. Abrahamsen,

R. Hauge, and O. Kolbjø rnsen, Eds. Oslo, Norway: Springer Science & Business Media Dordrecht, 2012, pp. 3–15.

[59] P. Goovaerts, *Geostatistics for Natural Resources Evaluation*. New York: Oxford University Press, 1997.

[60] K. Krivoruchko, "Chapter 9: Princeples of Modeling Geostatistical Data: Kriging," in *Spatial Statistical Data Analysis for GIS Users*, 1st ed. California, USA: Esri Press, 2011, pp. 349–389.

[61] V. Joseph, Y. Hung, and A. Sudjianto, "Blind kriging: A new method for developing metamodels," *ASME Journal of Mechanical Design*, vol. 130, no. 3, 2008.

[62] C. E. Rasmussen and C. K. I. Williams, *Gaussian Processes for Machine Learning*. Cambridge, Massachusetts: MIT Press, 2006.

[63] P. Hiemstra and R. Sluiter, "Interpolation of Makkink evaporation in the Netherlands," Royal Netherlands Meteorological Institute, De Bilt, Tech. Rep., 2011, [Jun. 6, 2014]. [Online]. Available: http://www.numbertheory.nl/files/report_evap.pdf

[64] D. Greenwood, J. Neeteson, and D. A, "Response of potatoes to N fertilizer," *Plant and Soil*, vol. 85, no. 2, pp. 185–203, 1985.

[65] S. M. Vicente-serrano, M. A. Saz-sánchez, and J. M. Cuadrat, "Comparative analysis of interpolation methods in the middle Ebro Valley (Spain): application to annual precipitation and temperature," *Climate Research*, vol. 24, pp. 161–180, 2003.

[66] J. Devore and N. Farnum, *Applied Statistics for Engineers and Scientists*, 2nd ed. Belmont, CA: Thomson Brooks/Cole, 2005.

[67] N. Walford, *Practical statistics for geographers and earth scientists*. Chichester, UK: John Wiley & Sons, Ltd., 2011.

[68] M. P. Battaglia, "Nonprobability sampling," in *Encyclopedia of Survey Research Methods2*, 2011, no. 1, pp. 523–526.

[69] M. Angjelicinoski, V. Atanasovski, and L. Gavrilovska, "Comparative analysis of spatial interpolation methods for creating Radio Environment Maps," in *19th Telecommunications forum (TELFOR)*. Belgrade, Serbia: IEEE, 2011, pp. 334–337.

[70] R. A. de By, M. C. Ellis, Y. Georgiadou, W. Kainz, R. A. Knippers, M. Kraak, M. M. Radwan, E. J. Sides, Y. Sun, M. J. C. Weir, and C. J. van Westen, *Principles of Geographic Information Systems - An introductory textbook*, R. A. de By, Ed., 2001.

[71] C. Phillips, M. Ton, D. Sicker, and D. Grunwald, "Practical radio environment mapping with geostatistics," in *IEEE International Symposium on Dynamic Spectrum Access Networks (DySPAN)*. Bellevue, WA: IEEE, Oct. 2012, pp. 399–410.

[72] A. Ferreira, A. Braga, G. Cavalcante, and H. Gomes, "Kriging Method Applied to Predict the Coverage Area of Digital TV," in *SIMPÓSIO BRASILEIRO DE TELECOMUNICAÇÕES*, 2012, pp. 1–2.

[73] C. Phillips, D. Sicker, and D. Grunwald, "A Survey of Wireless Path Loss Prediction and Coverage Mapping Methods," *IEEE Communications Surveys & Tutorials*, vol. 15, no. 1, pp. 255–270, 2013.

[74] S. Grimoud, B. Sayrac, S. B. Jemaa, and E. Moulines, "An Algorithm for Fast REM Construction," in *6th International ICST Conference on Cognitive Radio Oriented Wireless Networks and Communications (CROWNCOM)*. Osaka: IEEE, 2011, pp. 251–255.

[75] A. B. H. Alaya-feki, B. Sayrac, S. Ben, I. Moulineaux, and E. Moulines, "Interference Cartography for Hierarchical Dynamic Spectrum Access," in *3rd IEEE Symposium on New Frontiers in Dynamic Spectrum Access Networks*. Chicago, IL: IEEE, 2008, pp. 1–5.

[76] C. Phillips, "Geostatistical Techniques for Practical Wireless Coverage Mapping," Ph.D. dissertation, University of Colorado at Boulder, 2012.

[77] A. Achtzehn, J. Riihij, G. Mart, M. Petrova, and M. Petri, "Improving Coverage Prediction for Primary Multi-Transmitter Networks Operating in the TV Whites-

paces," in *9th Annual IEEE Communications Society Conference on Sensor, Mesh and Ad Hoc Communications and Networks (SECON)*. Seoul: IEEE, 2012, pp. 547–555.

[78] J. Ojaniemi, J. Poikonen, and R. Wichman, "Effect of geolocation database update algorithms to the use of TV white spaces," in *7th International ICST Conference on Cognitive Radio Oriented Wireless Networks and Communications (CROWNCOM)*. Stockholm: IEEE, 2012, pp. 18–23.

[79] A. Achtzehn and J. Riihij, "Improving Accuracy for TVWS Geolocation Databases : Results from Measurement-Driven Estimation Approaches," in *IEEE International Symposium on Dynamic Spectrum Access Networks (DYSPAN)*. McLean, VA: IEEE, 2014, pp. 392–403.

[80] J. Ojaniemi, J. Kalliovaara, A. Alam, J. Poikonen, and R. Wichman, "Optimal field measurement design for radio environment mapping," in *47th Annual Conference on Information Sciences and Systems (CISS)*. Baltimore, MD: IEEE, 2013, pp. 1–6.

[81] Y. Tillé and A. Matei, "sampling: Survey Sampling," *R package version 2.6*, 2013, [Aug. 12, 2014]. [Online]. Available: http://cran.r-project.org/package=sampling

[82] E. J. Pebesma, "Multivariable geostatistics in S: the gstat package," *Computers & Geosciences*, vol. 30, no. 7, pp. 683–691, Aug. 2004.

[83] P. A. Burrough and R. A. Mcdonnell, "Data Models and Axioms," in *Principles of Geographical Information Systems*, 1998, pp. 17–34.

[84] F. C. Collins and P. V. Bolstad, "A comparison of spatial interpolation techniques in temperature estimation," in *Third International Conference/Workshop on Integrating GIS and Environmental Modeling*, 1996.

[85] R. Webster and M. A. Oliver, "Sample adequately to estimate variograms of soil properties," *Journal of Soil Science*, vol. 43, pp. 177–192, 1992.

[86] T. J. Hastie and D. Pregibon, "Generalized linear models," in *Statistical Models in S*, J. M. Chambers and T. J. Hastie, Eds. Wadsworth & Brooks/Cole, 1992.

[87] W. N. Venables and B. D. Ripley, *Modern Applied Statistics with S*, 4th ed. New York: Springer, 2002.

[88] I. Couckuyt, A. Forrester, and D. Gorissen, "Blind Kriging: Implementation and performance analysis," *Advances in Engineering Software*, vol. 49, no. 0, pp. 1–13, 2012.

[89] I. Couckuyt, F. Declercq, T. Dhaene, H. Rogier, and L. Knockaert, "Surrogate-Based Infill Optimization Applied to Electromagnetic Problems," *International Journal of RF and Microwave Computer-Aided Engineering (RFMiCAE)*, vol. 20, no. 5, pp. 492–501, 2010.

[90] T. Dhaene, "ooDACE - A Matlab Kriging toolbox: Getting started," 2013, [Jan. 21, 2014]. [Online]. Available: http://www.sumo.intec.ugent.be/ooDACE_download

[91] P. Ribeiro JR and P. Diggle, "geoR: A package for geostatistical analysis," *R-News*, vol. 1, no. 2, 2001.

[92] E. J. Pebesma, "Multivariate geostatistics in S: the gstat package," *Computers & Geoscience*, vol. 30, pp. 683–691, 2004.

[93] R. Bivand, T. Keitt, and B. Rowlingson, "rgdal: Bindings for the Geospatial Data Abstraction Library," *R package version 0.8-16*, 2014, [Aug. 11, 2014]. [Online]. Available: http://cran.r-project.org/package=rgdal

[94] J. A. Magliacane, "SPLAT! Because the world isn't flat!" 2014, [Jan. 23, 2014]. [Online]. Available: http://www.qsl.net/kd2bd/splat.html

[95] J. A. Magliacane, D. McDonald, and R. Bentley, "SPLAT! user manual," no. February, pp. 1–19, 2011, [Mar. 26, 2014]. [Online]. Available: http://www.qsl.net/kd2bd/splat.html

[96] The Independent Communications Authority of South Africa, "ICASA - The Independent Communications Authority of South Africa," 2014, [Feb. 20, 2014]. [Online]. Available: https://www.icasa.org.za/

[97] "Terrestrial broadcasting frequency plan 2013," in *Government Gazette*, Republic of South Africa, 2 Apr. 2013, vol. 36321, notice 298.

[98] J. Schuenemeyer and L. Drew, *Statistics for earth and environmental scientists*. Hoboken, NJ, USA: John Wiley & Sons, Inc., 2011.

[99] N. Mantel, "The Detection of Disease Clustering and a Generalized Regression Approach," *Cancer Research*, vol. 27, no. 2, pp. 209–220, 1967.

[100] T. Hengl, D. Rossiter, and A. Stein, "Soil sampling strategies for spatial prediction by correlation with auxiliary maps," *Australian Journal of Soil Research*, vol. 41, pp. 1403–1422, 2003.

[101] R. A. Becker, J. M. Chambers, and A. R. Wilks, *The New S Language: A Programming Environment for Data Analysis and Graphics*. Monterey, CA, USA: Wadsworth and Brooks/Cole Advanced Books & Software, 1988.

[102] B. D. Ripley, *Stochastic Simulation*. John Wiley & Sons, Inc., 1987.

[103] H. Akima, "Algorithm 761: scattered-data surface fitting that has the accuracy of a cubic ploynomial," *ACM Transactions on Mathematical Software*, vol. 22, pp. 362–371, 1996.

Appendix A

SPLAT! input files

This appendix demonstrates the structure of the site information files required by SPLAT! to perform the Longley-Rice ITM. The information given in the QTH and LRP files are used in addition to the DEM data to model propagation.

A.1 QTH file

The QTH file is the site location file. This file contains the geographic coordinates of the TV broadcasting station as well as the height AGL of the antenna. The following example shows the QTH file for the first broadcasting station in the available database:

```
1               ; Station name
-32.4778        ; Latitude
-24.0506        ; Longitude
18m             ; Antenna height AGL
```

The geographic coordinates of the station can be expressed in the decimal format or in degree, minute, second (DMS) format [95]. Coordinates north of the equator are indicated by positive latitudes while coordinates east of the Greenwich Meridian are

indicated by negative longitudes.

The height of the antenna is assumed to be given in feet. However, the available data specifies the height in metres. Fortunately, SPLAT! allows the antenna height to be specified in metres by adding an m to the height.

A.2 LRP file

The LRP file defines the ITM parameters that affect the RF propagation. The following is an example of a generated LRP file:

```
15.000   ; Earth Dielectric Constant (Relative permittivity)
0.005    ; Earth Conductivity (Siemens per metre)
301.000  ; Atmospheric Bending Constant (N-units)
471.25   ; Frequency in MHz (20 MHz to 20 GHz)
5        ; Radio Climate (5 = Continental Temperate)
1        ; Polarization (0 = Horizontal, 1 = Vertical)
0.50     ; Fraction of situations (50% of locations)
0.90     ; Fraction of time (90% of the time)
5.0119   ; Effective Radiated Power (ERP) in Watts (optional)
```

Appendix B

Randomly selected sites

This appendix includes all details regarding the TV broadcasting transmitter stations that were used throughout this dissertation. All of these sites were selected using the random selection process discussed in section 3.2.1.

B.1 Test for the effect of the Longley-Rice prediction variance

Table B.1: Sites used in testing the effect of the Longley-Rice prediction variance

	Site nr	Station name	Latitude	Longitude	Channel antenna			
					Frequency (MHz)	AGL (m)	ERP (W)	Pol
A	318	LAINGSBURG WILGRBOME	-32.7636	20.9067	583.25	10	63.0957	V
B	341	LYDENBURG DOORNHOEK	-25.3564	30.3578	623.25	10	3.2359	V
C	498	REITZ	-27.7919	28.45	615.25	10	5.0119	V
D	566	STILBAAI	-34.3653	21.4236	719.25	30	3.2359	V
E	741	VILLA NORA	-23.7	28.35	498	189	40000	H

B.2 Test for the effect of prediction radius and sample density

Table B.2: Sites used in testing the effect of prediction radius and sample density

	Site nr	Station name	Latitude	Longitude	Channel antenna			
					Frequency (MHz)	AGL (m)	ERP (W)	Pol
A	146	ELLIOT	-31.1767	27.8658	767.25	72	398.1072	V
B	287	KLERKSDORP	-26.7539	26.4081	559.25	253	100000	H
C	323	LIME ACRES C69	-28.3575	23.465	647.25	22	6.0256	V
D	554	STEINKOPF	-29.2483	17.7386	607.25	20	3.9811	V
E	89	CALVINIA	-31.3842	19.7825	479.25	221	10000	H

B.3 Test for the effect of different covariates

Table B.3: Sites used in testing the effect of different covariates

	Site nr	Station name	Latitude	Longitude	Channel antenna			
					Frequency (MHz)	AGL (m)	ERP (W)	Pol
A	136	DORINGKRUIN	-26.8181	26.6833	847.25	24	19.9526	V
B	308	LADISMITH AMALIENSTN	-33.4911	21.4897	551.25	10	1.2882	V
C	422	NTL ANTH BOSHOEK	-27.8264	31.0456	663.25	10	5.0119	V
D	573	STRANDFONTEIN CP	-31.7569	18.2286	543.25	37	0.50119	V
E	712	KNYSNA	-34.0717	23.0431	498	24	500	V

B.4 Test for spatial autocorrelation

Table B.4: Sites used in testing for spatial autocorrelation

	Site nr	Station name	Latitude	Longitude	Channel antenna			
					Frequency (MHz)	AGL (m)	ERP (W)	Pol
1	136	DORINGKRUIN	-26.8181	26.6833	847.25	24	19.9526	V
2	221	HEIDELBERG CP	-34.0981	20.9489	495.25	10	3.9811	V
3	308	LADISMITH AMALIENSTN	-33.4911	21.4897	551.25	10	1.2882	V
4	422	NTL ANTH BOSHOEK	-27.8264	31.0456	663.25	10	5.0119	V
5	433	PAARL	-33.7147	18.94	599.25	137	1995.2623	V
6	459	PILGRIMSRUS VAK.OORD	-24.8531	30.7181	607.25	10	3.9811	V
7	554	STEINKOPF	-29.2483	17.7386	607.25	20	3.9811	V
8	573	STRANDFONTEIN CP	-31.7569	18.2286	543.25	37	0.50119	V
9	682	WILLOWMORE II	-33.2925	23.4956	471.25	30	2.5119	V
10	712	KNYSNA	-34.0717	23.0431	498	24	500	V

B.5 100 experimental sites

Table B.5: 100 randomly selected sites used in final experiment (1 of 2)

Site nr	Station name	Latitude	Longitude	Channel antenna			
				Frequency (MHz)	AGL (m)	ERP (W)	Pol
104	CERES C12.1	-33.2536	19.4589	503.25	10	125.8925	V
113	CLIFTON	-33.9417	18.3769	471.25	11	10	H
116	COLESBERG	-30.7083	25.0578	487.25	12	501.1872	V
12	AMANDA GLEN	-33.855	18.6758	471.25	9	19.9526	V
124	DANIELSKUIL	-28.1775	23.5483	471.25	10	3.9811	V
129	DELAREYVILLE	-26.705	25.4594	615.25	25	25.1189	V
134	DORDRECHT	-31.3853	27.0364	495.25	15	7.9433	V
136	DORINGKRUIN	-26.8181	26.6833	847.25	24	19.9526	V
150	ENGCOBO	-31.6719	28.0067	623.25	10	3.02	V
153	ENTSHATSHONGO	-32.1442	28.6694	511.25	40	50118.7234	V
163	FORT BEAUFORT LORR	-32.6425	26.6592	663.25	0	1.5849	V
166	FRANSCHHOEK	-33.9072	19.0739	727.25	23	3981.0717	V
173	GANYESA	-26.6033	24.2667	479.25	155	30199.5172	H
181	GLENCOE	-28.1511	29.9475	487.25	135	100000	H
191	GRAHAMSTOWN C9	-33.3283	26.5011	535.25	10	6.3096	V
193	GRAVELOTTE MURCHISON	-23.8856	30.7144	695.25	10	7.9433	V
201	GROOT BRAKRIVIER	-34.0419	22.2167	487.25	14	25.1189	V
205	GROOTDERM KODASPIEK	-28.2275	16.9931	519.25	10	50.1187	V
207	GROOTDERM SENDLNGDRF	-28.1233	16.8978	495.25	10	1	V
209	HANKEY	-33.8372	24.8856	615.25	12	10	V
221	HEIDELBERG CP	-34.0981	20.9489	495.25	10	3.9811	V
223	HEILBRON	-27.2914	27.9647	655.25	12	1	V
230	HEXR SANDHLS KANETVL	-33.5167	19.5356	807.25	10	0.1	V
232	HLOBANE ALPHA AN	-27.7242	31.1267	767.25	15	0.50119	V
234	HLOBANE COLLIERY	-27.715	30.9931	479.25	10	1.9953	V
237	HOEDSPRUIT	-24.5417	30.8689	615.25	160	100000	H
240	HOPETOWN	-29.6297	24.085	607.25	30	10	V
248	IFAFA MARINA	-30.4392	30.6397	559.25	10	1.9953	V
25	BARBERTON SHEBA LINK	-25.7017	31.1242	751.25	10	1.9953	V
260	KAKAMAS SEEKOEISTEEK	-28.4572	20.0472	735.25	10	5.6234	V
271	KESTELL O74.2	-28.3014	28.7142	543.25	10	6.3096	V
278	KKL KRAKEELRIVIER	-33.7911	23.7064	583.25	10	1.9953	V
295	KOKSTAD	-30.6117	29.49	575.25	12	398.1072	V
299	KOPPIES	-27.2347	27.5744	623.25	25	5.0119	V
308	LADISMITH AMALIENSTN	-33.4911	21.4897	551.25	10	1.2882	V
319	LAMBERTS BAY C20	-32.0942	18.3128	751.25	18	2.5119	V
323	LIME ACRES C69	-28.3575	23.465	647.25	22	6.0256	V
33	BARKLY EAST C37.1	-30.9806	27.6292	583.25	10	0.50119	V
332	LOUIS TRICHARDT	-22.9922	29.9019	639.25	10	100	V
338	LOXTON	-28.0428	23.1122	647.25	10	158.4893	V
339	LUTZVILLE	-31.5531	18.3422	607.25	10	1.9953	V
355	MARYDALE	-29.4144	22.0942	599.25	18	1.9953	V
358	MATATIELE LINK N51	-30.35	28.8097	655.25	10	3.9811	H
365	MESSINA LINK	-22.3531	29.9619	735.25	20	141.2538	V
375	MOGOBOYA	-23.9933	30.2164	599.25	17	50.1187	V
376	MONDEOR	-26.2811	27.9928	479.25	19	89.1251	V
387	MOUNT AYLIFF	-30.8364	29.3947	487.25	136	1000	H
390	MSAULI MINE LINK	-25.9203	31.1253	599.25	10	3.9811	V
394	MTSHANYANA	-31.8567	27.6708	727.25	10	1.9953	V
408	NEW PAN HELLENIC	-26.15	28.1314	832.5	10	100	H

Table B.6: 100 randomly selected sites used in final experiment (2 of 2)

Site nr	Station name	Latitude	Longitude	Channel antenna			
				Frequency (MHz)	AGL (m)	ERP (W)	Pol
410	NEWCASTLE	-27.7186	29.9533	663.25	61	1000	V
422	NTL ANTH BOSHOEK	-27.8264	31.0456	663.25	10	5.0119	V
426	OHRIGSTAD BRANDDRAAI	-24.5292	30.6392	599.25	0	6.3096	V
433	PAARL	-33.7147	18.94	599.25	137	1995.2623	V
437	PATENSIE BOERE C8.5	-33.7608	24.8269	815.25	10	7.9433	V
45	BETHANIE	-25.5606	27.5872	655.25	31	39.8107	V
456	PILGRIMSRUS BUFFELHK	-24.6878	30.7275	743.25	10	6.0256	V
459	PILGRIMSRUS VAK.OORD	-24.8531	30.7181	607.25	10	3.9811	V
464	POFADDER KLEINPELLA	-29.0053	18.9697	615.25	10	3.2359	V
465	POFADDER WILLEM OPD	-29.3642	19.8181	471.25	20	1.9953	V
468	PONGOLA	-27.5261	31.65	479.25	12	141.2538	V
469	PORT ALFRED	-33.6	26.8872	727.25	28	5.0119	V
470	PORT EDWARD EDEN	-31.0653	30.1897	687.25	10	0.19953	V
482	PRIESKA	-29.6686	22.7403	615.25	10	1	V
501	RICHARDS BAY	-28.7861	32.1067	647.25	12	190.5461	V
506	RIEMVASMAAK SENDING	-28.4603	20.3303	727.25	10	3.9811	V
513	ROOSSENEKAL MAPOCHS	-25.1975	29.9156	607.25	10	1.9953	V
516	RUSTENBURG PLATINM A	-24.8056	27.3369	695.25	34	19.9526	V
518	SABIE	-25.1289	30.7594	735.25	12	25.1189	V
52	BEZ VALLEY	-26.1947	28.0844	495.25	19	69.1831	V
53	BLIKANA	-30.58	27.6292	615.25	10	1.9953	V
531	SENEKAL	-28.2553	27.5072	607.25	222	1995.2623	H
540	SOMERSET EAST	-32.7125	25.5781	727.25	12	50.1187	V
544	SPRINGBOK MATJIESKLF	-29.6697	17.8792	623.25	10	1	V
552	STEELPOORT MOKOME	-24.7806	30.1322	495.25	10	19.9526	V
554	STEINKOPF	-29.2483	17.7386	607.25	20	3.9811	V
562	STEYTLERVILE	-33.3167	24.3447	751.25	10	3.02	V
573	STRANDFONTEIN CP	-31.7569	18.2286	543.25	37	0.50119	V
585	SUTHERLAND RHEN RIV.	-32.1756	20.6914	519.25	0	3.2359	V
586	SUTHERLAND TAFELBRGP	-32.2531	21.0961	759.25	10	3.9811	V
618	UGIE	-31.2111	28.2275	559.25	30	7.9433	V
625	UNDERBERG	-29.7992	29.5106	599.25	10	3.9811	V
649	VILLIERSDORP ELANDSK	-33.9078	19.2786	471.25	10	2.5119	V
65	BRANDVLEI	-30.1	20.4333	730	220	100000	H
664	WARDEN O74.3	-27.8339	28.9756	503.25	10	6.3096	V
665	WARRENTON	-28.1142	24.8489	647.25	10	19.9526	V
674	WILLISTON	-31.3439	20.9189	607.25	12	3.9811	V
680	WILLISTON TWEEMIK	-30.6861	21.1561	511.25	10	5.0119	V
682	WILLOWMORE II	-33.2925	23.4956	471.25	30	2.5119	V
683	WILLOWMORE STUDTIS	-33.6264	24.1117	511.25	10	3.9811	V
692	ZEERUST	-25.8603	26.0478	623.25	252	100000	H
699	ENGCOBO	-31.6556	28.0094	658	35	10000	V
712	KNYSNA	-34.0717	23.0431	498	24	500	V
721	MONDEOR	-26.2811	27.9978	738	19	20	V
729	SEVERN	-26.4	23.0667	690	251	40000	H
730	SHANZHA	-22.96	30.2333	594	8	2000	V
74	BUFFELSRIVIER	-29.6994	17.5989	743.25	18	3.9811	V
75	BURGERDORP	-31.0008	20.1208	679.25	0	10	V
76	BURGERSDORP	-31.0006	26.3392	615.25	12	100	V
81	BUTTERWORTH	-32.2764	28.2069	471.25	253	5011.8723	H

B.6 Verification of the created 10-fold CV algorithm

Table B.7: Sites used for the verification of the created 10-fold CV algorithm

	Site nr	Station name	Latitude	Longitude	Channel antenna			
					Frequency (MHz)	AGL (m)	ERP (W)	Pol
A	201	GROOT BRAKRIVIER	-34.0419	22.2167	487.25	14	25.1189	V
B	416	NONGOMA	-27.905	31.6575	562	194	10000	H
C	459	PILGRIMSRUS VAK.OORD	-24.8531	30.7181	607.25	10	3.9811	V
D	587	SUTHERLAND VYFFONTN	-32.4217	20.5839	535.25	10	0.1	H
E	588	SUTHERLAND WELG DE-K	-32.6775	20.7986	567.25	10	2.5704	V

B.7 Validation of OK implementation in R

Table B.8: Sites used for the validation of the OK implementation in R

	Site nr	Station name	Latitude	Longitude	Channel antenna			
					Frequency (MHz)	AGL (m)	ERP (W)	Pol
A	187	GRAAFF-REINET	-32.2617	24.5031	511.25	10	0.50119	V
B	202	GROOT MARICO	-25.6197	26.4356	647.25	48	199.5262	V
C	378	MONTAGU	-33.7872	20.1436	514	12	50.1187	V
D	568	STILBAAI MELKHOUTFNT	-34.3333	21.4092	495.25	10	3.02	V
E	702	GROOTDERM	-28.4333	17.0833	522	183	30000	H

Appendix C

Article published on this research

The following article was published in the proceedings of the *Southern Africa Telecommunication Networks and Applications Conference (SATNAC) 2014*. The conference is hosted by Telkom, annually. It was held in Port Elizabeth, South Africa, and the paper was presented as part of the *Standards, Regulatory & Environmental* sessions.

Received power prediction of a terrestrial TV broadcasting transmitter using ordinary kriging interpolation

Willem H. Boshoff, Magdalena J. Grobler, Melvin Ferreira
TeleNet Research Group
School of Electrical, Electronic and Computer Engineering
North-West University, Potchefstroom Campus
Email: {21625158, leenta.grobler, melvin.ferreira}@nwu.ac.za

***Abstract* – Radio Environment Mapping (REM) provides information useful for many different applications in the telecommunications field. In this paper the authors evaluate the ability of ordinary kriging (OK) to produce a REM without the large number of samples typically required. The kriging model is generated using different sizes of received power input sample sets over a 5 km radius surrounding a transmitter. The input sample selection is discussed as well as the implementation of the OK model in MATLAB. The authors compare contour maps of the received power predicted by the kriging model to the SPLAT generated map and the kriging model is validated through cross-validation and by inspecting the semi-variogram. The authors find that the OK model produces a Root-Mean-Squared Error (RMSE) of less than 6 dBm for sample set sizes larger than 500 samples as well as a very small ratio between the RMSE and the variation in the input data.**

***Index Terms* - Cognitive radio, Dynamic Spectrum Access, kriging interpolation, Longley-Rice ITM, ordinary kriging, Radio Environment Mapping, TV white space**

I. INTRODUCTION

The concept of cognitive radio (CR) is defined as a radio system with the ability to assess its surrounding geographical and operational environment, to obtain knowledge and accordingly adapt to changes in its operating parameters and protocols in a dynamic and autonomous way [1]. This is done in an effort to provide reliable communication, independent of its location and which is spectrally efficient [2].

A difficult task in the journey toward CR functionality is providing the ability to dynamically access the frequency spectrum. This can, in turn, lead to effective utilisation of spectral opportunity inside the spectrum. Recently, spatial re-use techniques enjoyed increasing attention, where CRs are allowed to transmit and receive within specified interference constraints [3]. Therefore, research on Power Spectral Density (PSD) maps became of interest as a method of obtaining information on Radio Frequency (RF) traffic in terms of time, space and frequency.

A proposed solution to improve utilisation of the frequency spectrum is Dynamic Spectrum Access (DSA). This involves wireless devices sharing locally available spectrum based on real time demands rather than making use of statically allocated frequencies [4]. Proposed solutions to characterise the spectral use in the area of interest, are the use of interference cartography, channel gain maps or PSD maps. These solutions can collectively be referred to as Radio Environment Mapping (REM).

In order to generate REMs, many measurement samples covering the entire area of interest are required. If a propagation modelling approach is followed, the transmitter data as well as the topographical information of the entire area of interest are required.

Taking the required amount of empirical measurements is, although preferred, usually very time consuming and the mobile measuring equipment needed is also expensive. Another problem arises when samples need to be measured using a grid fashioned approach. In this case, sampling locations can be difficult or impractical to reach with the equipment. A third problem is introduced by experimental variances due to the dynamic RF environment. Finally, in order to get a good resolution, a lot of measurements are required.

In this paper the authors evaluate the ability of ordinary kriging (OK) to produce a REM without the large number of samples typically required. The output of the Longley-Rice Irregular Terrain Model (ITM) is considered as measurements at designated points from which a randomly selected sample set is collected. For the purpose of this evaluation, the ITM output is taken as the ground truth. Hence, the authors will evaluate the ability of OK to aid in constructing a REM using significantly less sample points in comparison to what would be required if one were to measure these points in the field. More specifically as a case study, the authors consider the Aggeneys Black Mountain transmitter located in Aggeneys in the Northern Cape province of South Africa.

The remainder of this document is structured as follows: a brief background on OK and the Longley-Rice ITM are given in section II, followed by section III which elaborates on the simulation tools used for this experiment. Section IV will give more insight into the research methodology that was followed and precedes the experimental results in section V. The results are evaluated in section VI and the authors come to a conclusion in section VII.

II. BACKGROUND

A. Spatial Interpolation

There are numerous different spatial interpolation techniques, geostatistical and non-geostatistical. Each of these has their own advantages and disadvantages for certain situations [5]. The main purpose of interpolation methods is to make inferences of certain properties at locations using only limited data of the surrounding spatial area.

Due to its optimal results when input assumptions are met and its robustness when they are not met, the authors have chosen to investigate kriging as a candidate for effectively producing REMs using the least possible irregularly spaced samples.

B. Kriging Interpolation

Kriging is a very popular spatial interpolation technique used in geostatistics. Geostatistics is the area in statistics that focuses on geographical applications such as meteorology, mining exploration and other environmental sciences [6]. This technique was originally introduced by a South African mining engineer Danie Krige [7] by whom it was used to map mineral resources by using scattered measurements. The method is based on spatial autocorrelation which originates from the first law of geography (or Tobler's first law). This law states that everything is related to everything else, but near things are more related than distant things [6].

The kriging interpolation technique is generally used for spatial data and has a few variations of implementation. The three most common variations are: simple kriging (SK), ordinary kriging (OK) and universal kriging. Another variation is co-kriging. All of these variations are conceptually the same but differ in the parametrical assumptions that are made.

OK is a B.L.U.E. (Best Linear Unbiased Estimator) spatial interpolation method since the estimates are weighted linear combinations of the sample data used, it attempts to achieve a mean error of zero and minimises the error variance. Last mentioned feature distinguishes OK from other spatial interpolation techniques [8].

Another favourable characteristic of OK is the fact that the points are estimated using the covariances between the data samples and between the estimation point and the data samples. This means that the estimation does not depend on the locations of the sampled data points but rather the separation between them.

What defines OK as an spatial prediction method is the following two assumptions [9], [10]:

1. Model assumption:

$$Z(\boldsymbol{s}) = \mu + \delta(\boldsymbol{s}), \qquad \boldsymbol{s} \in \boldsymbol{D}, \quad \mu \in \mathbb{R}, \quad \textit{and } \mu \textit{ unknown.} \tag{1}$$

,where μ is an constant unknown regression function (i.e. $\mu = \alpha_0$ with α_0 being a constant unknown value) and δ is a Gaussian process constructed from the residuals. The constant regression function means that the technique assumes an unknown constant trend in the data [11].

2. Predictor assumption:

$$p(\boldsymbol{Z}; B) = \sum_{i=1}^{n} \lambda_i Z(\boldsymbol{s}_i), \sum_{i=1}^{n} \lambda_i = 1. \tag{2}$$

,where λ_i in this case represents the kriging weights [12], [13] which are assigned to each sample value, $Z(\boldsymbol{s}_i)$, and are used as a linear combination to predict the unknown value (p). The condition of the kriging weights summing to unity in equation (2) ensures the unbiasedness.

OK utilises a semi-variogram to determine the kriging weights. The model semi-variogram is a curve that is fitted to the experimental semi-variogram. The experimental semi-variogram is calculated by finding the average of the semi-variance cloud for each separation distance of the sample data points. It is also common practice to determine the semi-variogram from the correlogram. A correlogram is usually derived from the correlation matrix describing the correlation between the input samples. The relationship between the semi-variogram and the correlogram is shown in equation (3).

$$\gamma(h) = 1 - c(h) \tag{3}$$

where γ is the semi-variance function, h is the separation between sample points (known as the lag) and c is the correlation function of the correlogram. The model semi-variogram is an indication of how the point being estimated is related to the sample points considering the distance between them.

C. Longley-Rice Irregular Terrain Model

Currently, REMs are mainly generated by using radio wave propagation models. The Longley-Rice ITM is a very popular terrain specific model for this application.

The Longley-Rice model is a radio propagation model used to predict radio signal attenuation over irregular terrain relative to free-space transmission loss. This method is designed for the frequency range 20 MHz to 20 GHz and path lengths from 5 km to 2000 km [14]. It is also known as the Institute for Telecommunication Sciences (ITS) ITM. The model caters for two telecommunication links: point-to-point and point-to-area and it is path specific. The path parameters taken into account in this model are the effective antenna heights, horizon distances and elevation angles, terrain irregularity and reference attenuation. The reference attenuation includes line of sight, diffraction and forward scatter attenuation.

D. ICASA data

The transmitter data used for this research is provided by ICASA (The Independent Communications Authority of South Africa). The data contains information of all analogue and digital broadcasting stations in South Africa as given by the ICASA final terrestrial broadcasting plan of 2013 [15].

III. SIMULATION TOOLS

A. MATLAB ooDACE toolbox

For this research application a kriging toolbox called "ooDACE" (object-oriented Design and Analysis of Computer Experiments) [16], [17] will be used. This

toolbox implements the "Gaussian Process based Kriging surrogate models" [18]. ooDACE [16], [17] is capable of implementing SK, OK, co-kriging, blind kriging and stochastic kriging and supplies several accuracy metrics such as the prediction variance, the process variance and cross-validation prediction error. These metrics can be used to determine the accuracy of the kriging model generated.

B. SPLAT!

SPLAT! is an acronym for a RF Signal Propagation, Loss and Terrain analysis tool. This tool implements the Longley-Rice ITM with enhancements and one of its main applications is in analogue and digital television and radio broadcasting [19]. SPLAT! is a very popular tool among researchers in the radio propagation field [19]. Interoperability with Google Earth also provides scaled and good quality graphical presentation of results.

SPLAT! has different option for point-to-point predictions as well as area predictions. The output is given in the form of two text files, a portable pixmap (ppm) image and a data file.

The output file of importance for this experiment is the alphanumerical data file. This file contains the boundaries of the analysed area as well as the coordinates, azimuths, elevations to first obstruction and the received power in dBm (decibels of the power referenced to one milliwatt) at that specific point [20]. Another file of interest to us is the '.dcf' (SPLAT colour definition) file. This colour definition file assigns a RGB colour value to each 10 dBm increment of received power and it is used to plot the ppm image which marks the transmitter location and shows the received power in dBm for the specified radius.

IV. Methodology

A. Experimental flow

As described in section III, the OK model is implemented in the MATLAB software environment using the ooDACE kriging toolbox. The kriging model considers no topographical information whatsoever but does require measured samples of the received power over the entire area of interest.

The authors gather data for the experiment by implementing the Longley-Rice ITM in SPLAT using the information of the Aggeneys Black Mountain transmitter. The only information regarding the transmitting antenna that SPLAT requires for a received power analysis is the name of the transmitter, the latitude, longitude, transmitter height above ground level and the ERP in watts (W). Both the latitude and longitude can be specified in either decimal format or DMS (degrees, minute, second) format. The alphanumerical output data file used to obtain the samples to be used as input to the kriging model. The authors randomly select 1%, 5%, 10% and 20% of the SPLAT output points as the input sample sets for the OK model. After the samples are obtained, they need to be transformed into a format suitable for kriging.

One of the most important transformations is to convert the LatLon (Latitude/Longitude) geographical coordinates specifying the location at which the samples are taken, into a flat plane. The reason for this is the fact that the kriging model is based on the Euclidean distances between the samples and the geographical coordinates give the locations on the ellipsoidal surface of the earth (i.e. locations are separated by arc lengths). Although the effect of the ellipsoidal coordinates on the relatively small area of analysis is not great, it still affects the accuracy of the kriging predictions. For this experiment, the geographical coordinates were converted to UTM (Universal Transverse Mercator). The reference ellipsoid used is the World Geodetic System 1984 (WGS84). Thus, the input to the kriging model is UTM coordinates which can be used to calculate the distances between samples.

The authors in [12] and [21]–[23] propose *k*-fold and leave-one-out cross-validation (LOO-CV) to evaluate the kriging model. The authors implement a 10-fold cross-validation as well as the LOO-CV using ooDACE.

B. Analysis parameters

The following command was used in SPLAT in order to implement the Longley-Rice ITM on the Aggeneys Black Mountain transmitter for a radius of 5 km.

-t Aggeneys.qth -L 10.0 -R 5.0 -olditm -erp 10000 -dbm -metric -ano ReceivedPower_Aggeneys

SPLAT automatically finds the required SRTM topographical data files stored in the execution directory, based on the location of the transmitter defined in the *.qth* file and the specified area of interest. The command also specifies the receiver antenna height to be 10 m and the *-metric* switch indicates that the specifications are in meters and kilometres instead of feet and miles. The *-erp* and *-dbm* switches invoke the received power analysis with the ERP antenna ERP specified in watts. For the implementation of the Longley-Rice ITM, SPLAT uses the 3-arc-second Satellite Radar Topography Mission (SRTM) data. 3-arc-seconds can be approximated to roughly 90 meters on the surface of the earth. This means that the points predicted by SPLAT are separated by approximately 90 m. Thus, 10533 points are predicted over the 5 km radius area.

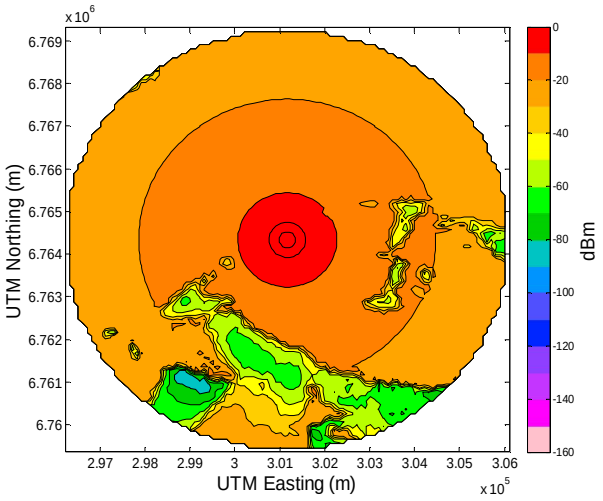

Figure 1: Received power contour plot of the points predicted using the Longley-Rice ITM for a radius of 5 km

V. Kriging Results

One of the conditions for kriging is that it requires a normally distributed data set. Thus, before the model is fitted to the input data, samples are normalised.

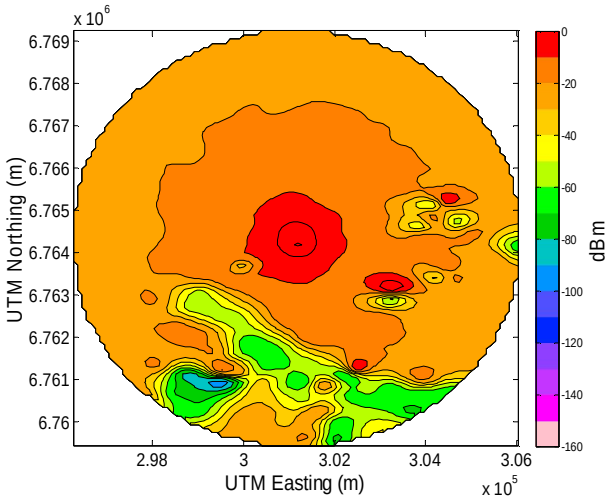

(a) Contour plot of kriging model for 5% samples

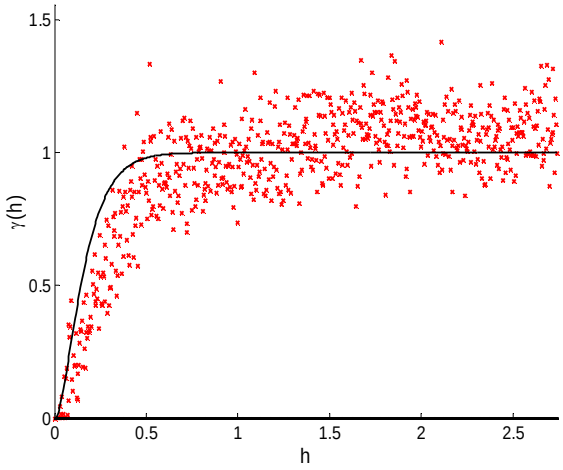

(b) Semi-variogram for 5% samples

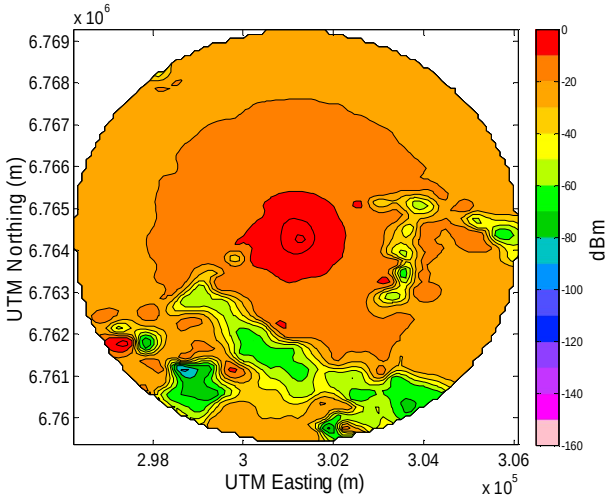

(c) Contour plot of kriging model for 10% samples

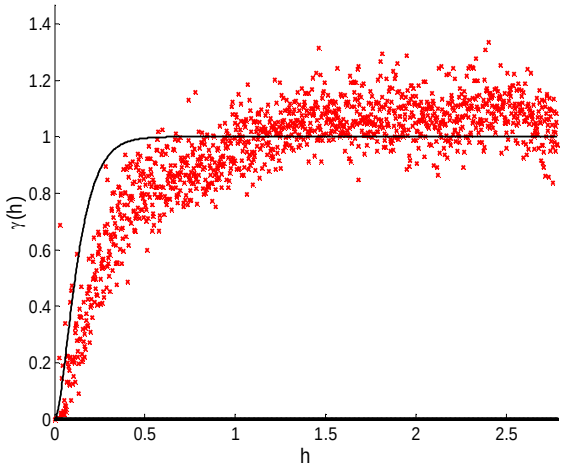

(d) Semi-variogram for 10% samples

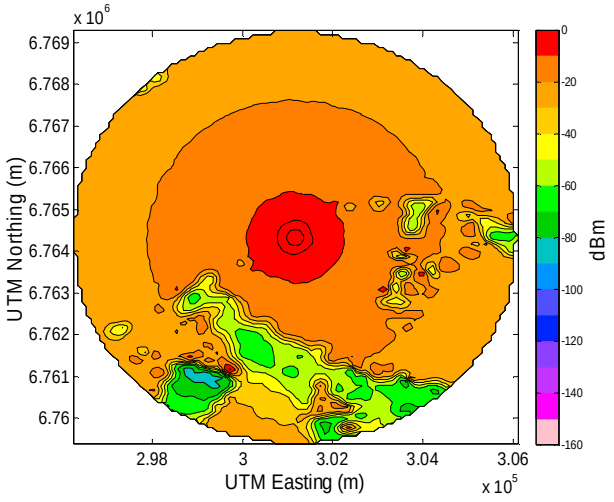

(e) Contour plot of kriging model for 20% samples

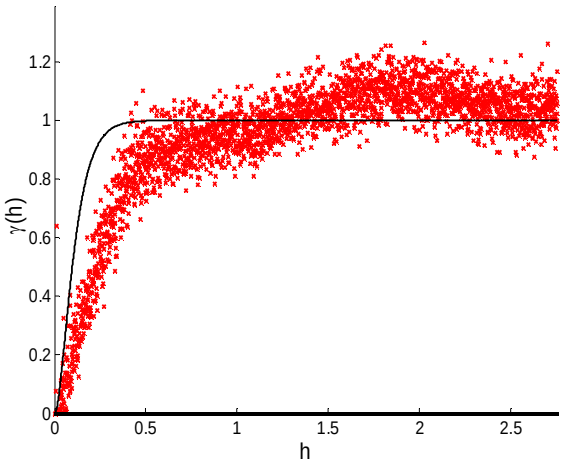

(f) Semi-variogram for 20% samples

Figure 2: Contour plots and semi-variograms of the models fitted to different sample set size

The colour scale specified in the SPLAT colour definition file was used to create a colour map in MATLAB. This colour map was used for the contour plot in order to visually compare the results to the received power map generated by the Longley-Rice ITM in SPLAT (see Figure 1).

Since the authors are interested in mapping the received power of the broadcast signal, contour maps of the OK model output are plotted. Figure 2 shows the OK model contour maps as well as the experimental and the model semi-variograms fitted to the normalised data for three

different input sample set sizes. The ooDACE toolbox uses equation (3) to derive the model semi-variogram from the correlation matrix.

Figure 2 shows visually how the kriging model contour plot becomes more accurate in comparison to the contour plot produced by SPLAT for 5%, 10% and 20% samples in figures 2.a, 2.c and 2.e, respectively. This is also evident in the three semi-variograms for 5%, 10% and 20% samples in figures 2.b, 2.d and 2.f, respectively. The semi-variogram plots show both the experimental semi-variogram (designated by red x's) and the model semi-variogram (solid line) for each case. The semi-variances of the input sample data in the experimental semi-variogram becomes less scattered as the number of input sample points increase, which also leads to a better fit of the model semi-variogram.

VI. Results Evaluation

As mentioned in section IV, the authors evaluate the generated OK model using two forms of cross-validation namely, 10-fold and LOO-CV. The authors cross-validate the model by dividing the sample set into disjoint subsets. One subset is then used for validation, while the remaining subsets are used to fit the kriging model. The subset of sample points (or a single sample point in the case of LOO-CV) kept for validation is then predicted using the fitted model. These results are compared to actual sample values using the Root-Mean-Squared Error (RMSE) function. Since the larger errors are given more weight in this approach, the RMSE values also give an indication of the variation in the errors. The authors also considered the RMSE relative to the standard deviation (SD) of the input data using equation (4). This value is expressed as a ratio and is proposed to be a better representation of the actual performance of the model [24]. The RMSE relative to the SD is given by:

$$RMSE_{SD} = \frac{\sqrt{\frac{1}{n}\sum_{i=1}^{n}\left(Z_{CV,i} - Z(s_i)\right)^2}}{\sqrt{\frac{1}{n-1}\sum_{i=1}^{n}(Z(s_i) - \bar{Z})^2}} \qquad (4)$$

,where n is the number of sample locations, $Z_{CV,i}$ is the cross-validation predicted value at sample location s_i and $\bar{Z}$ is the mean of the input values of all sample locations.

For the *k*-fold cross-validation, the authors used a *k*-value of 10, which means that the sample data set is divided into 10 disjoint subsets. In order to divide the sample set into 10 disjoint subsets, it must be a factor of 10. Thus, each sample set size was rounded to the nearest factor of 10.

For the evaluation of the kriging model the authors inspected the accuracy of the model using sample set sizes of 1%, 5%, 10% and 20%. Refer to Table 1. It was found that both the 10-fold cross-validation and the LOO-CV produced similar RMSE results. The calculated SDs (in dBm) of the input data was 13.83, 15.55, 14.39, and 14.17 for the respective sample sets in ascending order of sample set sizes. The SDs were calculated in order to obtain $RMSE_{SD}$ as suggested in equation (4).

Table 1: RMSE value results from cross-validation

Number of samples		**10-fold CV**		**LOO-CV**	
Count	***%***	***RMSE (dBm)***	***$RMSE_{SD}$***	***RMSE (dBm)***	***$RMSE_{SD}$***
120	1	7.9224	0.5728	7.7679	0.5617
520	5	5.9992	0.3858	5.8019	0.3731
1040	10	5.6444	0.3922	5.4098	0.3759
2100	20	4.1140	0.2903	3.8956	0.275

It is evident throughout the different sizes of sample sets, that LOO-CV yields the smaller RMSE of the two. This is to be expected since the subset of sample data used to train the kriging model is always larger than the 10-fold cross-validation. Furthermore, the decrease in the RMSE value as the size of the sample data sets increase was also found as expected. The small values for $RMSE_{SD}$ indicate very good performance of the OK model relative to the extent of the variation in the input data.

The results shown in Table 1 are quite remarkable considering the fact that the largest number of samples used to predict the 78.5 km^2 area, was 2100 samples (i.e. 1 sample for every 37380 m^2). In research it was found that the accuracy of empirical propagation models is in the order of 8-10 dB for urban areas and between 10 and 15 dB in rural areas [25]–[27].

VII. Conclusion

This paper introduced the problem of evaluating OK interpolation as a tool for REM. A brief background on the applicable study fields was given and the methodological approach taken to evaluate OK was discussed. It can be concluded that the OK results are comparable to results obtained using SPLAT with low RMSE as well as a very low $RMSE_{SD}$. This is noteworthy considering the small number of samples used to predict the received power for the entire area as well as the fact that the kriging model requires no topographical information at all. For future research, the authors will look into various methods to increase the accuracy of the OK model fit, which could lead to a reduction in the number of samples required and predictions with lower error. It can thus be concluded that OK shows great promise for effectively aiding in the generation of REMs. A case is therefore to be made for the use of a hybrid approach – measurements combined with kriging as an alternative to pure radio propagation modelling.

VIII. Acknowledgement

The authors acknowledge the financial support of the Telkom Centre of Excellence (CoE) at the North-West University, Potchefstroom Campus.

IX. References

[1] IEEE Standards Association, "IEEE Standard Definitions and Concepts for Dynamic Spectrum Access: Terminology Relating to Emerging Wireless Networks, System Functionality, and Spectrum Management," *IEEE Std 1900.1a-2012*, no. January, 2013.

[2] S. Haykin, "Cognitive Radio : Brain-Empowered Wireless Communications," *IEEE Journal on Selected Areas in Communication*, vol. 23, no. 2, pp. 201–220, 2005.

[3] S. Kim, "Cooperative spectrum sensing for cognitive radios using kriged kalman filtering," *IEEE Journal of Selected Topics in Signal Processing*, vol. 5, no. 1, pp. 24–36, 2011.

[4] L. Cao and H. Zheng, "Balancing Reliability and Utilization in Dynamic," vol. 20, no. 3, pp. 651–661, 2012.

[5] J. Li and A. D. Heap, "A review of spatial interpolation methods for environmental scientists." Geoscience Australia, Record 2008/23, p. 137, 2008.

[6] A. B. H. Alaya-Feki, S. Ben Jemaa, B. Sayrac, P. Houze, and E. Moulines, "Informed spectrum usage in cognitive radio networks: Interference cartography," *2008 IEEE 19th International Symposium on Personal, Indoor and Mobile Radio Communications*, pp. 1–5, Sep. 2008.

[7] D. G. Krige, "A Statistical Approach To Some Basic Mine Valuation Problems on the Witwatersrand," *Journal of Chemical Metallurgical and Mining Society of South Africa*, pp. 201–215, 1952.

[8] E. H. Isaaks and R. M. Srivastava, *An Introduction to Applied Geostatistics*. New York, United States of America: Oxford University Press, 1989.

[9] G. Matheron, *The Theory of Regionalized Variables and Its Applications*, 5th ed. Fontainebleau, France, 1971.

[10] A. G. Journel and C. J. Huijbregts, *Mining Geostatistics*. Academic Press, London, 1978, p. 304.

[11] W. Kresse and D. M. Danko, Eds., "Geostatistics," in *Handbook of Geographic Information*, Springer, 2012, pp. 43–59.

[12] N. A. C. Cressie, "Spatial Prediction and Kriging," in *Statistics for Spatial Data*, Revised., Wiley Interscience, 1993, pp. 105–210.

[13] D. Arroyo, X. Emery, and M. Peláez, "Sequential Simulation with Iterative Methods," in *Quantitative Geology and Geostatistics*, 17th ed., P. Abrahamsen, R. Hauge, and O. Kolbjørnsen, Eds. Oslo, Norway: Springer Science & Business Media Dordrecht, 2012, pp. 3–15.

[14] O. Thoke, "The Longley-Rice Propagation Model and TV White Space for Ultra WiFi," 2011. [Online]. Available: http://www.brighthubengineering.com/consumer-appliances-electronics/102752-the-longley-rice-propagation-model-and-tv-white-space-for-ultra-wifi/. [Accessed: 16-Sep-2013].

[15] "Final terrestrial broadcasting frequency plan, 2013," *Government Gazette*, Republic of South Africa, vol. 574, no. 36321, 2013.

[16] I. Couckuyt, A. Forrester, and D. Gorissen, "Blind Kriging: Implementation and performance analysis," *Advances in Engineering Software*, vol. 49, no. February 2012, pp. 1–13, 2012.

[17] I. Couckuyt, F. Declercq, T. Dhaene, H. Rogier, and L. Knockaert, "Surrogate-Based Infill Optimization Applied to Electromagnetic Problems," *International Journal of RF and Microwave Computer-Aided Engineering (RFMiCAE)*, vol. 20, no. 5, pp. 492–501, 2010.

[18] T. Dhaene, "ooDACE toolbox," no. June, 2013.

[19] J. A. Magliacane, "SPLAT! Because the world isn't flat!," 2014. [Online]. Available: http://www.qsl.net/kd2bd/splat.html. [Accessed: 23-Jan-2014].

[20] J. A. Magliacane, D. McDonald, and R. Bentley, "SPLAT user manual," no. February, pp. 1–19, 2011.

[21] T. Hengl, *A Practical Guide to Geostatistical Mapping*, Second. 2009.

[22] V. Joseph, Y. Hung, and A. Sudjianto, "Blind kriging: A new method for developing metamodels," *ASME Journal of Mechanical Design*, vol. 130, no. 3, 2008.

[23] C. E. Rasmussen and C. K. I. Williams, *Gaussian Processes for Machine Learning*. Cambridge, Massachusetts: MIT Press, 2006.

[24] P. Hiemstra and R. Sluiter, "Interpolation of Makkink evaporation in the Netherlands," De Bilt, 2011.

[25] C. Phillips, D. Sicker, and D. Grunwald, "Bounding the Practical Error of Path Loss Models," *International Journal of Antennas and Propagation*, vol. 2012, pp. 1–21, 2012.

[26] N. Faruk, A. A. Ayeni, and Y. A. Adediran, "On the study of empirical path loss models," *Progress In Electromagnetics Research B*, vol. 49, no. February, pp. 155–176, 2013.

[27] C. Phillips, S. Raynel, J. Curtis, S. Bartels, and D. Sicker, "The efficacy of path loss models for fixed rural wireless links," in *Passive and Active Measurement: 12th International Conference*, 2011, pp. 42–51.

Willie Boshoff received his B.Eng. degree in Computer and Electronic Engineering from the North West University Potchefstroom in 2012 and started pursuing a Master of Engineering degree in 2013 at the same institution. He is a Telkom CoE student and his research interests include efficient spectrum usage methods and radio environment mapping.